

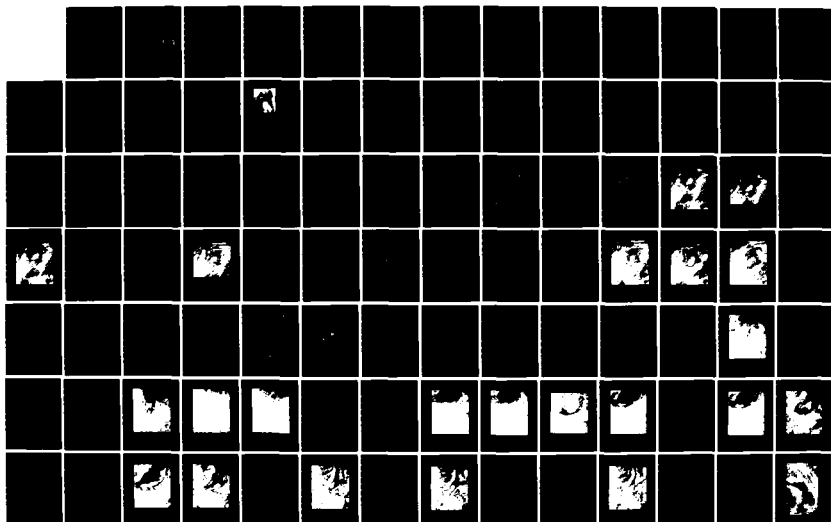
AD-A145 384

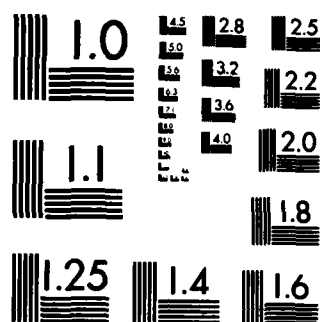
THE ARC CLOUD COMPLEX A CASE STUDY(U) AIR FORCE INST OF 1/2
TECH WRIGHT-PATTERSON AFB OH R L MILLER AUG 84
AFIT/CI/NR-84-52T

UNCLASSIFIED

F/G 4/2

NL





MICROCOPY RESOLUTION TEST CHART
NATIONAL BUREAU OF STANDARDS-1963-A

UNCLASS

SECURITY CLASSIFICATION OF THIS PAGE (When Data Entered)

REPORT DOCUMENTATION PAGE		READ INSTRUCTIONS BEFORE COMPLETING FORM
1. REPORT NUMBER AFIT/CI/NR 84-52T	2. GOVT ACCESSION NO.	3. RECIPIENT'S CATALOG NUMBER
4. TITLE (and Subtitle) The Arc Cloud Complex: A Case Study		5. TYPE OF REPORT & PERIOD COVERED THESIS/DISSERTATION
		6. PERFORMING ORG. REPORT NUMBER
7. AUTHOR(s) Robert Loren Miller		8. CONTRACT OR GRANT NUMBER(s)
9. PERFORMING ORGANIZATION NAME AND ADDRESS AFIT STUDENT AT: Texas A&M		10. PROGRAM ELEMENT, PROJECT, TASK AREA & WORK UNIT NUMBERS
11. CONTROLLING OFFICE NAME AND ADDRESS AFIT/NR WPAFB OH 45433		12. REPORT DATE Aug 84
		13. NUMBER OF PAGES 101
14. MONITORING AGENCY NAME & ADDRESS (if different from Controlling Office)		15. SECURITY CLASS. (of this report) UNCLASS
		15a. DECLASSIFICATION/DOWNGRADING SCHEDULE
16. DISTRIBUTION STATEMENT (of this Report) APPROVED FOR PUBLIC RELEASE; DISTRIBUTION UNLIMITED		
17. DISTRIBUTION STATEMENT (of the abstract entered in Block 20, if different from Report) B		
18. SUPPLEMENTARY NOTES APPROVED FOR PUBLIC RELEASE: IAW AFR 190-1 5 Sept 84 LYNN E. WOLAVER Dean for Research and Professional Development AFIT, Wright-Patterson AFB OH		
19. KEY WORDS (Continue on reverse side if necessary and identify by block number)		
20. ABSTRACT (Continue on reverse side if necessary and identify by block number) ATTACHED		

AD-A145 384

DTIC FILE COPY

DD

FORM

1473

EDITION OF 1 NOV 65 IS OBSOLETE

UNCLASS

84 - 09 13 022

SECURITY CLASSIFICATION OF THIS PAGE (When Data Entered)

ABSTRACT

The Arc Cloud Complex: A Case Study. (August 1984)

Robert Loren Miller, B.S., Texas A&M University

Chairman of Advisory Committee: Dr. Kenneth C. Brundidge

A detailed investigation of an arc cloud complex (ACC) using satellite, radar, rawinsonde, surface, and hourly precipitation data is documented. The fields of divergence and equivalent potential temperature were numerically determined. The ACC was produced by a mesoscale convective system (MCS) which was associated with a mid-tropospheric short-wave trough. The wind field at the surface within the ACC was highly divergent. It was deduced that the origin of the low-level air within the ACC was near the 700 mb level and that the origin of the updraft air was from a southerly low-level jet across West Texas. The edge of the ACC was characterized by strong wind shear. The precipitation structure of and behind the gust front while it was under the MCS cloud shield was similar to that in tropical convective systems. Convection which developed along the arc cloud became more intense than the convection which produced the arc cloud, and resulted in the formation of a larger, more significant MCS.

AFIT RESEARCH ASSESSMENT

The purpose of this questionnaire is to ascertain the value and/or contribution of research accomplished by students or faculty of the Air Force Institute of Technology (AU). It would be greatly appreciated if you would complete the following questionnaire and return it to:

AFIT/NR
Wright-Patterson AFB OH 45433

RESEARCH TITLE: The Arc Cloud Complex: A Case Study

AUTHOR: Robert Loren Miller

RESEARCH ASSESSMENT QUESTIONS:

1. Did this research contribute to a current Air Force project?

☐ a. YES

☐ b. NO

2. Do you believe this research topic is significant enough that it would have been researched (or contracted) by your organization or another agency if AFIT had not?

☐ a. YES

☐ b. NO

3. The benefits of AFIT research can often be expressed by the equivalent value that your agency achieved/received by virtue of AFIT performing the research. Can you estimate what this research would have cost if it had been accomplished under contract or if it had been done in-house in terms of manpower and/or dollars?

☐ a. MAN-YEARS _____

☐ b. \$ _____

4. Often it is not possible to attach equivalent dollar values to research, although the results of the research may, in fact, be important. Whether or not you were able to establish an equivalent value for this research (3. above), what is your estimate of its significance?

☐ a. HIGHLY
SIGNIFICANT

☐ b. SIGNIFICANT

☐ c. SLIGHTLY
SIGNIFICANT

☐ d. OF NO
SIGNIFICANCE

5. AFIT welcomes any further comments you may have on the above questions, or any additional details concerning the current application, future potential, or other value of this research. Please use the bottom part of this questionnaire for your statement(s).

NAME _____ GRADE _____ POSITION _____

ORGANIZATION _____ LOCATION _____

STATEMENT(s):

THE ARC CLOUD COMPLEX: A CASE STUDY

A Thesis

by

ROBERT LOREN MILLER

**Submitted to the Graduate College of
Texas A&M University
in partial fulfillment of the requirements for the degree of
MASTER OF SCIENCE**

August 1984

Major Subject: Meteorology

84 : 09 13 022

THE ARC CLOUD COMPLEX: A CASE STUDY

A Thesis

by

ROBERT LOREN MILLER

Approved as to style and content by:

Kenneth C. Brundidge
Kenneth C. Brundidge
(Chairman of Committee)

Walter K. Henry
Walter K. Henry
(Member)

Marshall J. McFarland
Marshall J. McFarland
(Member)

James R. Scoggins
James R. Scoggins
(Head of Department)



August 1984

Accession For	
NTIS GRA&I	<input checked="checked" type="checkbox"/>
DTIC TAB	<input type="checkbox"/>
Unannounced	<input type="checkbox"/>
Justification	
By _____	
Distribution/	
Availability Codes	
Dist	Avail and/or Special
A-1	

ABSTRACT

The Arc Cloud Complex: A Case Study. (August 1984)

Robert Loren Miller, B.S., Texas A&M University

Chairman of Advisory Committee: Dr. Kenneth C. Brundidge

A detailed investigation of an arc cloud complex (ACC) using satellite, radar, rawinsonde, surface, and hourly precipitation data is documented. The fields of divergence and equivalent potential temperature were numerically determined. The ACC was produced by a mesoscale convective system (MCS) which was associated with a mid-tropospheric short-wave trough. The wind field at the surface within the ACC was highly divergent. It was deduced that the origin of the low-level air within the ACC was near the 700 mb level and that the origin of the updraft air was from a southerly low-level jet across West Texas. The edge of the ACC was characterized by strong wind shear. The precipitation structure of and behind the gust front while it was under the MCS cloud shield was similar to that in tropical convective systems. Convection which developed along the arc cloud became more intense than the convection which produced the arc cloud, and resulted in the formation of a larger, more significant MCS.

DEDICATION

To my wonderful wife, Karen, for her love and patience throughout this adventure, and to our daughter, Kate, who did not get to see Daddy as much as she wanted. Without the support of my family, this work would not have been possible.

ACKNOWLEDGEMENTS

I wish to thank the United States Air Force and the Air Force Institute of Technology for making this study possible. I am also grateful to the members of the Atmospheric Science Division, Marshall Space Flight Center, Huntsville, Alabama, who helped procure and process data via McIDAS. Thanks go to Tammy Rippetoe who plotted numerous surface charts and upper-air soundings. Most of all, I thank Dr. Kenneth C. Brundidge for his guidance and assistance during the research phase of this study, and for his help, advice, and patience in the preparation of this manuscript.

TABLE OF CONTENTS

	Page
ABSTRACT	iii
DEDICATION.	iv
ACKNOWLEDGEMENTS	v
TABLE OF CONTENTS	vi
LIST OF TABLES	vii
LIST OF FIGURES.	viii
INTRODUCTION	1
A CASE STUDY: THE ACC of 26 JUNE 1982	13
Overview.	13
Significant Weather	13
Products Used in the Study	14
Conditions Leading to the First Arc Cloud	17
Conditions Leading to the Second Arc Cloud	41
SUMMARY AND RECOMMENDATIONS	92
Summary.	92
Recommendations	96
REFERENCES	98
VITA	101

LIST OF TABLES

TABLE		Page
1	Mesoscale Convective Complex (MCC) definition, based upon analysis of enhanced IR satellite imagery	2
2	MB enhancement	4
3	D/VIP levels and categories of intensity and rainfall rate	16

LIST OF FIGURES

FIGURE		Page
1	MB enhancement curve description	3
2	Schematic cross-section of arc-line penetration results .	6
3	The four stages of a thunderstorm gust front	8
4	Cloud pattern types associated with thunderstorm gust fronts	9
5	500 mb height (dm) and temperature (°C) for 0000 GMT 26 June 1982	19
6	300 mb height (dm) and temperature (°C) for 0000 GMT 26 June 1982	20
7	700 mb height (dm) and temperature (°C) for 0000 GMT 26 June 1982	21
8	850 mb height (dm) and temperature (°C) for 0000 GMT 26 June 1982	23
9	GOES infrared image with MB enhancement at 0330 GMT 26 June 1982	24
10	GOES infrared image with MB enhancement at 0430 GMT 26 June 1982	25
11	Radar summary chart for 0435 GMT 26 June 1982	26
12	GOES infrared image with MB enhancement at 0500 GMT 26 June 1982	27
13	Radar summary chart for 0535 GMT 26 June 1982	28
14	GOES infrared image with MB enhancement at 0630 GMT 26 June 1982	30
15	Radar summary chart for 0635 GMT 26 June 1982	31
16	Radar summary chart for 0735 GMT 26 June 1982	33
17	Surface temperature and pressure fields for 0800 GMT 26 June 1982	34

Continued

FIGURE		Page
18	Radar summary chart for 0835 GMT 26 June 1982	36
19	GOES infrared image with MB enhancement at 0830 GMT 26 June 1982	37
20	GOES infrared image with MB enhancement at 1000 GMT 26 June 1982	38
21	GOES infrared image with MB enhancement at 1201 GMT 26 June 1982	39
22	Surface temperature and pressure fields for 1200 GMT 26 June 1982	42
23	500 mb height (dm) and temperature (°C) for 1200 GMT 26 June 1982	43
24	300 mb height (dm) and temperature (°C) for 1200 GMT 26 June 1982	45
25	850 mb height (dm) and temperature (°C) for 1200 GMT 26 June 1982	46
26	Midland sounding at 1200 GMT 26 June 1982	48
27	Surface divergence for 1200 GMT 26 June 1982	49
28	850 mb θ_e (K) for 1200 GMT 26 June 1982	50
29	Surface θ_e (K) for 1200 GMT 26 June 1982	52
30	300 mb divergence overlaid upon GOES image for 1200 GMT 26 June 1982	53
31	300 mb θ_e (K) for 1200 GMT 26 June 1982	54
32	700 mb θ_e (K) for 1200 GMT 26 June 1982	56
33	700 mb divergence overlaid upon GOES image for 1200 GMT 26 June 1982	57
34	Surface divergence overlaid upon GOES image for 1200 GMT 26 June 1982	58

Continued

FIGURE		Page
35	850 mb divergence overlaid upon GOES image for 1200 GMT 26 June 1982	59
36	Radar summary chart for 1435 GMT 26 June 1982	61
37	Surface divergence overlaid upon GOES image for 1400 GMT 26 June 1982	62
38	Surface θ_e (K) overlaid upon GOES image for 1400 GMT 26 June 1982	63
39	GOES IR/Visual composite (C9 enhancement) for 1502 GMT 26 June 1982	64
40	Surface divergence overlaid upon GOES image for 1600 GMT 26 June 1982	65
41	Surface temperature and pressure fields for 1600 GMT 26 June 1982	66
42	Surface θ_e (K) overlaid upon GOES image for 1600 GMT 26 June 1982	67
43	GOES IR/Visual composite (C9 enhancement) for 1602 GMT 26 June 1982	68
44	Radar summary chart for 1735 GMT 26 June 1982	70
45	Surface θ_e 2-h change pattern (1800-1600 GMT) overlaid upon 1800 GMT GOES image for 1800 GMT 26 June 1982	71
46	GOES IR/Visual composite (C9 enhancement) for 1902 GMT 26 June 1982	72
47	GOES IR/Visual composite (C9 enhancement) for 2102 GMT 26 June 1982	74
48	GOES IR/Visual composite (C9 enhancement) for 2202 GMT 26 June 1982	76
49	Midland sounding at 0000 GMT 27 June 1982	78

Continued

FIGURE		Page
50	GOES IR/Visual composite (C9 enhancement) for 2302 GMT 26 June 1982	79
51	500 mb height (dm) and temperature (°C) for 0000 GMT 27 June 1982	80
52	Surface divergence overlaid upon GOES image for 0000 GMT 27 June 1982	82
53	850 mb divergence overlaid upon GOES image for 0000 GMT 27 June 1982	83
54	300 mb divergence overlaid upon GOES image for 0000 GMT 27 June 1982	84
55	GOES IR/Visual composite (C9 enhancement) for 0002 GMT 27 June 1982	85
56	GOES infrared image with MB enhancement at 0330 GMT 27 June 1982	86
57	GOES infrared image with MB enhancement at 0430 GMT 27 June 1982	87
58	GOES infrared image with MB enhancement at 0530 GMT 27 June 1982	88
59	GOES infrared image with MB enhancement at 0630 GMT 27 June 1982	89
60	GOES infrared image with MB enhancement at 0800 GMT 27 June 1982	90

INTRODUCTION

Large, long-lived convective weather systems, termed mesoscale convective systems (MCSs), that frequently occur over the United States during the spring and summer, have received much attention in the literature lately. This is a consequence of the fairly recent development of the Geostationary Operational Environmental Satellite (GOES) which has allowed observation of atmospheric phenomena on scales which had previously been unobservable. The satellite imagery helps fill the observational gaps between the synoptic scale, mesoscale, and cumulus scale. The most important reason for the attention given to MCSs is the significant impact of these MCSs and their associated features on human activities. Tornadoes, large hail, heavy rain, and damaging wind gusts are often associated with MCSs. More will be said of these aspects at a later point.

Maddox (1980a) established a definition for a mesoscale convective complex (MCC) which is an MCS meeting the criteria in Table 1. The criteria are based on the areal extent and duration of specific cloud top temperatures observed in enhanced GOES infrared (IR) imagery. The MB enhancement curve (U. S. Department of Commerce, 1983) is described in Fig. 1 and Table 2.

At mid-levels in an MCS, entrainment of environmental air produces strong, evaporationally-driven downdrafts. At the surface,

The citations on the following pages follow the style of The Journal of the Atmospheric Sciences.

TABLE 1. Mesoscale Convective Complex (MCC) definition, based upon analysis of enhanced IR satellite imagery (after Maddox, 1980a).

Physical Characteristics	
Size:	<p>A: Cloud shield with IR temperature less than or equal to -32° C must have an area greater than or equal to 100,000 square km</p> <p>B: Interior cold cloud region with temperature less than or equal to -52° C must have an area greater than or equal to 50,000 square km</p>
Initiate:	Size definitions A and B first satisfied
Duration:	Size definitions A and B must be met for a period greater than or equal to 6 h.
Maximum extent:	Contiguous cold cloud shield (IR temperature less than or equal to -32° C) reaches maximum size
Shape:	Eccentricity (minor axis/major axis) greater than or equal to 0.7 at time of maximum extent
Terminate:	Size definitions A and B no longer satisfied

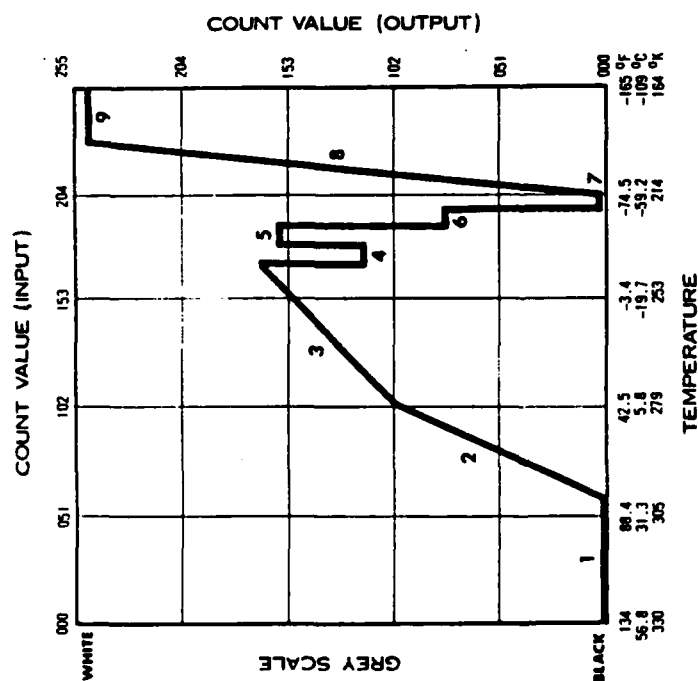


Fig. 1. MB Enhancement Curve Description. The steep slope of segments 1, 2, and 3 in Fig. 1a will give definition to the low and mid clouds. Segments 4 through 7 contours convective areas. Segment 8 slopes with a factor greater than zero from -63° C to -80° C which allows for good definitions of very cold domes (see Table 2). This enhancement applied to a satellite image is seen in Fig. 1b. Although specific temperatures can not be obtained, it better isolates the coldest tops by gradually going to white rather than producing a complete white-out at all temperatures colder than -65° C (after U. S. Department of Commerce, 1983).

TABLE 2. MB Enhancement (after U. S. Department of Commerce, 1983).

SEGMENT NUMBER	°C TEMPERATURE	COMMENTS
1	58.8 to 29.3	Little or no useful Met Data (Black)
2	28.8 to 6.8	Low Level/Sea Surface Difference
3	6.3 to -31.2	Middle Level - No Enhancement
4	-32.2 to -42.2	First Level Contour (Med Gray)
5	-43.2 to -53.2	(Light Gray)
6	-54.2 to -59.2	Thunderstorm (Dark Gray)
7	-60.2 to -63.2	Enhancement (Black)
8	-64.2 to -80.2	Overshooting Tops Enhancement
9	-81.2 to -110.2	(White)

cold outflow from individual storm downdrafts merge to produce a large mesohigh. The mesohigh created in the surface pressure field by the thunderstorm downdrafts had previously been explained by Byers and Braham (1949) and Fujita (1963). Along the leading edge of the mesohigh is often a cloud formation termed an "arc cloud" by Purdom (1973), which is discernible in GOES imagery. Vertical motions along the forward edge of the spreading, cooler air generate the arc cloud. A schematic cross-section of an arc-line depicting vertical motions and temperature changes based on the results of research aircraft penetrations is shown in Fig. 2 (Sinclair and Purdom, 1982). An MCS which produces an arc cloud has been termed an arc cloud complex (ACC) by Brundage (1983). An ACC may or may not meet the criteria established by Maddox for an MCC; however it seems likely that an ACC often is an MCC undergoing dissipation. One of the reasons Maddox (1980a) suggests for the demise of an MCC is, "The cold air dome beneath the system may become so intense that the surface convergence zone moves away from the region of mean mesoscale ascent into a region of mid-and upper-level subsidence". This scenario seems to match the behavior of and conditions associated with an arc cloud complex.

The thunderstorm outflow boundary, commonly termed a gust front, moves like a density current and in many ways resembles a cold front. Numerous studies (Charba, 1974; Goff, 1976; Mitchell and Hovermale, 1977; Wakimoto, 1982) explain its structure. To an observer, the effects of a gust front passage are normally an abrupt change in wind speed and direction, decreasing temperatures, and pressure rise. An observer also may note an arc cloud accompanying the gust front which

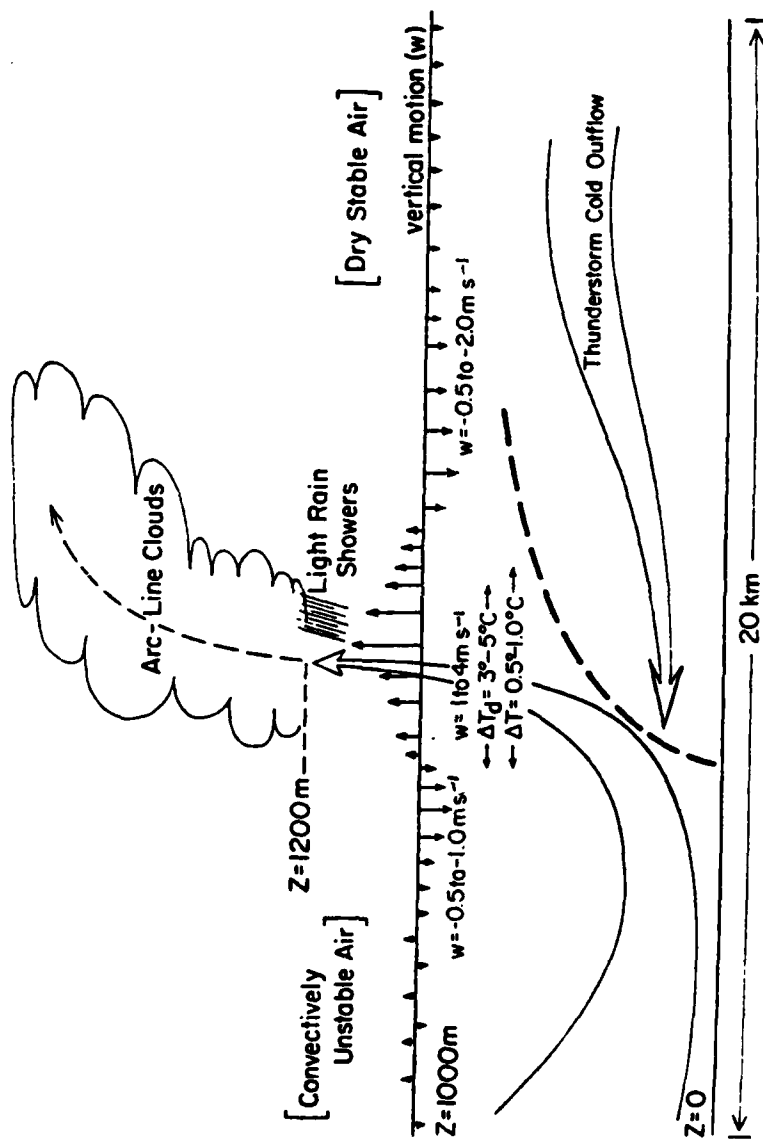


Fig. 2. Schematic cross-section of arc-line penetration results. The dew point change, temperature change, and vertical motion are for $Z = 1000 \text{ m}$. The dashed line represents the thunderstorm outflow boundary (after Sinclair and Purdom, 1982).

may appear as a roll cloud, shelf cloud, cumulus, towering cumulus, cumulus congestus, or cumulonimbus. The heaviest precipitation often is associated with the thunderstorm producing the outflow. Thus, heavy precipitation can accompany the gust front near its origin. As the gust front moves away from the parent thunderstorm, lighter precipitation may accompany its passage due to the "precipitation roll" described by Wakimoto (1982) in his study of individual severe thunderstorms (Fig. 3). However, the arc cloud is on a larger time and space scale than the gust front for an individual thunderstorm. Although the arc cloud may at times contain the precipitation roll feature, precipitation more often is associated with convective clouds which develop along it.

In a study of gust fronts, Gurka (1976) divided the cloud patterns associated with gust fronts into four categories shown in Fig. 4. The wind direction behind the gust front is indicated by the arrows. A Type 2 pattern has a clear-cut, arc-shaped leading edge with vigorous convection along most of the arc. This pattern sometimes replaces a Type 1 pattern in an area where the winds aloft are turning to northerly or northeasterly with time and becoming more anticyclonic. A Type 3 gust front is a narrow arc-shaped line of convective clouds with fairly uniform tops and no vigorous development along the arc. The arc is clearly separated from the originating cumulonimbus cell or cluster which is usually in its dying stage. The Type 4 pattern has a similar appearance to a thunderstorm gust front, but is formed along a sea-breeze front. The category that relates to this case study is the Type 1 which was previously described by Purdom

FOUR STAGES of a GUST FRONT

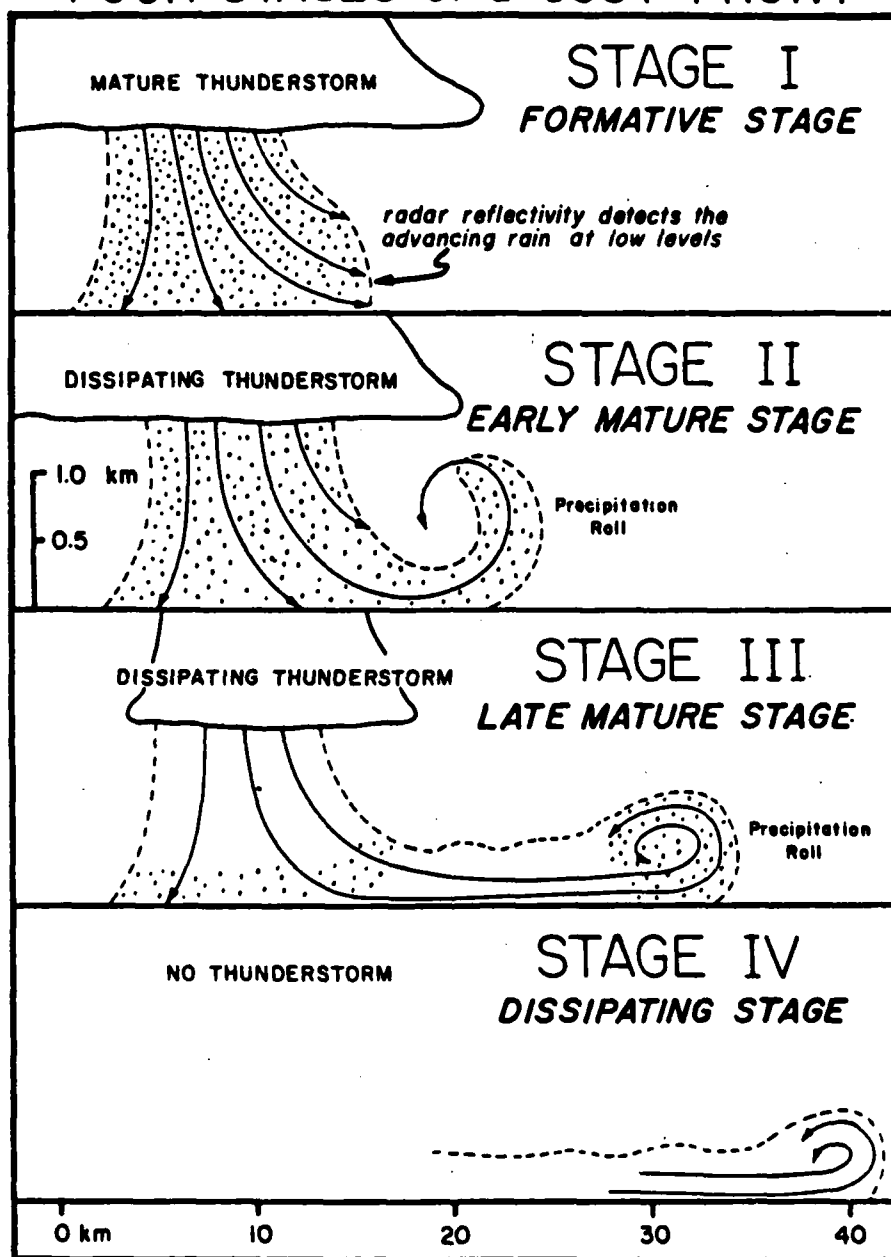


Fig. 3. The four stages of a thunderstorm gust front. The advancing precipitation at low levels is detected by the radar. The "precipitation roll" is a horizontal roll formed by airflow that is deflected upwards by the ground (after Wakimoto, 1982).

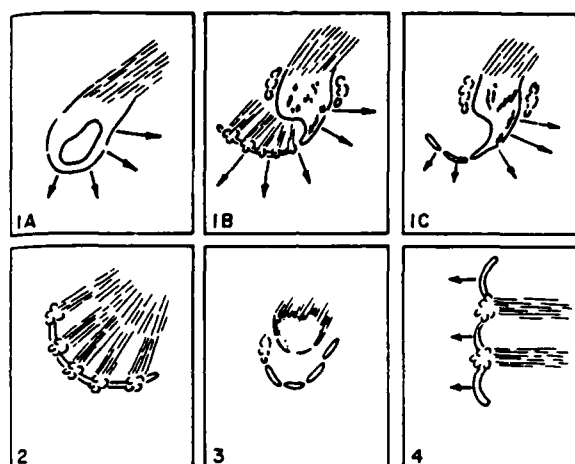


Fig. 4. Cloud pattern types associated with thunderstorm gust fronts (after Gurka, 1976).

(1974) as a large thunderstorm cluster with an oval-shaped leading edge and with the anvil cirrus curving anticyclonically out of the rear of the cluster. The majority of these storms were, "generally formed by a short-wave trough embedded in a northwesterly flow aloft or in the southwesterly flow ahead of a large-scale upper trough. With an eastward moving system, the gust front will generally be found on the eastern and southern portion of the convective cluster...". The Type 1 cloud patterns were broken down into three categories. Type 1A thunderstorm cluster has an oval-shaped leading edge, but with no "comma tail"; Type 1B has growing convection along a comma tail which extends from the southern portion of the parent cumulonimbus cell; Type 1C is similar to Type 1B except that the comma tail consists of weak low-level convection. In the case study to be reported on here, the pattern changes from Type 1A to 1C to 1B at which point the convection along the comma tail dominates and becomes the genesis of a larger MCS.

Fritsch et al. (1981) showed that MCCs produce widespread regions of measurable rainfall and that they account for a significant portion of growing-season rainfall over much of the United States' corn and wheat belts. Maddox (1980a) stated that many MCCs produced locally intense rainfalls and flash flooding. The arc cloud complex also can be responsible for severe weather, especially along the gust front and associated arc cloud. Proper identification of these features is important. The gust front is a dangerous source of potential aircraft accidents (Greene, 1977). Goff (1976) notes that imbedded within the outflow air mass are secondary surges of outflow.

Each is characterized by strong horizontal shears and large updrafts and downdrafts. All of these wind factors make aircraft operation at low levels difficult and unsafe. Buildings and other stationary structures vulnerable to high winds also may be adversely affected. Purdom (1979) stated another very important reason to properly identify (and possibly forecast) the location of the arc cloud. It may travel hundreds of kilometers from its outflow source, be maintained for several hours after dissipation of the MCS, and can trigger new and intense convection. It can become part of a chain of storm events which may extend over several days.

Before MCSs can be quantitatively described and a theory developed for their behavior, we must first learn all we can through examination of features from past occurrences. The leading researcher of MCCs, Robert Maddox, in summarizing his 1983 study stated, "Although this study has provided answers to some basic questions concerning mid-latitude MCCs, a number of important scientific questions were beyond the scope of this effort. Some of the more important considerations yet to be addressed include...

"Are there small-scale controls that govern initial thunderstorm formation in the MCC precursor environment?
What is the role of thunderstorm-scale downdrafts and downdraft interactions within a nascent MCC?
What are the details of the precipitation structure of the system?"

In summary, MCSs play an important role in human activities. Detailed analysis and discussion of individual ACC cases is needed to

better understand the workings of mesoscale convective systems. For the case at hand, convective cells along the arc-cloud line eventually became the progenitors of a significant MCS. Aspects of the ACC such as gust front movement, origins of the updraft and downdraft air, precipitation structure, surface weather changes, upper air changes, changes in the satellite imagery, divergence field changes, equivalent potential temperature (θ_e) field changes, and significant weather events will be documented. It is hypothesized that ACCs form through a specific sequence of events. This paper describes the formation of two arc clouds and, through analysis of all available observations, attempts to establish this sequence. Research of this type will help us to understand and forecast significant weather events.

A CASE STUDY: THE ACC of 26 JUNE 1982

Overview

The storm chosen for this study had its origins during the afternoon of 25 June 1982 just to the lee of the Rocky Mountain chain through Colorado and New Mexico. The study extends over the period from 0330 GMT 26 June 1982 to 0000 GMT 27 June 1982. During this period the storm moved eastward into the Texas Panhandle and western Oklahoma. It first intensified and produced copious precipitation. Within 6 h of the most intense precipitation, an arc cloud appeared in the satellite imagery. Later, through a process similar to that of the first arc cloud, a second arc cloud appeared.

The second arc cloud was the more significant of the two and became a source of new and deep convection as the original storm area dissipated. This new convection became more intense than the convection which produced the arc cloud, and resulted in the formation of a larger, more significant MCS.

Significant Weather

Numerous severe thunderstorm watches and warnings, flash flood watches and warnings, and tornado watches and warnings were issued by the National Weather Service (NWS) for areas along the arc cloud. A tornado uprooted several large trees 80 km northwest of Abilene. Reports of golf ball size hail came from Taylor, Brown, Mills, Reagan,

Sterling, and San Saba Counties. Strong winds, accompanied with marble size hail, ripped roofs off two commercial buildings, snapped numerous power and telephone poles, downed fences, and caused considerable crop damage in Martin County. Several large plate glass windows were broken out of a high rise building in Fort Worth. Lightning critically injured a woman in Garland, Texas. These severe weather events were either described in Storm Data (U. S. Department of Commerce, 1982a) or were transmitted over the NOAA weather wire.

Products Used in the Study

Several products and sources of information were used to aid this investigation of the arc cloud complex. These were as follows:

1. Hourly surface maps corresponding to the time and location of the ACC's development and existence were plotted and analyzed by hand for temperature and altimeter setting.
2. Standard pressure-level charts (300, 500, 700, and 850 mb) from the NWS were reanalyzed by hand in order to seek indications of the mesoscale features aloft which may have been smoothed in the original analysis. The upper level height and temperature pattern changes during the life cycle of the ACC were documented.
3. Radar summary charts from the NWS were transposed to opaque maps with the same scale as the hourly surface maps. Patterns of radar reflectivity intensity were correlated with features of the ACC. The determination of intensity was done by an intensity processor known as the Digital Video Integrator and Processor [D/VIP (U. S. Department of Commerce, 1981)]. Contours on these charts

correspond to the 1, 3, and 5 D/VIP levels. Estimated rainfall rates for these levels are shown in Table 3 (U. S. Department of Commerce, 1982b). These charts were used to help determine the rainfall pattern and intensity at the surface.

4. Pertinent atmospheric soundings at 0000 GMT and 1200 GMT in and around the ACC were plotted and analyzed to aid in determination of the ACC's structure, outflow origin, and stability of the atmosphere.

5. Hourly precipitation amounts (U. S. Department of Commerce, 1982c) were plotted for the recording gage stations within Texas to help determine the rainfall pattern at the surface.

6. GOES imagery, both visual and IR, was used for the following:

- a. Location of the outer boundary, or arc cloud portion of the ACC.
- b. Determination of the cloud top temperatures.
- c. Determination of when and where convective development or dissipation was occurring.

7. The Man-Computer Interactive Data Access System (McIDAS) of the Atmospheric Sciences Division of the Systems Dynamics Laboratory, Marshall Space Flight Center, provided the following products:

- a. Surface divergence field at 2 h intervals
- b. Upper level divergence fields at 12 h intervals
- c. Surface θ_e field at 2 h intervals
- d. Upper level θ_e fields at 12 h intervals
- e. 2 h surface θ_e field change

TABLE 3. D/VIP Levels and Categories of Intensity and Rainfall Rate (after U. S. Department of Commerce, 1982b).

D/VIP Level	Echo Intensity	Precipitation Intensity	dBZ [#]	Rainfall Rate (in/hr)	
				Stratiform*	Convective**
1	Weak	Light	Less than 30	Less than 0.1	Less than 0.2
2	Moderate	Moderate	30-41	0.1-0.5	0.2-1.1
3	Strong	Heavy	41-46	0.5-1.0	1.1-2.2
4	Very Strong	Very Heavy	46-50		2.2-4.5
5	Intense	Intense	50-57		4.5-7.1
6	Extreme	Extreme	More than 57		More than 7.1

*Based on $Z = 200R^{1.6}$. Stratiform rain of D/VIP levels 4, 5, and 6 does not occur.

**Based on $Z = 55R^{1.6}$, except that levels 5 and 6 are empirically determined. Hail is likely at these levels.

#dBZ = $\log_{10} Z_e \text{ mm}^6 \text{ m}^{-3}$, where Z_e is the equivalent radar reflectivity.

f. Vertical atmospheric cross sections

The analysis and contours provided by McIDAS are computer products obtained objectively by use of the Barnes (1973) interpolation scheme. This objective analysis does not separate mesoscale features from the synoptic environment. One should note that an objective technique for separating macroscale and mesoscale features in meteorological data has been established by Maddox (1980b). MCSs have been shown to modify their near environment on horizontal scales detected by synoptic upper-air observations [Fritsch et al. (1979), and Maddox et al. (1979)]. Therefore, the resultant fields of θ_e and divergence shown in this paper are a combination of mesoscale and synoptic scale features. The correlation of McIDAS products with each other, and their correlation with features in the other products such as surface maps, upper air charts, and rainfall patterns is discussed later from the point of view of their contribution to the sequence of events in the storm's history.

Conditions Leading to the First Arc Cloud

Initial convection developed to the lee of the Wyoming, Colorado, and northern New Mexico Rockies during the afternoon of 25 June 1982. This convection moved eastward. During the evening hours an MCS developed over the western Plains stretching from the Texas Panhandle to southwestern South Dakota. This sequence agrees with Wetzel et al. (1982) who found that afternoon orogenic thunderstorms such as those that develop along the foothills of the Rockies often move and provide the beginnings of significant Plains mesosystems.

On 26 June 1982 at 0000 GMT that portion of the MCS from which the ACC developed was located over northeast New Mexico and southeast Colorado. Fig. 5 shows that it was located along and extended to the rear of a 500 mb short-wave ridge. The temperature field was leading the height field which may indicate that the MCS, which stretched from the Texas Panhandle to South Dakota, had already altered its environment. It is hypothesized that the short-wave trough contributed to convective development, after which time the convection contributed to altering the trough. The MCS was located downstream of the thermal trough and upstream of the thermal ridge. Dew point depressions were less in this thermal trough than in the surrounding area. The amplitude of the height trough was not as great as the thermal trough. There was cold advection in the vicinity of the MCS. Cold advection extended into the ridge east of the MCS while warm advection was occurring in the trough west of the MCS. The overall 500 mb pattern over the United States was dominated by short waves. In addition to the short-wave trough/ridge pattern described above, another trough extended from northeast Texas to Wisconsin and a ridge extended from southern California to northern Idaho.

At 300 mb (Fig. 6) the MCS was located as it was at 500 mb, i.e., to the rear of a short-wave ridge and in an area of cold advection. The MCS was between a warm pocket located over Kansas and a cold pocket located over Utah. Ahead of the MCS the temperature was -36°C , behind it -38°C . The flow at both 300 and 200 mb over the MCS was diffluent, indicating the likelihood of convergence below.

At 700 mb (Fig. 7) the MCS was located near the inflection point

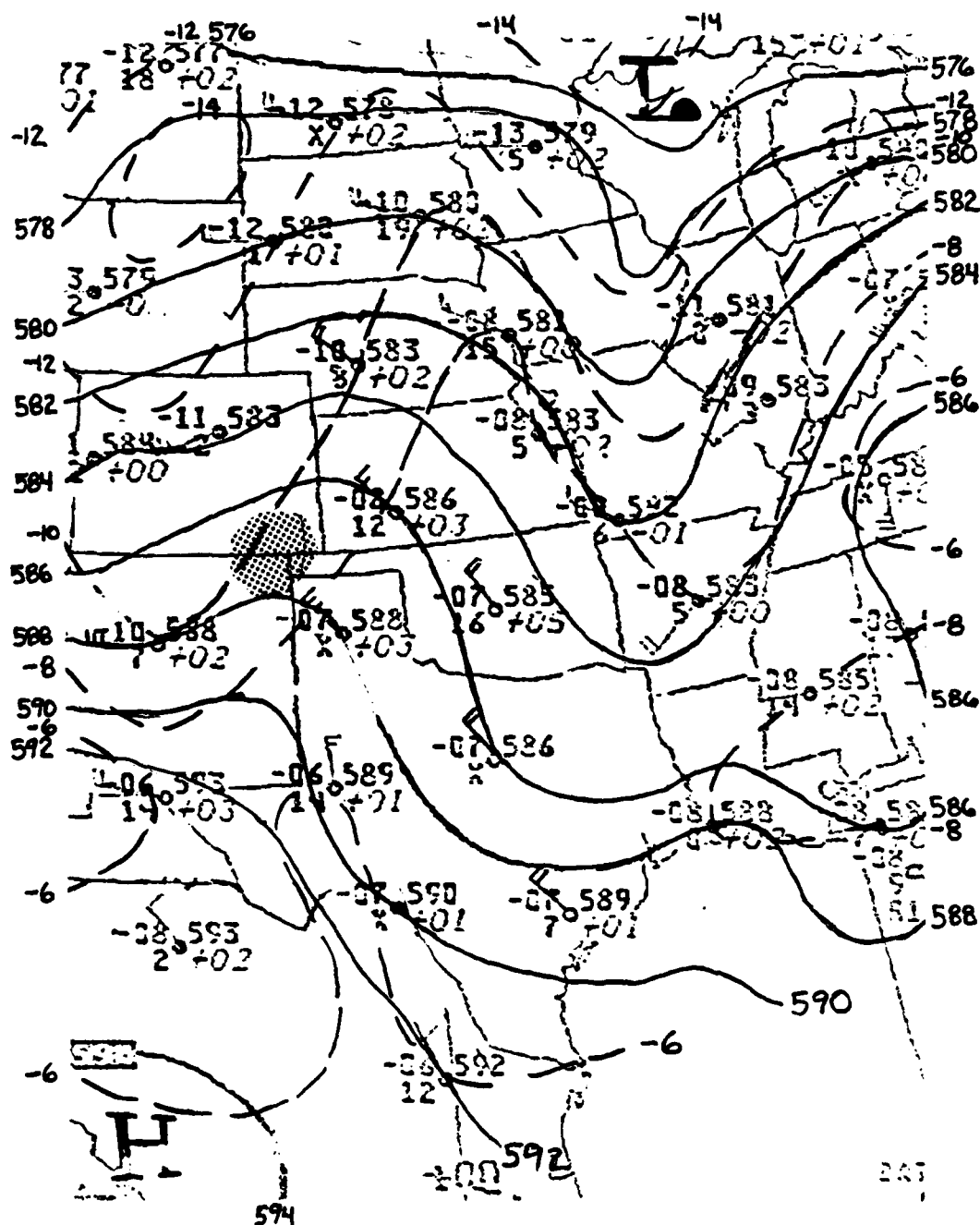


Fig. 5. 500 mb height (dm) and temperature (°C) for 0000 GMT 26 June 1982. Height contours (solid lines) are every 20 m; isotherms (dashed lines) are every 2°C. The location of the MCS corresponds to the dotted area.

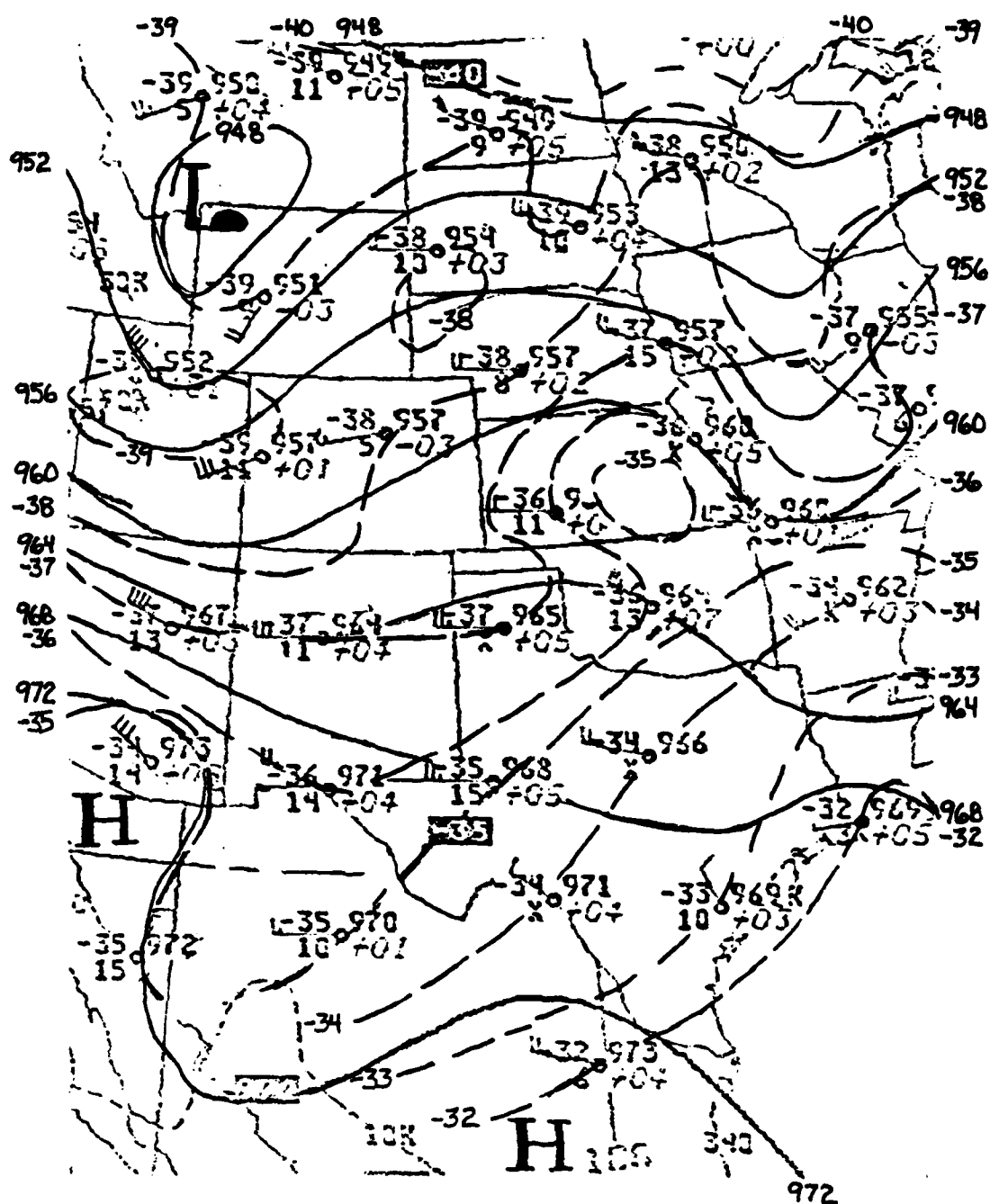


Fig. 6. 300 mb height (dm) and temperature (°C) for 0000 GMT 26 June 1982. Height contours (solid lines) are every 40 m; isotherms (dashed lines) are every 1°C.

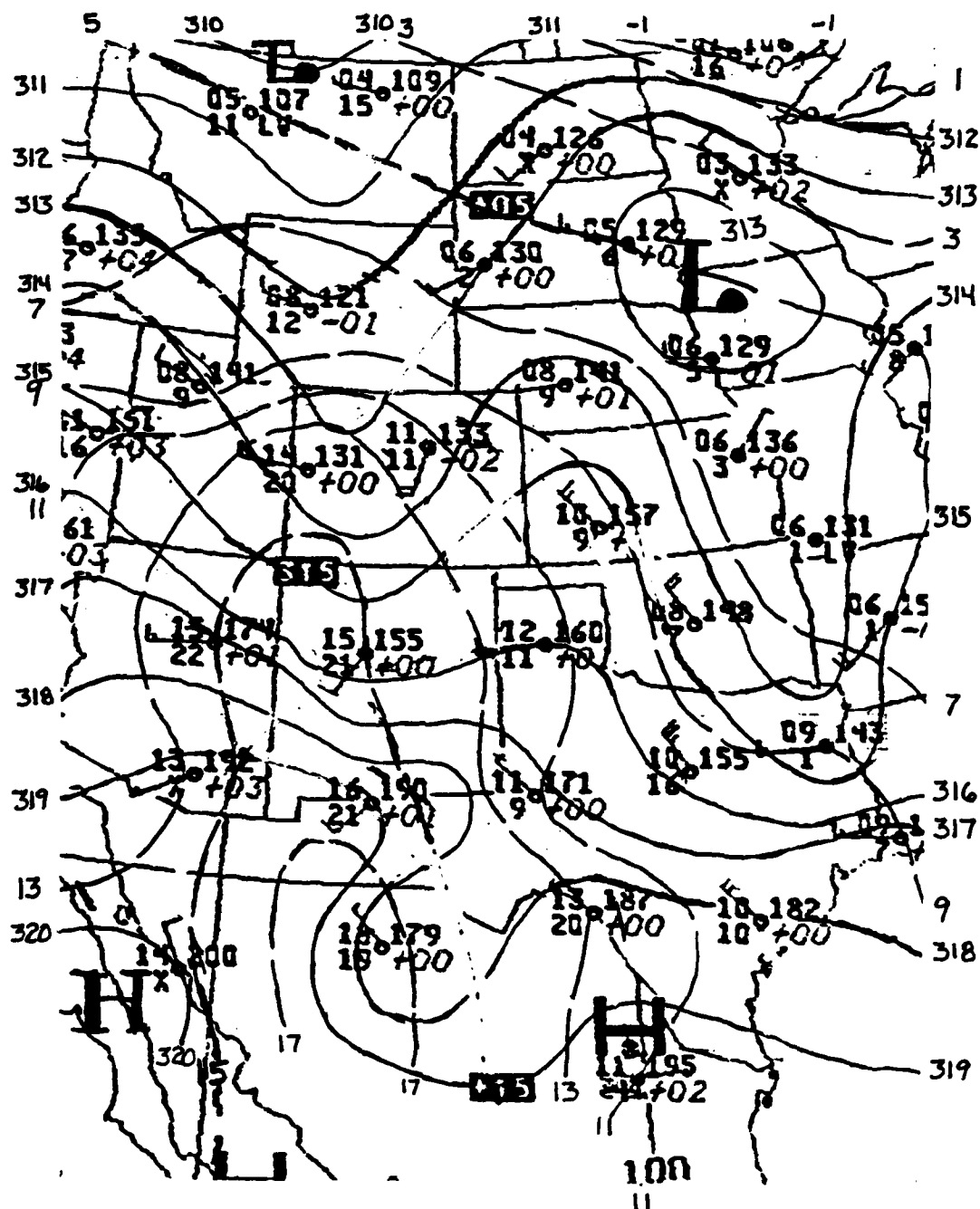


Fig. 7. 700 mb height (dm) and temperature (°C) for 0000 GMT 26 June 1982. Height contours (solid lines) are every 10 m; isotherms (dashed lines) are every 2°C.

on the east side of a short-wave trough. At this level the trough is warm-core so that warm air advection is occurring in the vicinity of the MCS. With respect to the 850 mb winds, the 700 mb winds veered, indicating warm-air advection throughout this layer. At 850 mb (Fig. 8) there was slight warm-air advection near the MCS. Thus, the troposphere is undergoing destabilization due to differential advection. A low level jet was not apparent.

Fig. 9 shows the enhanced IR satellite imagery for 0330 GMT 26 June 1982. Two storm areas on the eastern slope of the Rocky Mountains were present at this time. Attention in this paper is given to the southern storm marked with an arrow which already had developed cloud-top temperatures of $T < -58^{\circ}\text{C}$. The arc cloud complex began its life cycle from downdraft air originating in this nearly circular MCS of about 270 km in diameter. From 0330 GMT to 0430 GMT (Fig. 10) the black enhanced area (-58°C to -62°C) enlarged, spreading into the Oklahoma Panhandle. The 0435 GMT radar summary chart (Fig. 11) indicates a nearly circular ($D=160\text{ km}$) area of precipitation (labeled "A"), matching the satellite image. The D/VIP levels 3 and 5 were well-correlated with the area of coldest temperature in the satellite image. At 0500 GMT two overshooting tops, denoted as a lighter area ($T < -62^{\circ}\text{C}$) within the black area of the satellite image, appeared over the western Oklahoma Panhandle and northeast New Mexico (Fig. 12). The 0535 GMT radar summary chart (Fig. 13) indicated that the precipitation pattern changed from a nearly circular area to an arc-shaped band of heavier ($D/VIP=3$) precipitation located between these overshooting tops. Note that the maximum height of the radar

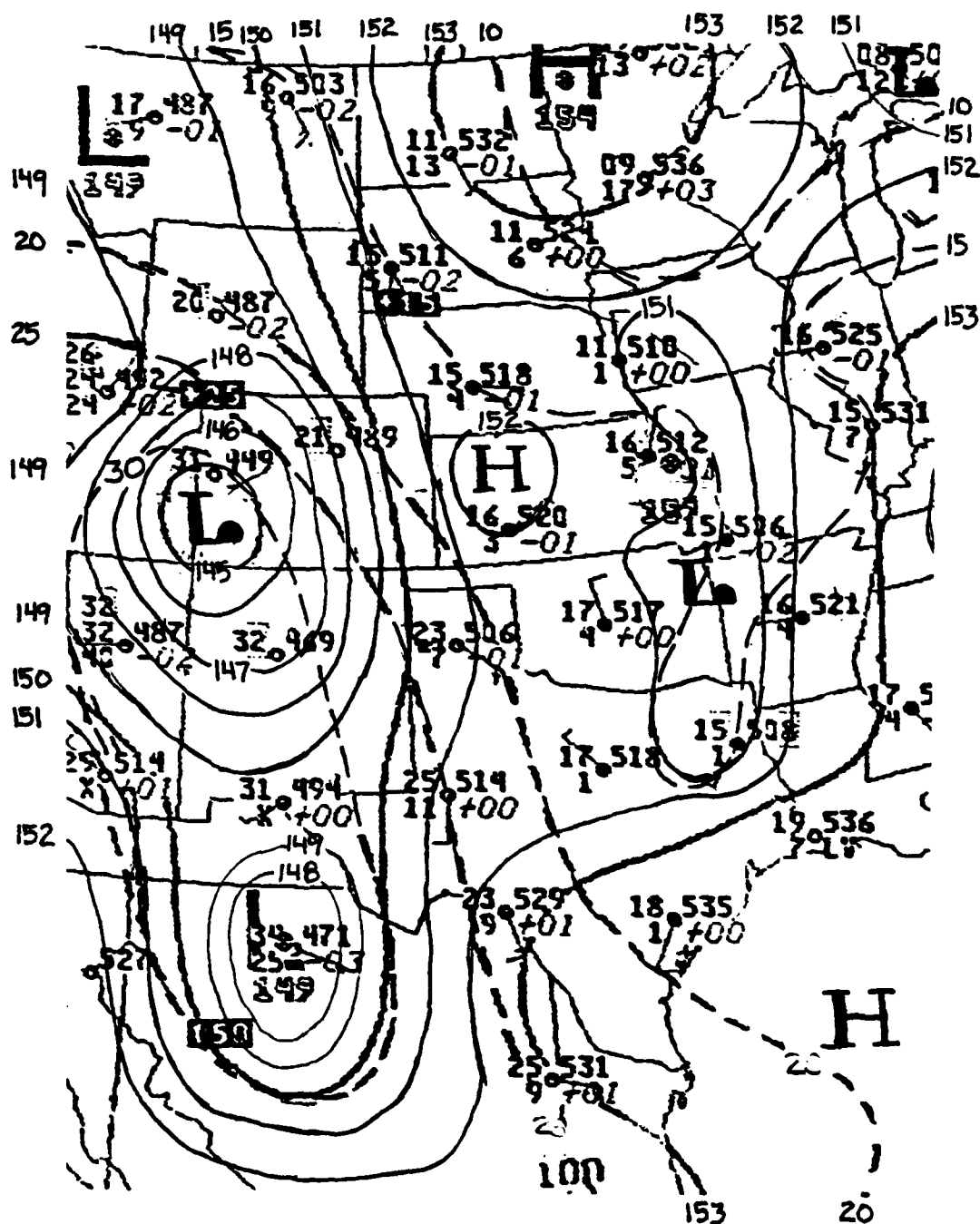


Fig. 8. 850 mb height (dm) and temperature (°C) for 0000 GMT 26 June 1982. Height contours (solid lines) are every 10 m; isotherms (dashed lines) are every 5°C.

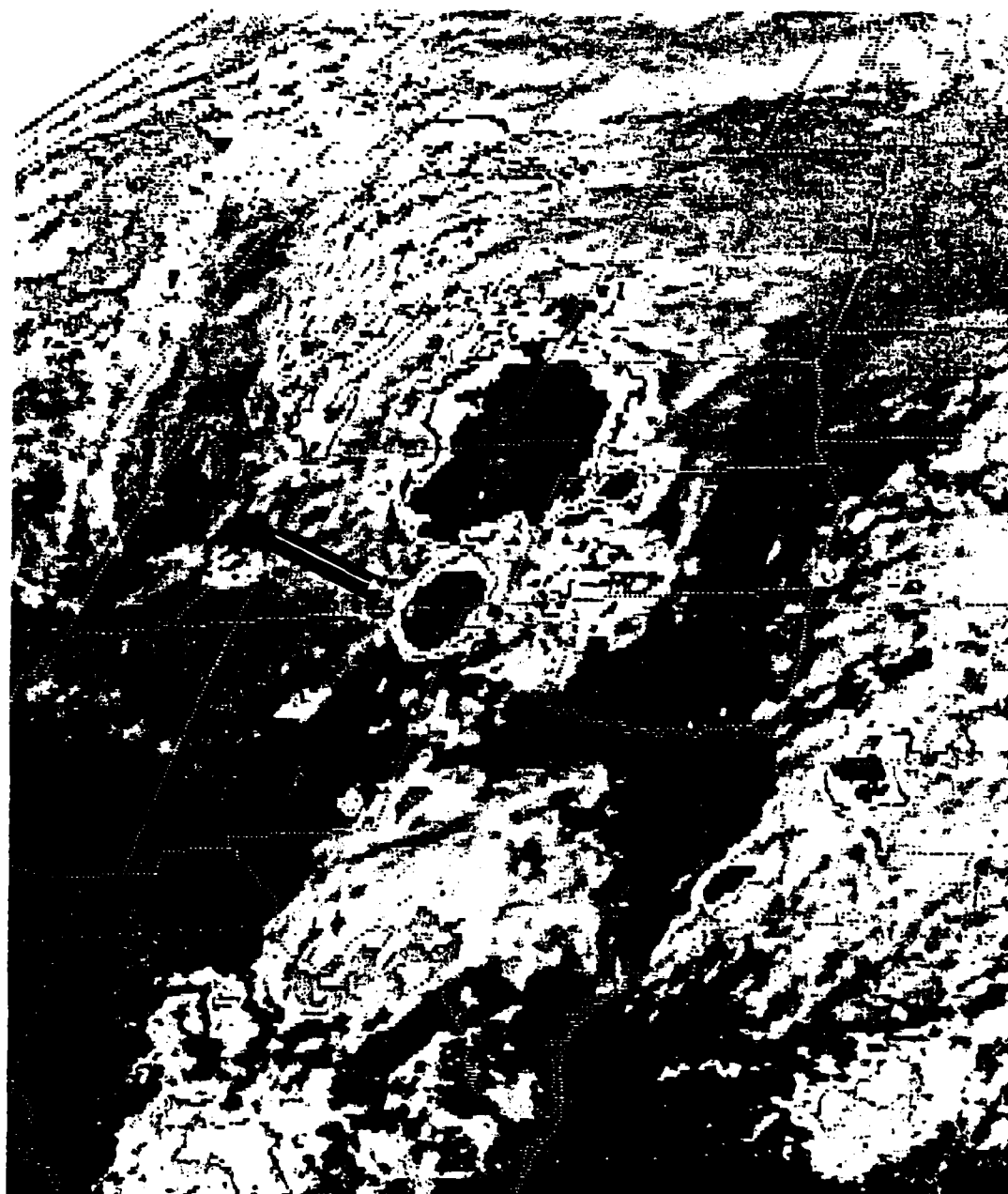


Fig. 9. GOES infrared image with MB enhancement at 0330 GMT 26 June 1982. The arrow points out the storm area given attention in this paper.



Fig. 10. GOES infrared image with MB enhancement at 0430 GMT 26 June 1982.

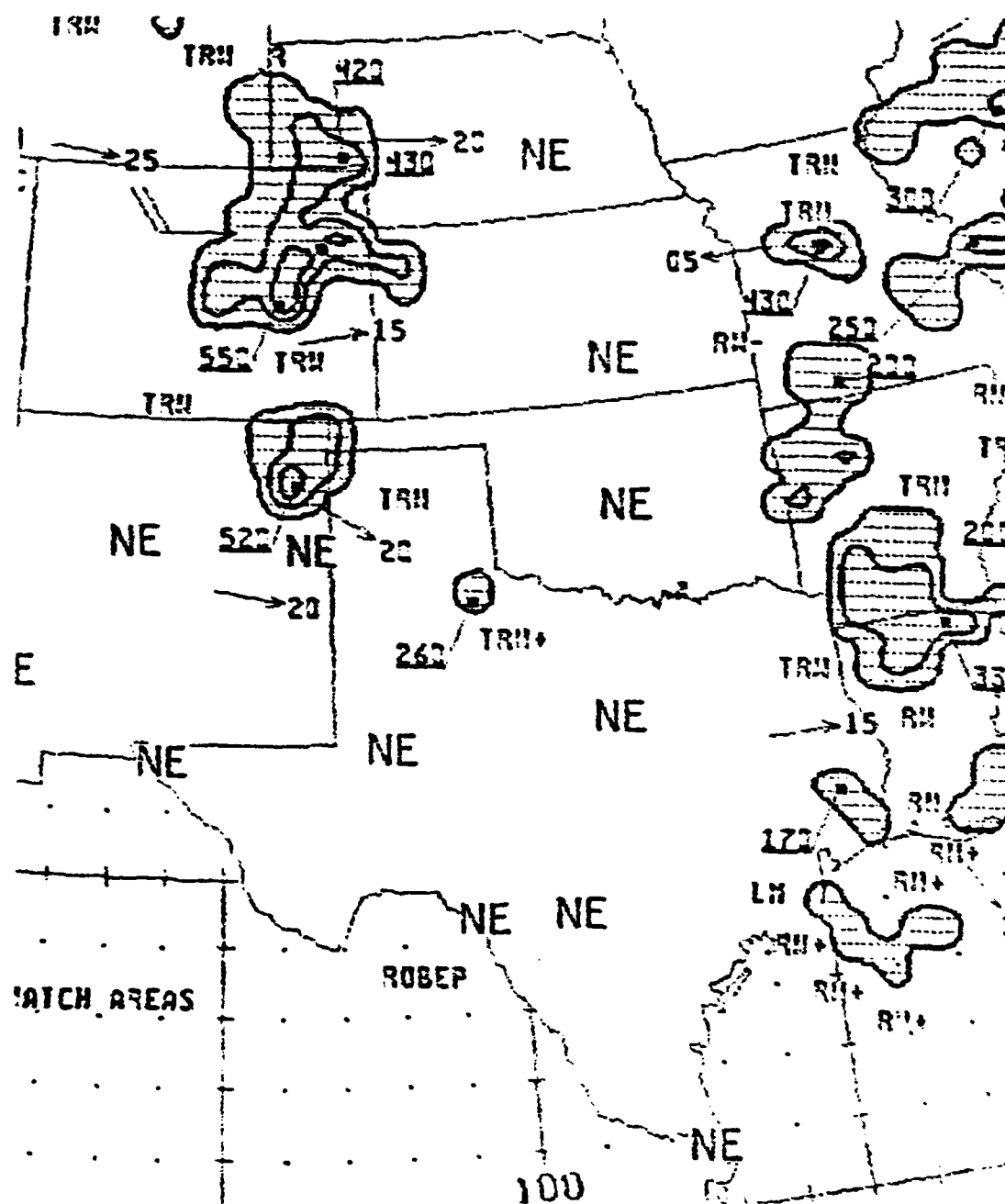


Fig. 11. Radar summary chart for 0435 GMT 26 June 1982. Shading indicates echo areas. Contours at echo intensities 1, 3, and 5; echo heights are in thousands of feet; cell movement given at end of arrows in knots; area and line movement given by pennant with full barb = 10 kt (U. S. Department of Commerce, 1981). The subject cell is denoted "A".

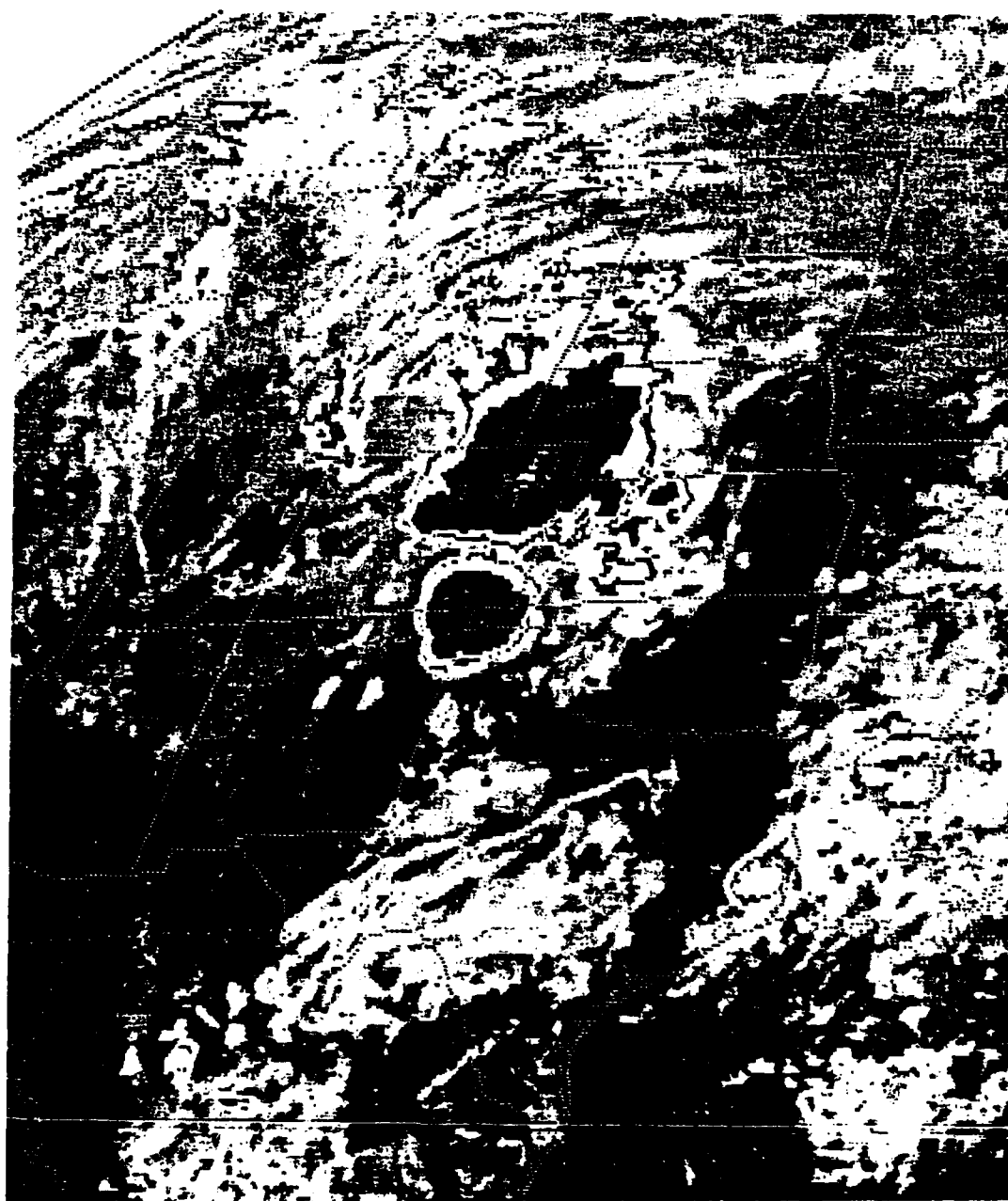


Fig. 12. GOES infrared image with MB enhancement at 0500 GMT 26 June 1982.

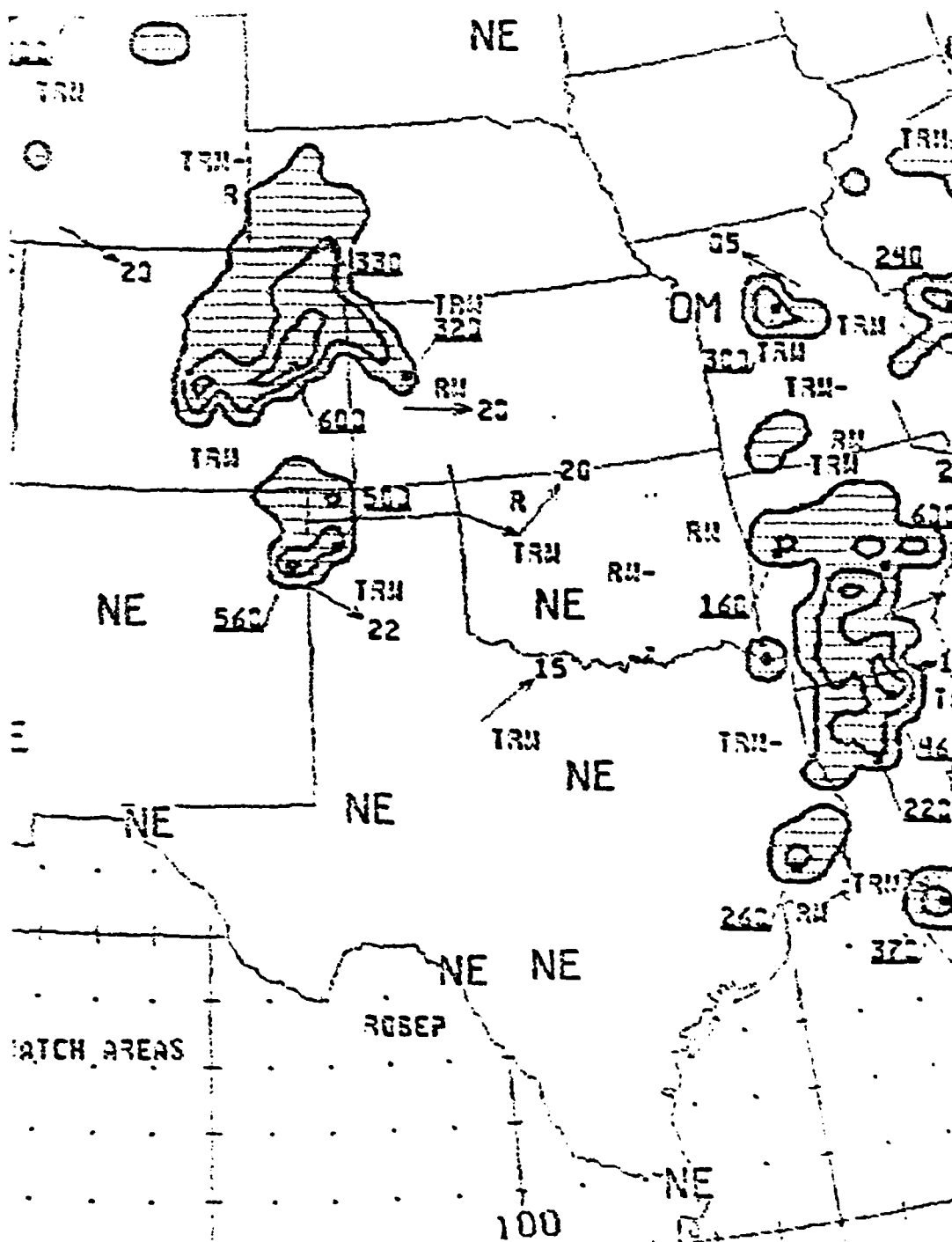


Fig. 13. Radar summary chart for 0535 GMT 26 June 1982. Shading indicates echo areas. Contours at echo intensities 1, 3, and 5; echo heights are in thousands of feet; cell movement given at end of arrows in knots; area and line movement given by pennant with full barb = 10 kt (U. S. Department of Commerce, 1981).

echo had reached 56,000 ft. It is probable that a gust front existed along this arc-shaped area of heavier precipitation. The exact location and onset of the downdraft air is not known because the density of surface stations is not great enough. The details of the structure of the gust front as described in previous studies (Charba, 1974; Goff, 1976; Mitchell and Hovermale, 1977; Wakimoto, 1982) are not adequately resolved by conventional surface data.

The 0630 GMT GOES imagery (Fig. 14) shows a continuing eastward motion plus expansion of the MCS under study. Also, a merging with the MCS to the north had occurred. Two interesting features may be noted. The first is the large IR temperature gradient along the east, south, and west sides of the storm complex. The gust front most likely is behind but parallel with this "isotherm" packing according to Gurka (1976) who stated that the gust front is found close to the greatest IR temperature gradient in satellite imagery. The second item of interest is the further decrease in temperature of the central portion of the storm complex (labeled "A") located along the Texas-Oklahoma Panhandle border, indicating an increase in cloud top height. Top height changes may be important in understanding the relation of cloud dynamics to arc cloud complex formation. This overshooting top was above a mesohigh in the surface pressure analysis (not shown). Radar at this time (Fig. 15) indicated that significant changes had occurred in the precipitation structure of the MCS. An arc-shaped squall line was now evident along the gust front. Note that the heaviest precipitation was associated with this squall line, not with the convection which was responsible for the outflow and gust

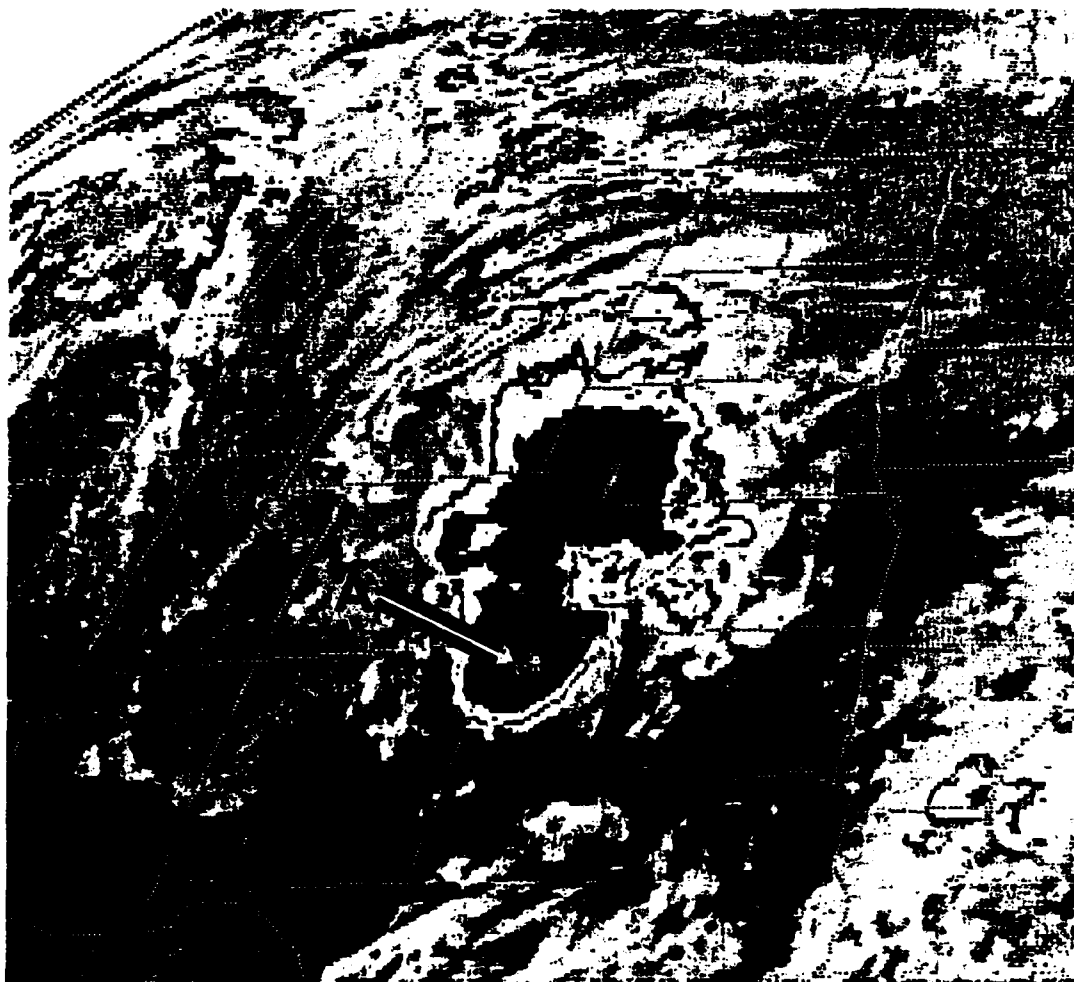


Fig. 14. GOES infrared image with MB enhancement at 0630 GMT 26 June 1982. Arrow "A" points out the central portion of the storm complex.

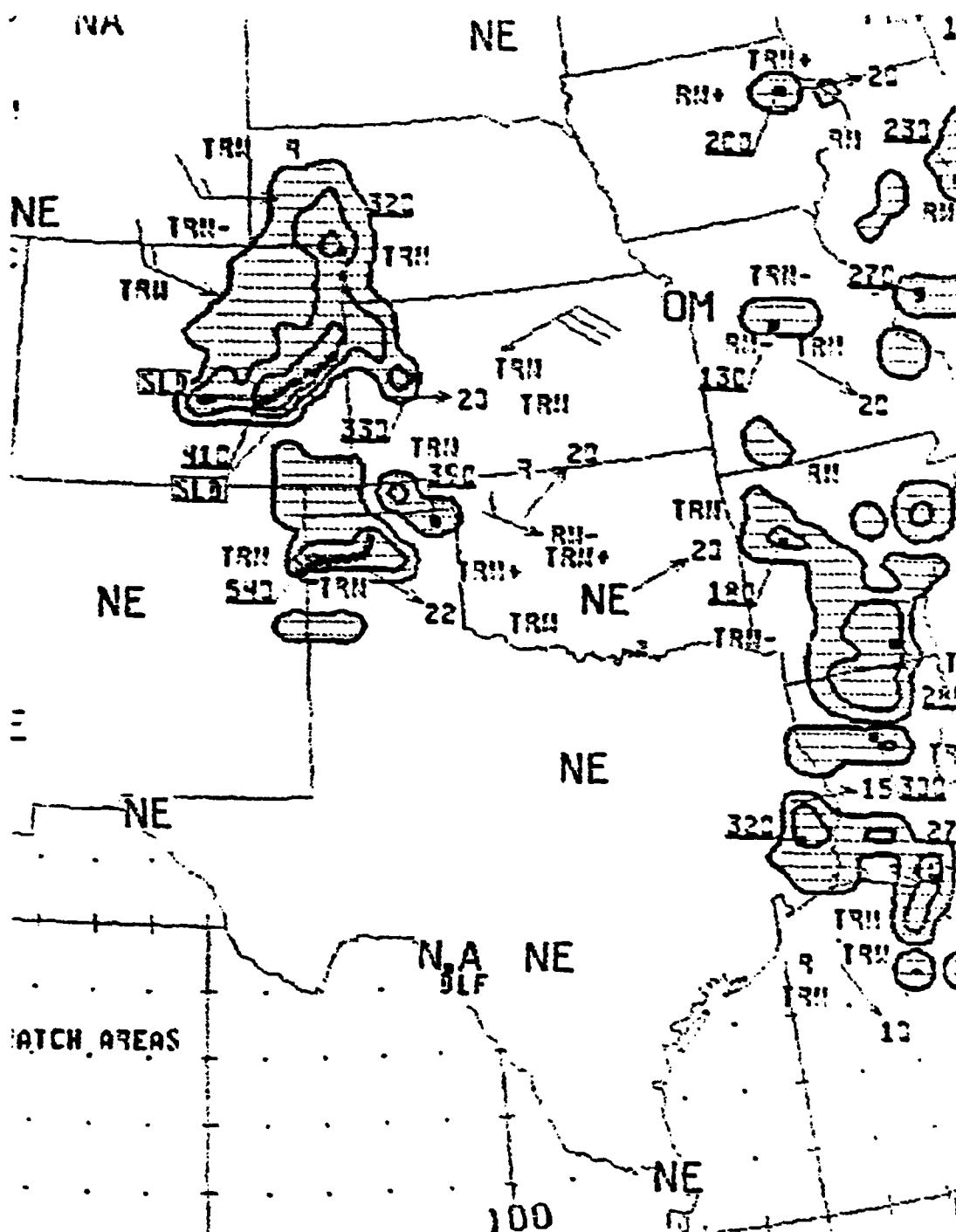


Fig. 15. Radar summary chart for 0635 GMT 26 June 1982. Shading indicates echo areas. Contours at echo intensities 1, 3, and 5; echo heights are in thousands of feet; cell movement given at end of arrows in knots; area and line movement given by pennant with full barb = 10 kt (U. S. Department of Commerce, 1981).

front.

The 0735 GMT radar chart (Fig. 16) reveals that the squall line was now solid along the eastern and southern sections of the gust front. A region of more stratiform precipitation continues to trail behind the arc-shaped squall line. This precipitation pattern is similar to the pattern described by Zipser (1977), Houze (1977), and Gamache and Houze (1982) who studied tropical squalls. Gamache and Houze (1982) stated, "The squall-line region is characterized by mesoscale boundary-layer convergence, which feeds deep convective updrafts, and mid-to-upper-level divergence associated with outflow from the cells". A discussion of the convergence and divergence within the ACC is presented later in this paper.

The surface analysis for 0800 GMT is shown in Fig. 17. The location of the gust front is denoted by a cold front symbol. The contour interval of altimeter setting isolines is 0.03 in Hg (about 1 mb). Isotherms are every 4° F. Note the moist, southeasterly surface flow across West Texas ahead of the gust front. The cold-core mesohigh at this time is centered just east of Dalhart. The first surface-observation evidence of the gust front was at Amarillo, Tx. The passage of the gust front occurred at 0728 GMT when the winds shifted from 140° at 13 kt to 010° at 20 kt, gusting to 29 kt. The altimeter setting rose 0.08 in of mercury (about 3 mb). The temperature dropped 10° F. Rain began 15 min after windshift; thunder began 20 min after windshift. The gust front is associated with a rainy downdraft, thus rain typically begins soon after gust front passage. An arc cloud was not visible at this time in the satellite

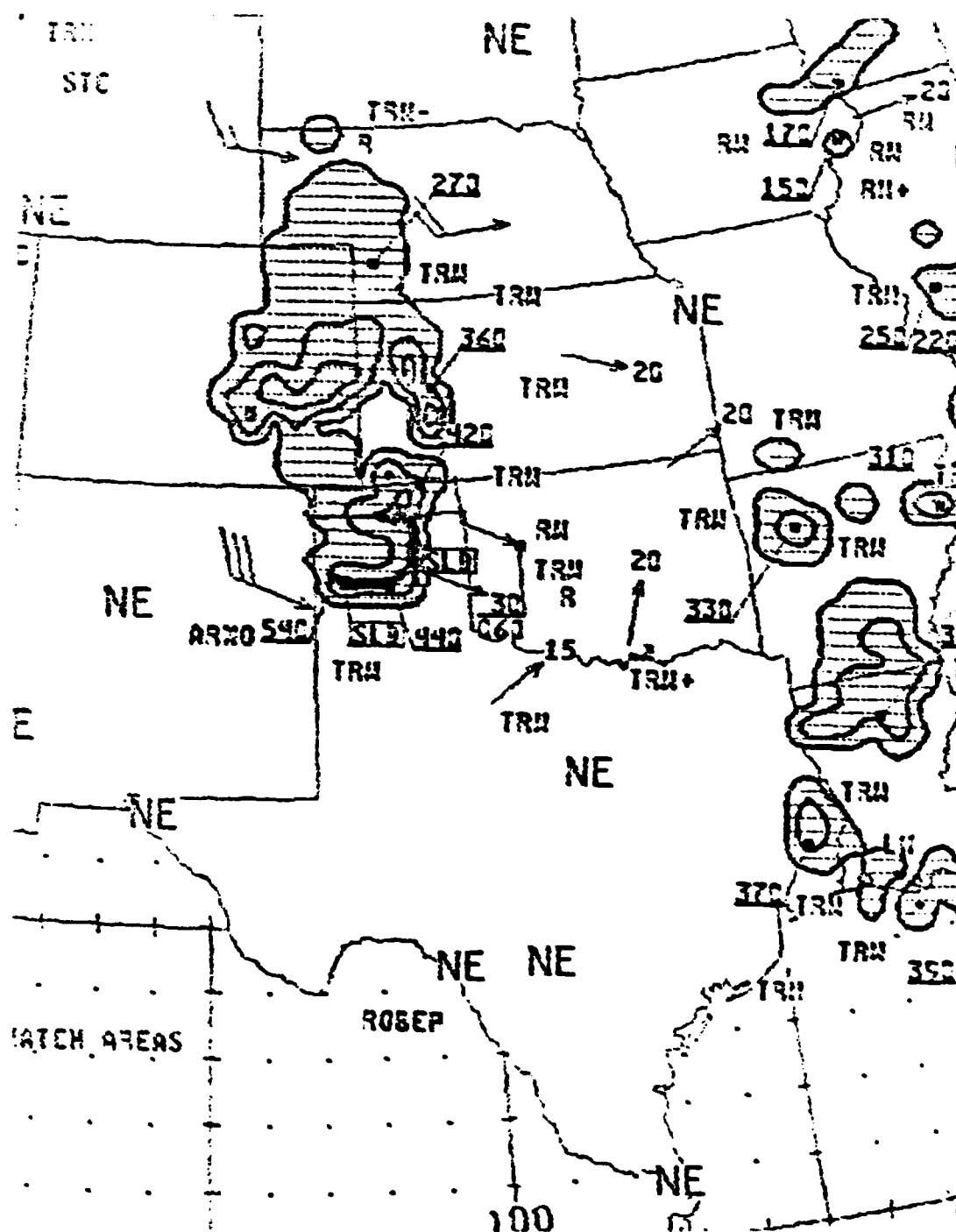


Fig. 16. Radar summary chart for 0735 GMT 26 June 1982. Shading indicates echo areas. Contours at echo intensities 1, 3, and 5; echo heights are in thousands of feet; cell movement given at end of arrows in knots; area and line movement given by pennant with full barb = 10 kt (U. S. Department of Commerce, 1981).

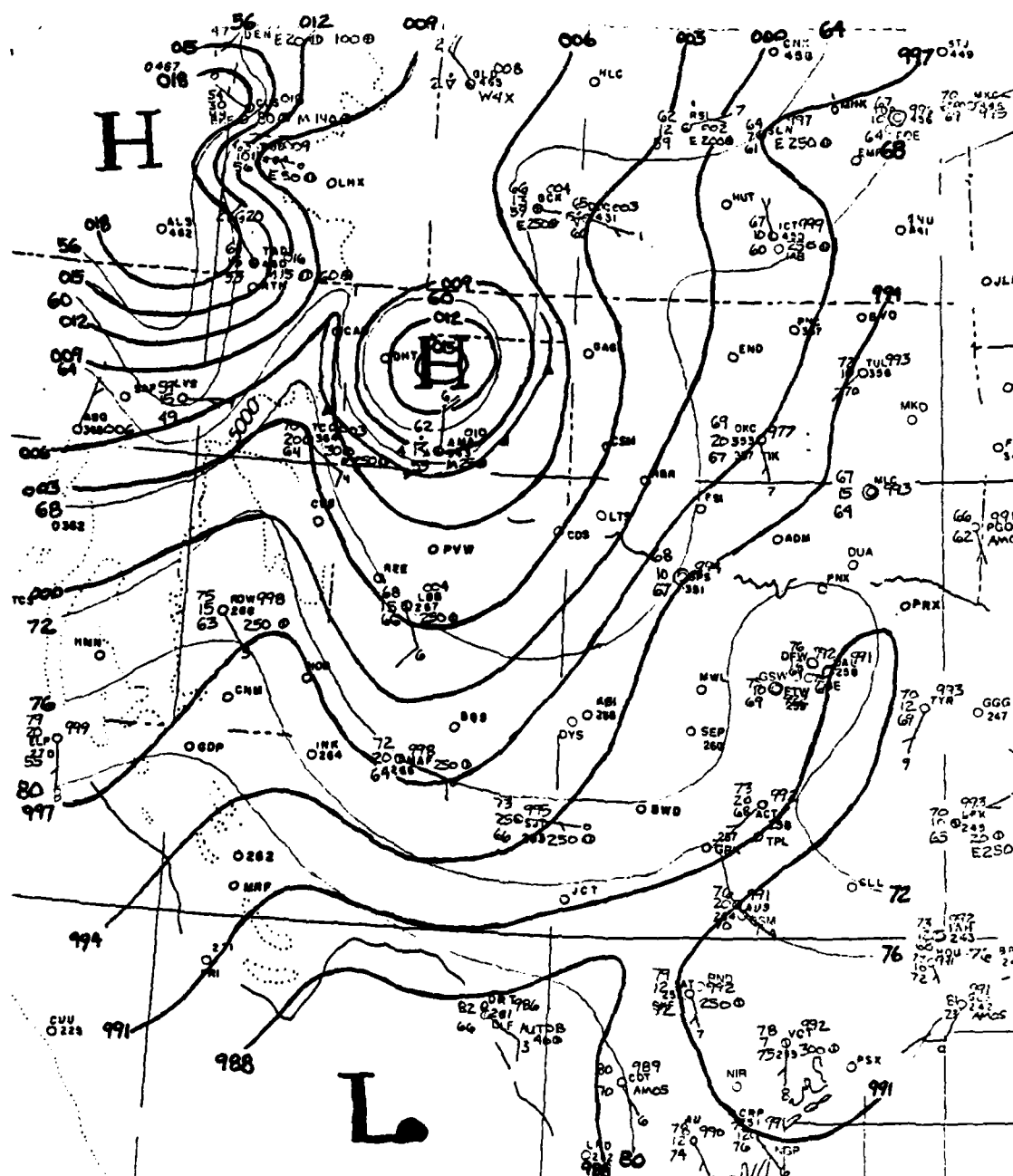


Fig. 17. Surface temperature and pressure fields for 0800 GMT 26 June 1982. Altimeter setting contours (thick lines) are every 0.03 in Hg; isotherms (thin lines) are every 4°F. The gust front is denoted by a cold front symbol.

imagery because the MCS cloud shield covered all but the southern portion of the Texas Panhandle.

Radar reports indicate that by 0835 GMT the solid squall line had decayed into isolated thunderstorms along the gust front (Fig. 18). Behind this decayed line the stratiform type rain continued to cover most of the Texas and Oklahoma Panhandles. The highest radar echo (labeled "B") indicated along the gust front is 48,000 ft, down 6,000 ft from 2 h earlier. The greatest reflectivity, $D/VIP=5$, corresponds to this highest cell. Another $D/VIP=5$ cell (labeled "C") was located along the northeastern portion of the gust front, over the Oklahoma Panhandle. The corresponding GOES image (Fig. 19) indicated that the cloud-top temperatures of this cell were the coldest in the area.

The areal extent of clouds with temperatures less than -58°C over the eastern and central Texas Panhandle decreased significantly from 1000 to 1200 GMT (Figs. 20 and 21). By 1200 GMT only a small area of clouds colder than -58°C remained, primarily located over the southeast corner of the Texas Panhandle. The first arc cloud is discernable in Fig. 21, having moved southeastward from the MCS cloud shield. Its location is marked with arrows. While the gust front was under the MCS cloud shield it was associated with heavy precipitation. Once it became visible in the satellite imagery as an arc cloud it acted as a "dry" gust front. Numerous stations experienced gust front passage without precipitation.

At this point, it is useful to summarize the sequence of events involved in the formation of the first arc cloud. Initial convection

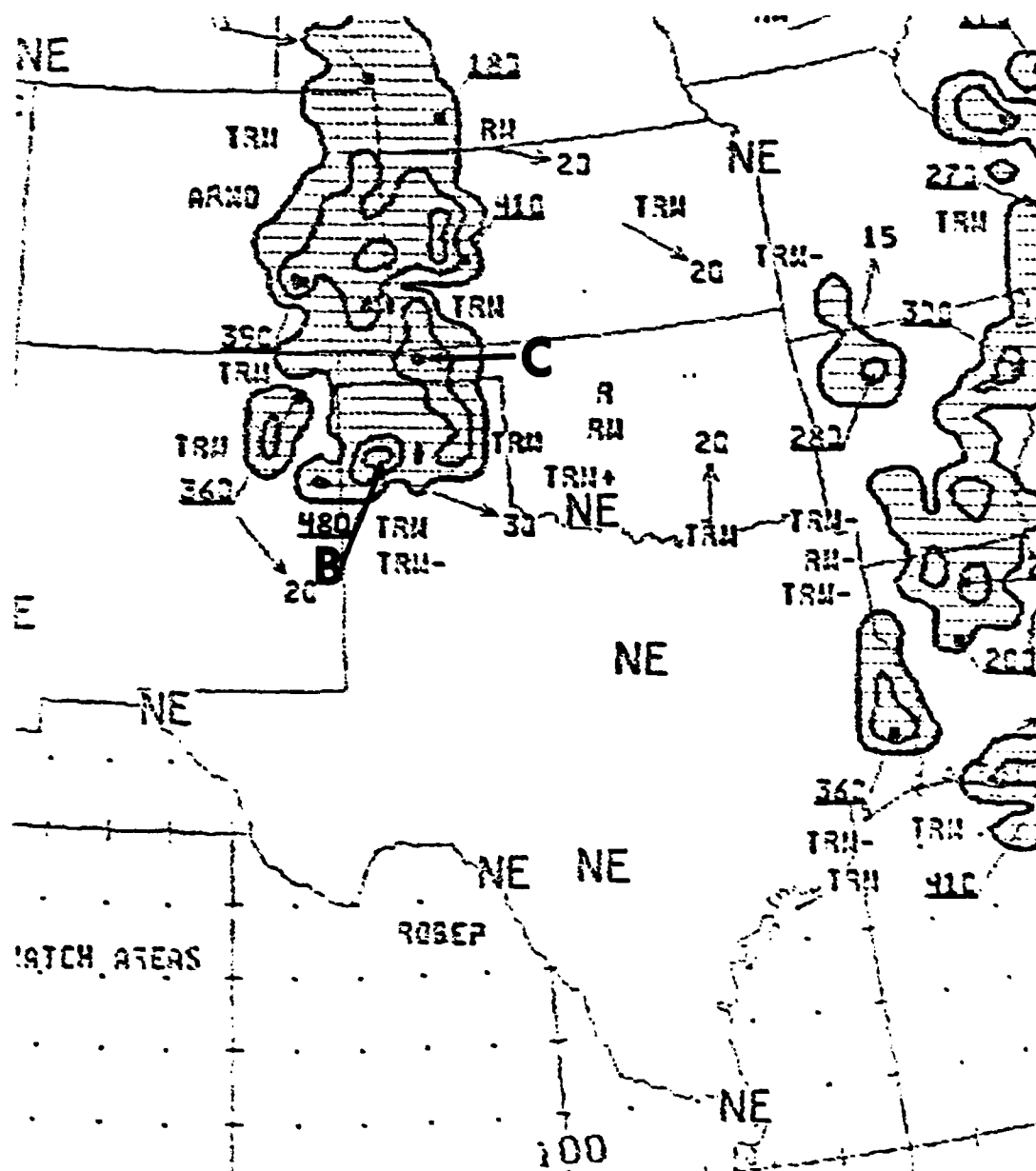


Fig. 18. Radar summary chart for 0835 GMT 26 June 1982. Shading indicates echo areas. Contours at echo intensities 1, 3, and 5; echo heights are in thousands of feet; cell movement given at end of arrows in knots; area and line movement given by pennant with full barb = 10 kt (U. S. Department of Commerce, 1981). Cell "B" was the highest cell along the gust front. Cell "C" had the coldest cloud-top temperature in the area.

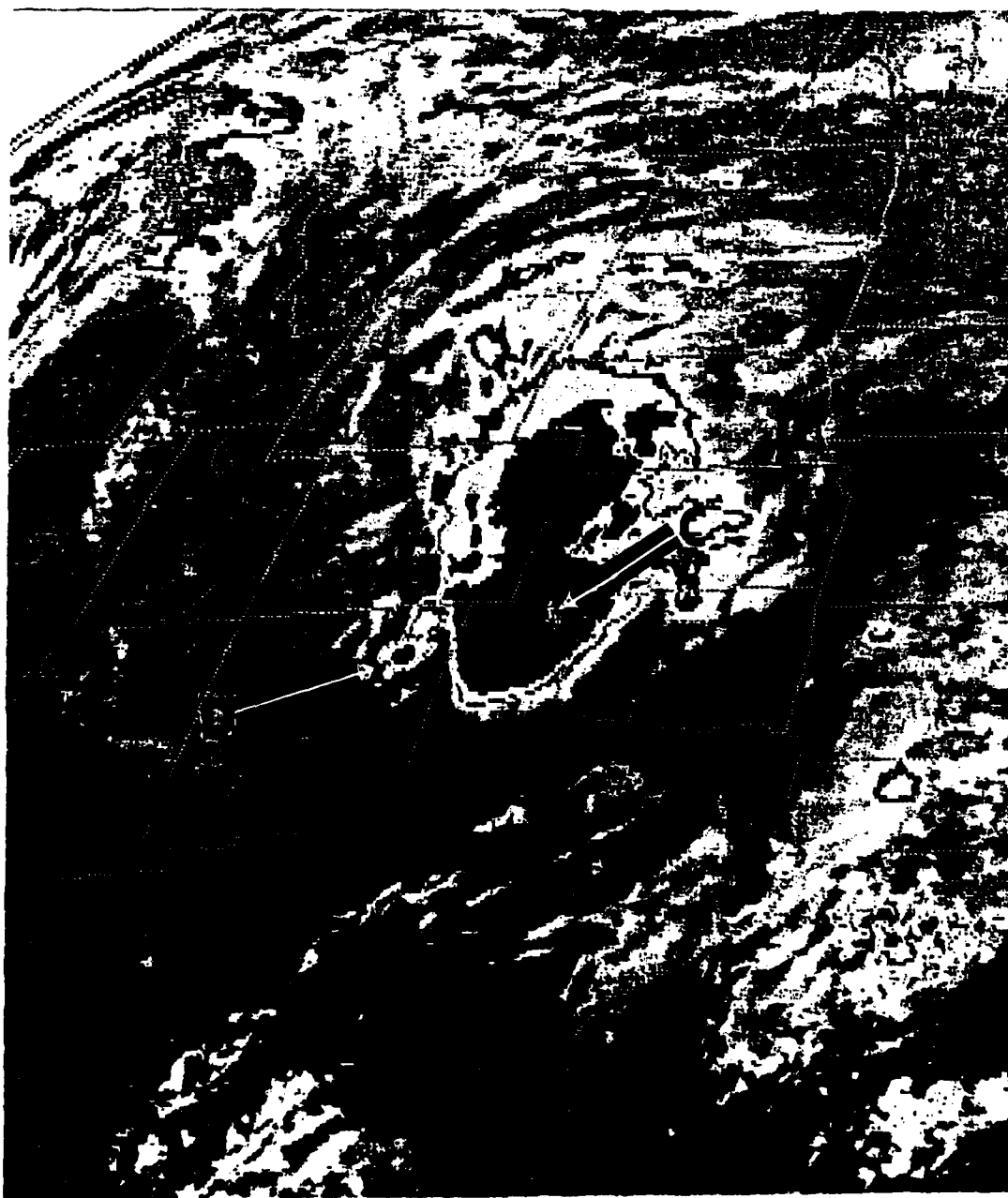


Fig. 19. GOES infrared image with MB enhancement at 0830 GMT 26 June 1982. Area "C" indicates overshooting tops. A new cell, "D", was moving eastward.

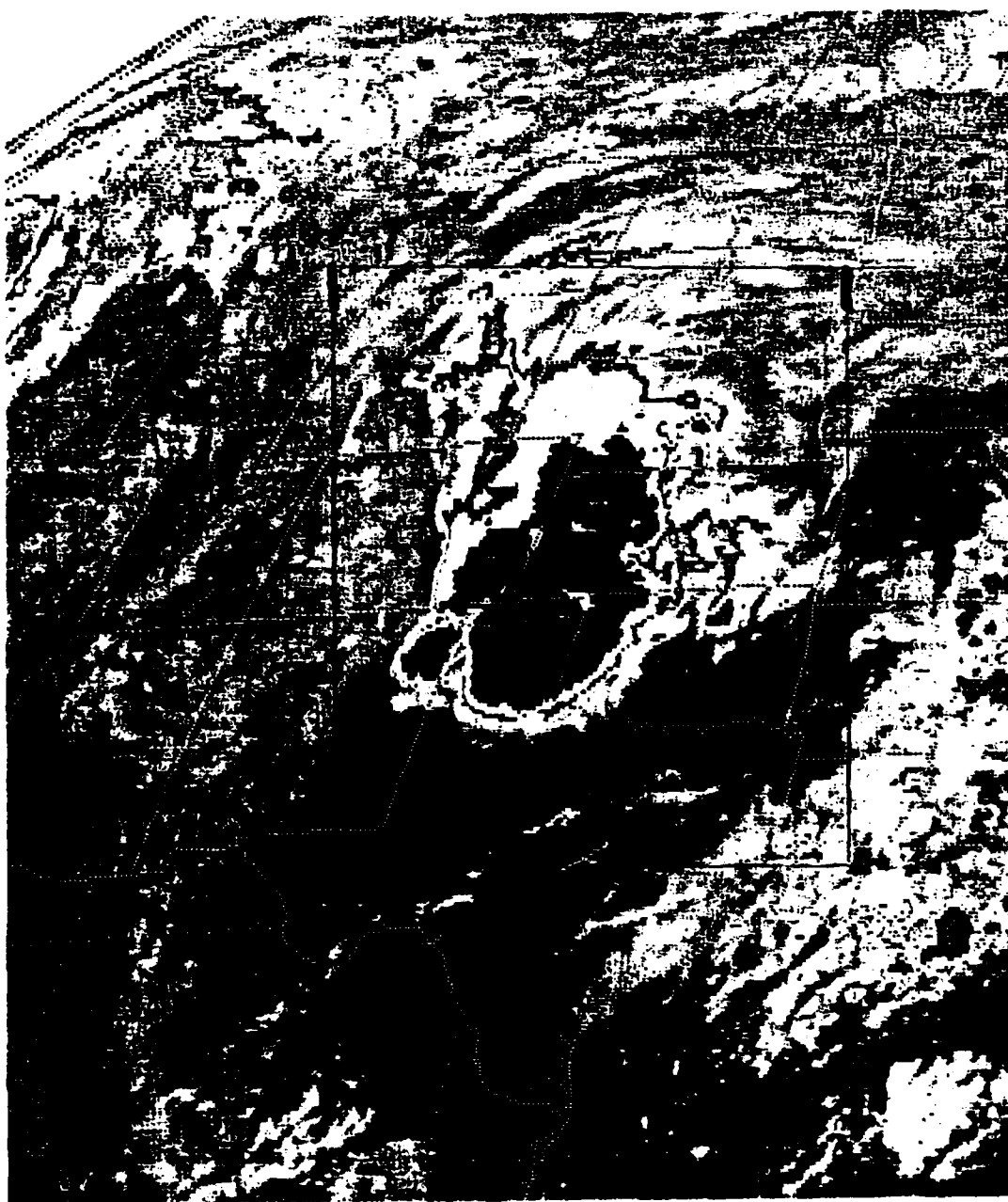


Fig. 20. GOES infrared image with MB enhancement at 1000 GMT 26 June 1982.

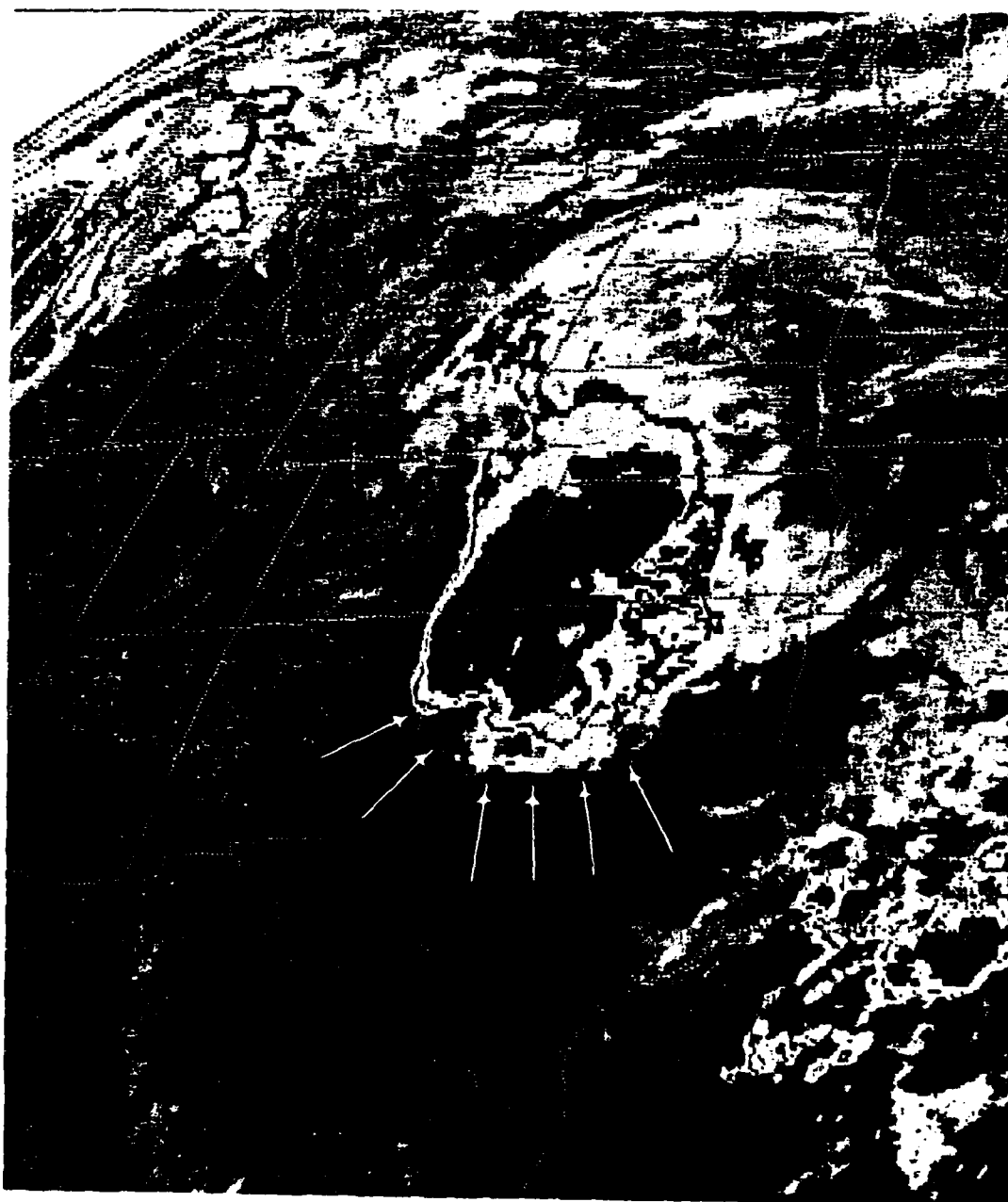


Fig. 21. GOES infrared image with MB enhancement at 1201 GMT 26 June 1982. The arrows point out the first arc cloud.

developed to the lee of the Rockies and moved eastward with an upper-level short-wave trough. In the area where the MCS formed, the troposphere was undergoing destabilization due to differential advection, with cold advection above a level of about 550 mb and warm advection below this level. As observed in the satellite imagery, the areal extent of the coldest cloud enlarged, followed by the appearance of overshooting tops. The downdraft and associated gust front were formed near the time the overshooting tops appeared, because soon afterward a surface mesohigh and arc-shaped line of precipitation along the gust front were detected. The location of the gust front correlated well with the location of the greatest IR temperature gradient in the satellite imagery. The heaviest precipitation was associated with convection just to the rear of the gust front while the gust front was under the MCS cloud shield. In other words, the parent storm which produced the downdraft and gust front was not detected in the radar charts as an area of heavier precipitation. Convection formed along the gust front at different times during its life, thus a chain of storm events occurred. The pattern of precipitation was similar to that observed in tropical squalls, i.e., a region of more stratiform precipitation trailed a squall line. As the squall line moved out from under the MCS cloud shield, it decayed into isolated cells. Soon afterward, the areal extent of the coldest cloud tops decreased and an arc cloud appeared. It moved as a dry gust front until it encountered areas favorable for convective development, as will be discussed later in this paper.

Conditions Leading to the Second Arc Cloud

A sequence of events similar to that of the first arc cloud is involved with the second surge. In the preceeding section it was noted that the areal extent of cold tops decreased from 1000 to 1200 GMT over the central and eastern Texas Panhandle. Also note in Figs. 19-21 the development and eastward movement of a convective cell (marked "D" in Fig. 19) across the New Mexico-Texas border which resulted in an increase of cold cloud top coverage over the western Texas Panhandle. This cell developed along the foothills of the New Mexico Rockies, moved eastward, and collided with the gust front which had passed Tucumcari between 0900 and 1000 GMT. The gust front did not travel much farther west, probably due to the increasing terrain elevation. Its location is identified with a cold front symbol in the 1200 GMT surface analysis (Fig. 22). The second gust front is found in the northern Texas Panhandle. Note that it too is along the edge of a surface mesohigh. It can be seen in Fig. 21 that the southern portion of this second gust front is beneath an area of large IR temperature gradient. The white center ($T < -64^{\circ} \text{C}$) in Fig. 21 between Tucumcari and Amarillo denotes the overshooting top which first appeared at 1130 GMT.

At 1200 GMT the highest (and coldest) tops of the MCS (from Fig. 21) were no longer located along and to the rear of a 500 mb short-wave ridge, but were found along the short-wave trough which was located over the Texas Panhandle, extending to eastern Wyoming (Fig. 23). The temperature trough was still somewhat to the west of the ACC. The amplitudes of both the thermal and height waves were

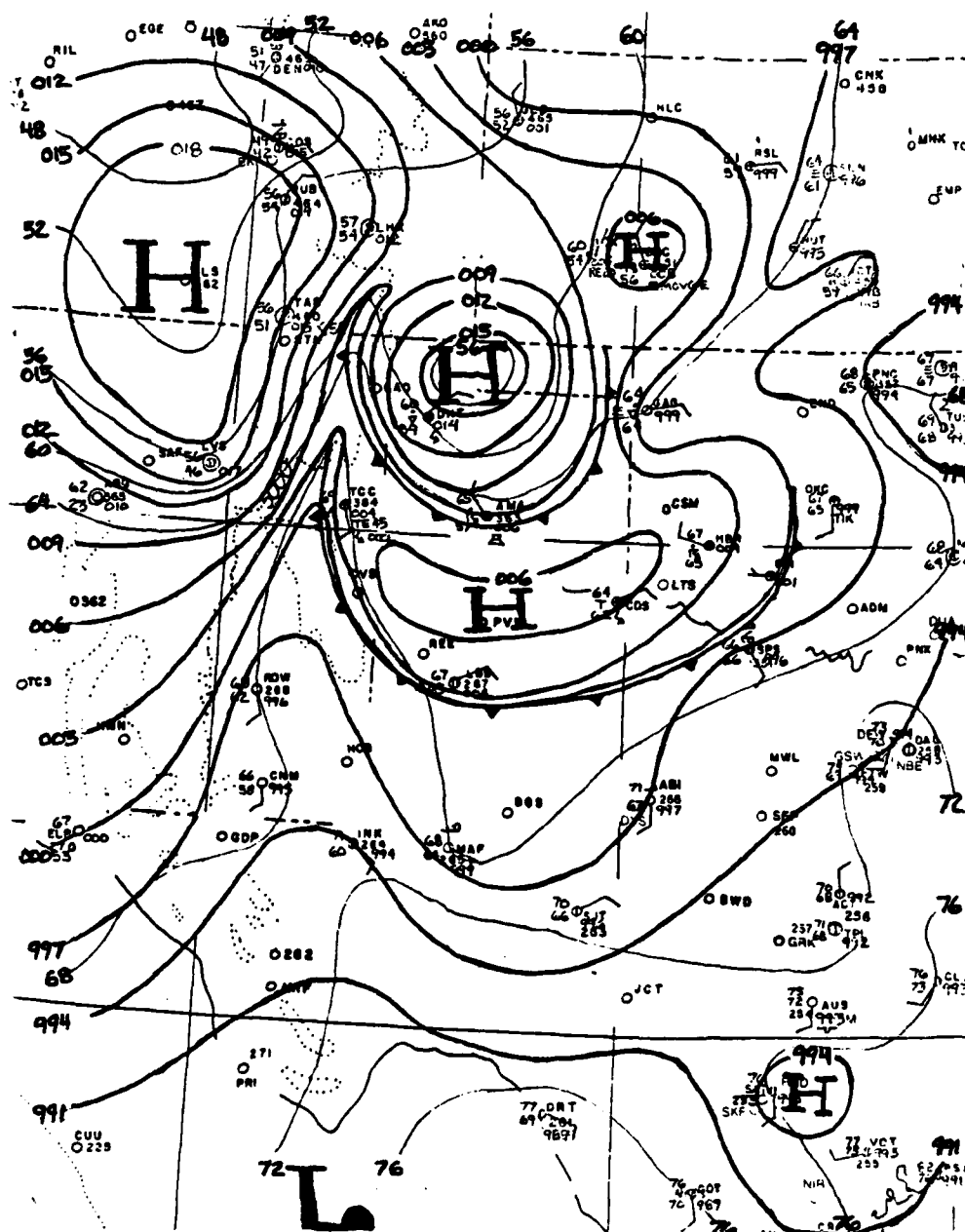


Fig. 22. Surface temperature and pressure fields for 1200 GMT 26 June 1982. Altimeter setting contours (thick lines) are every 0.03 in Hg; isotherms (thin lines) are every 4°F. The gust fronts are denoted by cold front symbols.

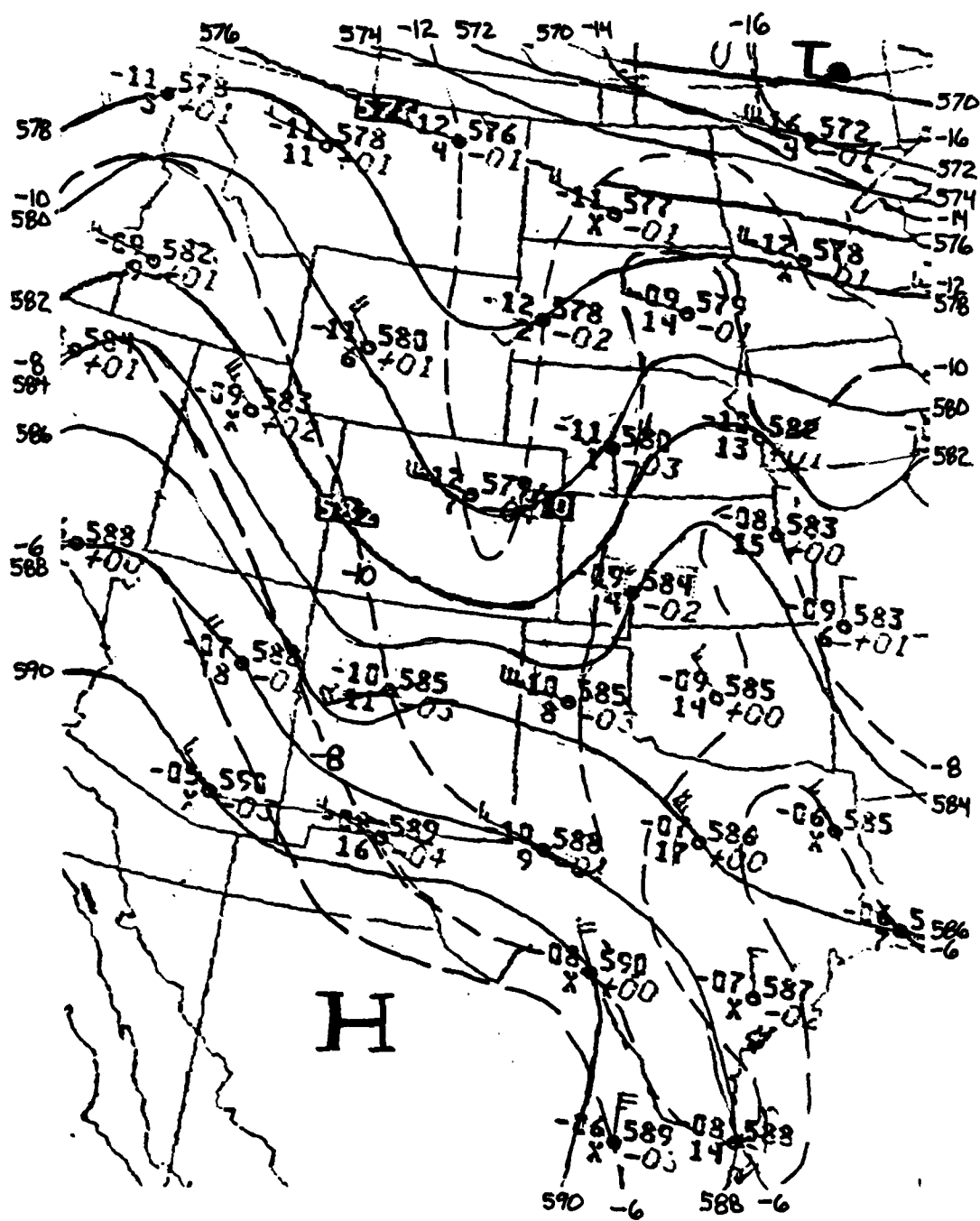


Fig. 23. 500 mb height (dm) and temperature (°C) for 1200 GMT 26 June 1982. Height contours (solid lines) are every 20 m; isotherms (dashed lines) are every 2°C.

greater than they were 12 h prior. Thus, colder air was still being advected from the west into eastern New Mexico and west Texas.

Amarillo's temperature was 3°C lower than 12 h earlier.

Significant changes were evident at 300 mb (Fig. 24). The warm-core high now centered over Dodge City, Kansas, had become warmer. Its axis ran from the eastern Texas Panhandle to Western Kansas. This axis was along the major axis of the storm area as a whole. More specifically, the axis was along the eastern side of the region of highest cloud tops, as can be seen in Fig. 21. It would appear to represent an updraft region in the storm. The flow over the ACC at 200 mb had become even more diffluent indicating continued upper-level outflow from the storm. Over Amarillo at 200 mb the winds were southwest at 25 kt while over Midland winds were northwest at 25 kt.

At 700 mb the short-wave ridge extended from Altus, Oklahoma to central Nebraska. The highest cloud tops were located along the inflection point of the ridge and trough. The amplitude did not change much over the previous 12 h, but the trough did move southeast. The 700 mb winds at both Amarillo and Midland veered with respect to the 850 mb winds, indicating warm-air advection throughout this layer, and continued tropospheric destabilization due to differential advection. Midland's wind speed increased from 10 kt at 700 mb to 30 kt at 850 mb. The 850 mb analysis is shown in Fig. 25. The presence of the 30 kt south wind over Midland at 850 mb was significant. A mois (dew point depression of 3°C) low-level jet had developed in west Texas. Note that the wind maximum is above the nocturnal

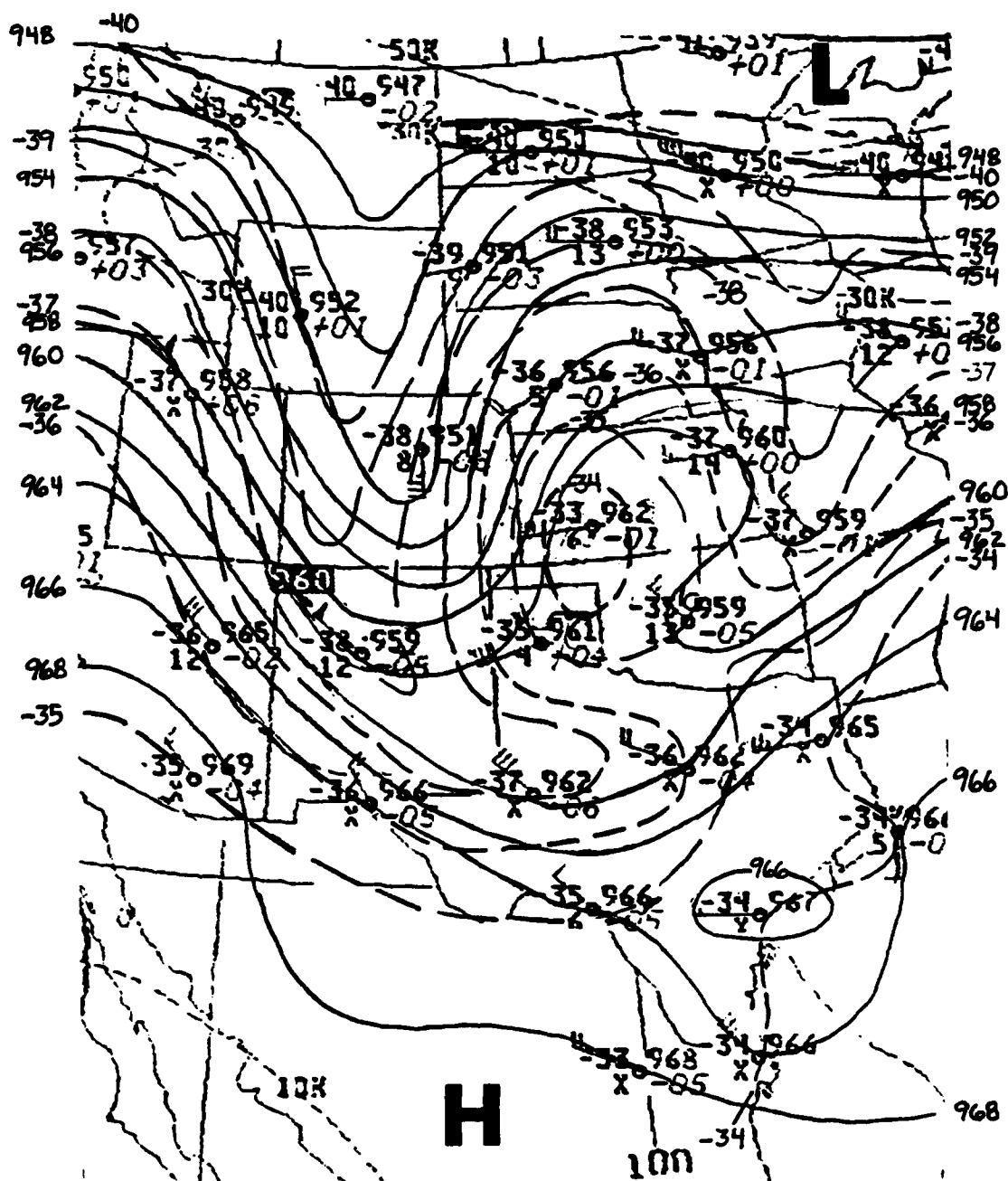


Fig. 24. 300 mb height (dm) and temperature (°C) for 1200 GMT 26 June 1982. Height contours (solid lines) are every 40 m; isotherms (dashed lines) are every 1°C.

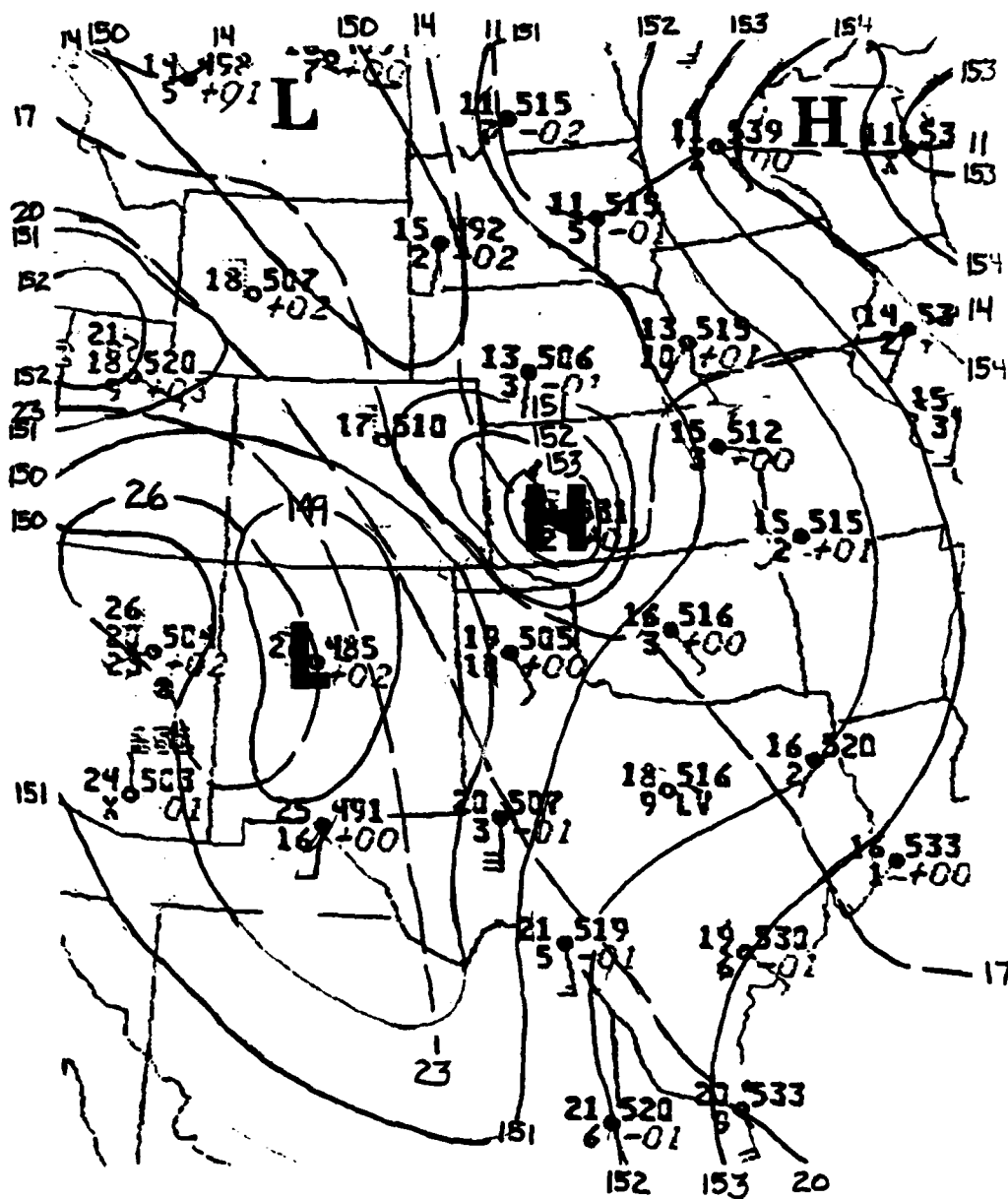


Fig. 25. 850 mb height (dm) and temperature (°C) for 1200 GMT 26 June 1982. Height contours (solid lines) are every 10 m; isotherms (dashed lines) are every 3°C.

inversion over Midland in Fig. 26. Latent instability was indicated from 780-880 mb. This instability could have extended to the surface with daytime heating. The discussion in the following paragraphs shows that this jet was feeding the convection in the center of the ACC. Deep convection near Midland occurred later in the day where this jet was flowing over the ACC boundary. Another feature worth noting in Fig. 25 is the cold-core mesohigh located over western Kansas most likely due to downdraft and outflow. Also note that the wind is northwesterly at 50 kt. The mesohigh also is resolved in the surface analysis (Fig. 22).

An examination of the McIDAS-derived fields of divergence and equivalent potential temperature (θ_e) helps to determine the source of the cold air within the ACC and the source of the updraft air within the ACC parent storm. The θ_e of an air parcel is conserved during both dry and saturated adiabatic processes, thus making it an excellent tracer. Figs. 27 and 28 represent analyses of horizontal divergence and θ_e , respectively. A leading digit, 3, is missing from the θ_e values. Lines of equal divergence values are drawn at an increment of $1 \times 10^{-5} \text{ s}^{-1}$. The wind was not adjusted for topographical influences. Because the objective analysis used synoptic data, only meso-alpha (Orlanski, 1975) scale features, which range in size from 200-2000 km, can be resolved.

It is hypothesized that the updraft air of the ACC parent storm originated near the Texas-Mexico border at low levels, moved northward across Texas in a low-level jet, then lifted to the 300 mb level within the ACC. This conclusion is based on the following features

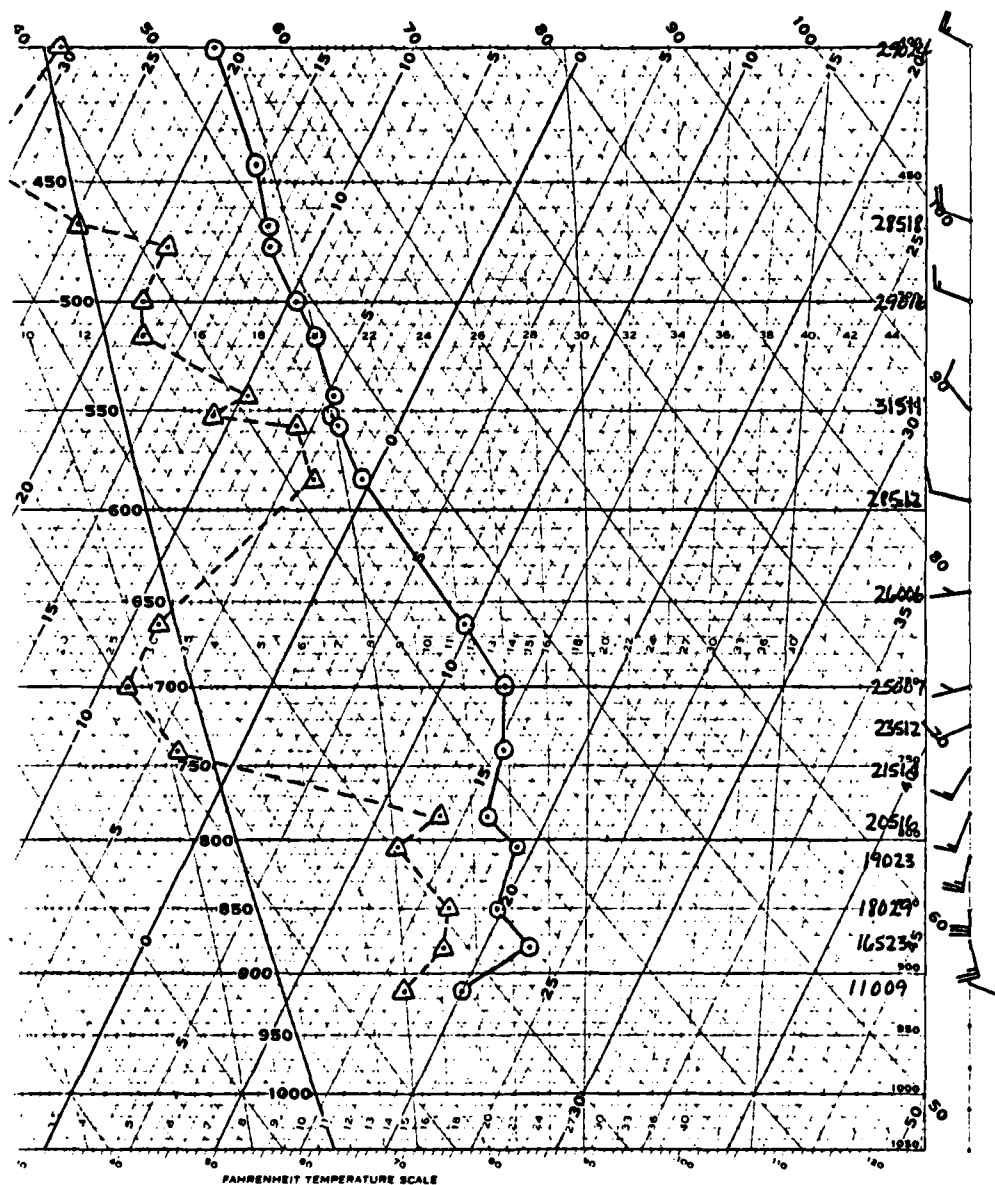


Fig. 26. Midland sounding at 1200 GMT 26 June 1982. Plot is on a skew-T log-P diagram.

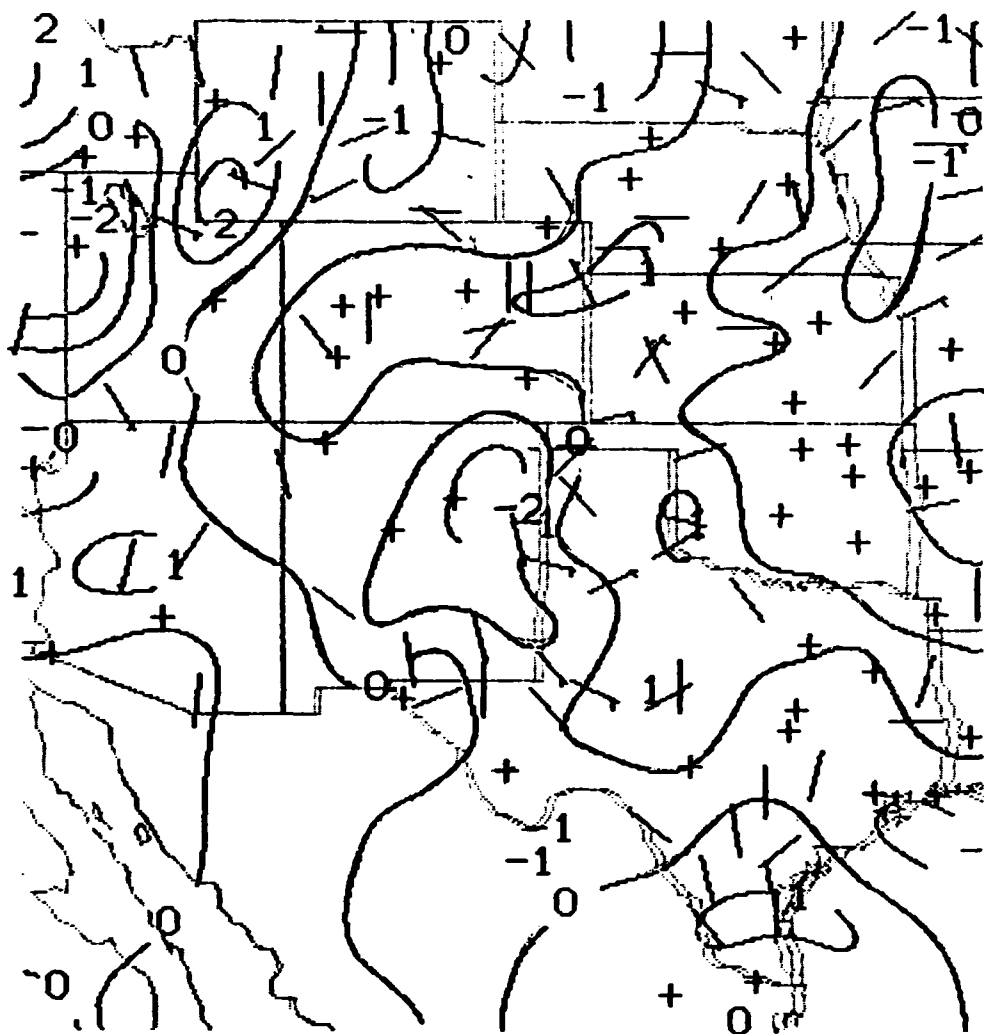


Fig. 27. Surface divergence for 1200 GMT 26 June 1982. Values are times 10^{-5} s^{-1} .

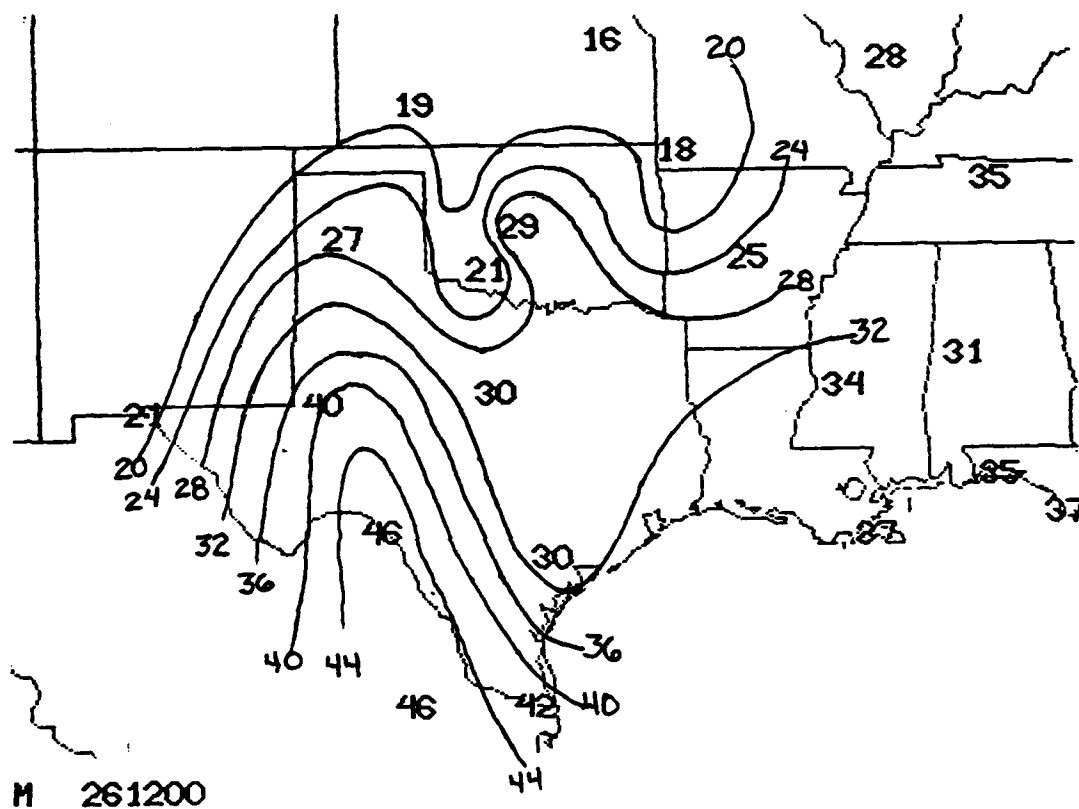


Fig. 28. 850 mb θ_e (K) for 1200 GMT 26 June 1982. The leading digit, 3, is missing from the values.

found in Figs. 27 and 28 and others to follow. Surface convergence is noted in Fig. 27 in the area along the Texas-New Mexico border. As was noted in Figs. 25 and 26, the southerly low-level jet was over this area. In Fig. 28, a tongue of higher θ_e values at 850 mb extends from Mexico, across West Texas, toward the Panhandle. Values at the northern extremity of this tongue ranged from 332 K to 336 K. The higher values ended abruptly in western Oklahoma at a pocket of low values associated with the first arc cloud (see Fig. 22). An axis of higher θ_e values at the surface along the Texas-New Mexico border is revealed in Fig. 29. As noted in Fig. 21, new convection was developing over the western half of the Panhandle. It is hypothesized that the low-level moisture streaming from the south into the convergent region in the western Panhandle and eastern New Mexico provided the ingredients needed to maintain the convection. In Fig. 30 it is seen that a divergence maxima appears over the northern Texas Panhandle at 300 mb with strong convergence to the west. As seen in Fig. 31, θ_e values over the Panhandle at 300 mb correspond to the θ_e values found in the tongue at 850 mb (Fig. 28). The interpretation applied to these observations is that the divergence maximum represents an updraft center. It already has been seen in Fig. 24 that there is a pocket of warmer temperatures in this same region. The strong convergence to the west is interpreted as a barrier effect produced by the flow from the west at this level encountering the ACC.

The source of the low-level cold air within the ACC is hypothesized to be near 700 mb just upstream of the parent

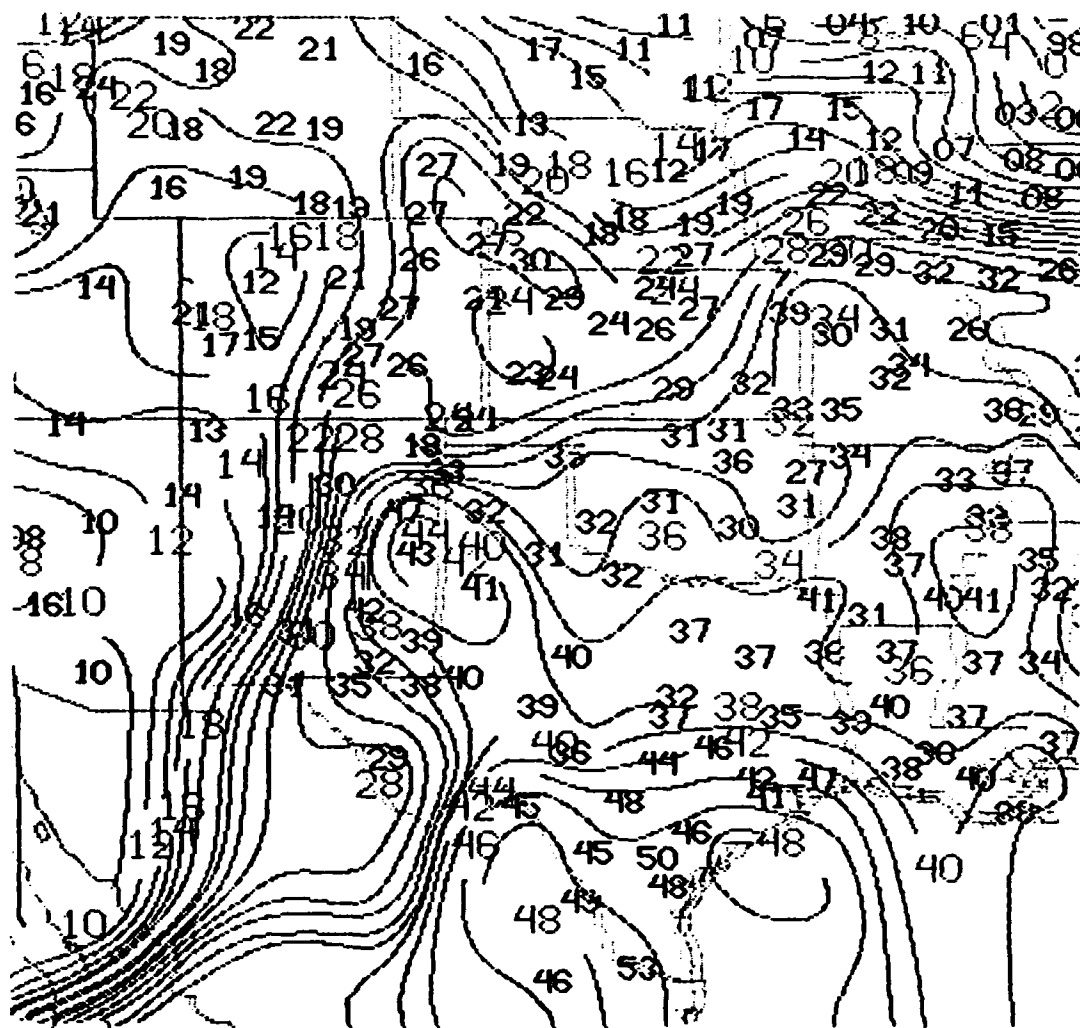


Fig. 29. Surface θ_e (K) for 1200 GMT 26 June 1982. The leading digit, 3, is missing from the values.



Fig. 30. 300 mb divergence overlaid upon GOES image for 1200 GMT 26 June 1982. Values are times 10^{-5} s^{-1} .

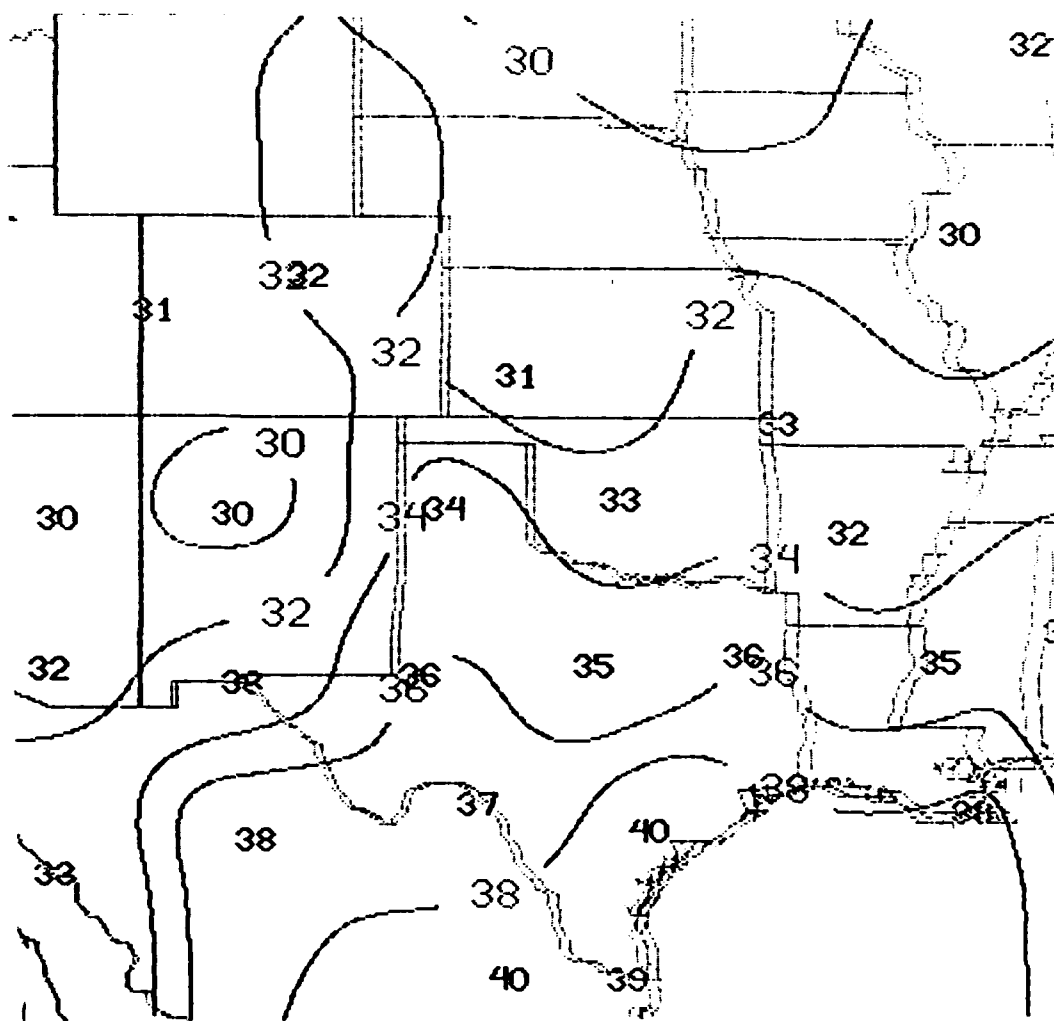


Fig. 31. 300 mb θ_e (K) for 1200 GMT 26 June 1982. The leading digit, 3, is missing from the values.

thunderstorm, where θ_e values (Fig. 32) ranged from 326-330 K. Within the surface mesohigh (Fig. 22) located over the northern Texas and Oklahoma Panhandles, θ_e values correspond to those identified at 700 mb (Fig. 32). Convergence is found in this area at 700 mb (Fig. 33) while divergent flow is found at the surface (Fig. 34). These findings are similar to those of Mader (1979) which indicated that midlevel (3-6 km) air was the main source of the downdraft air responsible for strong surface outflow. He also noted that mid-level convergence may be characteristic of storms which produce a strong downdraft and subsequently strong outflow. Note that local maxima of divergence occurred behind the first arc cloud at the surface (labeled "E" in Fig. 34) and at 850 mb (Fig. 35).

The remarks portion of the airways reports can be very useful when analyzing for a gust front in surface charts. Goff (1976) explains that vertical motion diminishes as the air flows over the top of the gust front's leading edge. If the displaced air is moist enough the lifting action may be sufficient to produce a small roll cloud just above the head. When the outflow is close to the parent thunderstorm this cloud formation is often the shelf-like cloud connected to the thunderstorm. The remarks portion of the 1355 GMT report from Childress stated, "TRWU N-NE MOVG SLOWLY E/ROLL CLD N...". The 1400 GMT surface analysis (not shown) placed the second gust front about 25 km northeast of Childress. With passage of the second gust front the wind shifted from 100° at 6 kt (1400 GMT) to 310° at 18 kt (1500 GMT). Over this same period the altimeter setting rose 0.09 in of mercury.

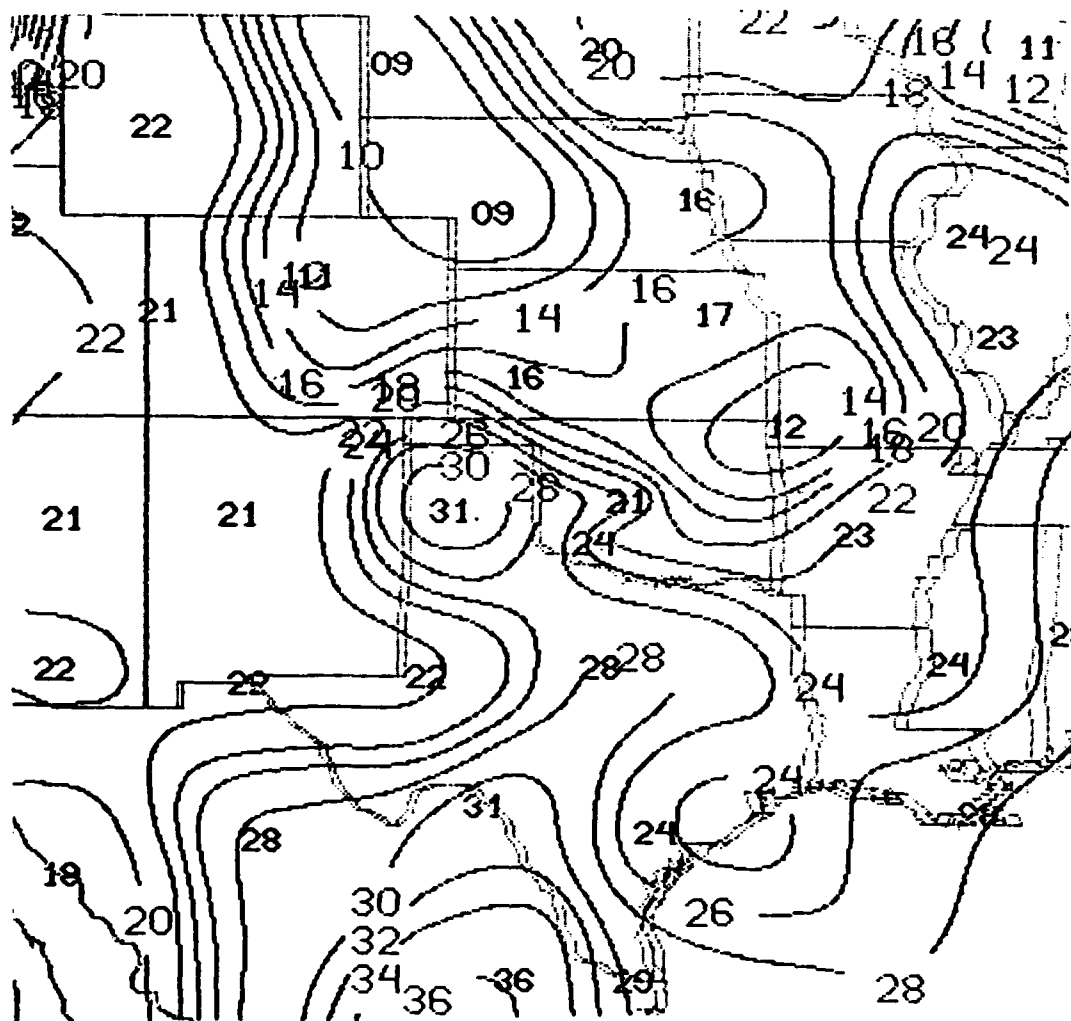


Fig. 32. 700 mb θ_e (K) for 1200 GMT 26 June 1982. The leading digit, 3, is missing from the values.



Fig. 33. 700 mb divergence overlaid upon GOES image for 1200 GMT 26 June 1982. Values are times 10^{-5} s^{-1} .

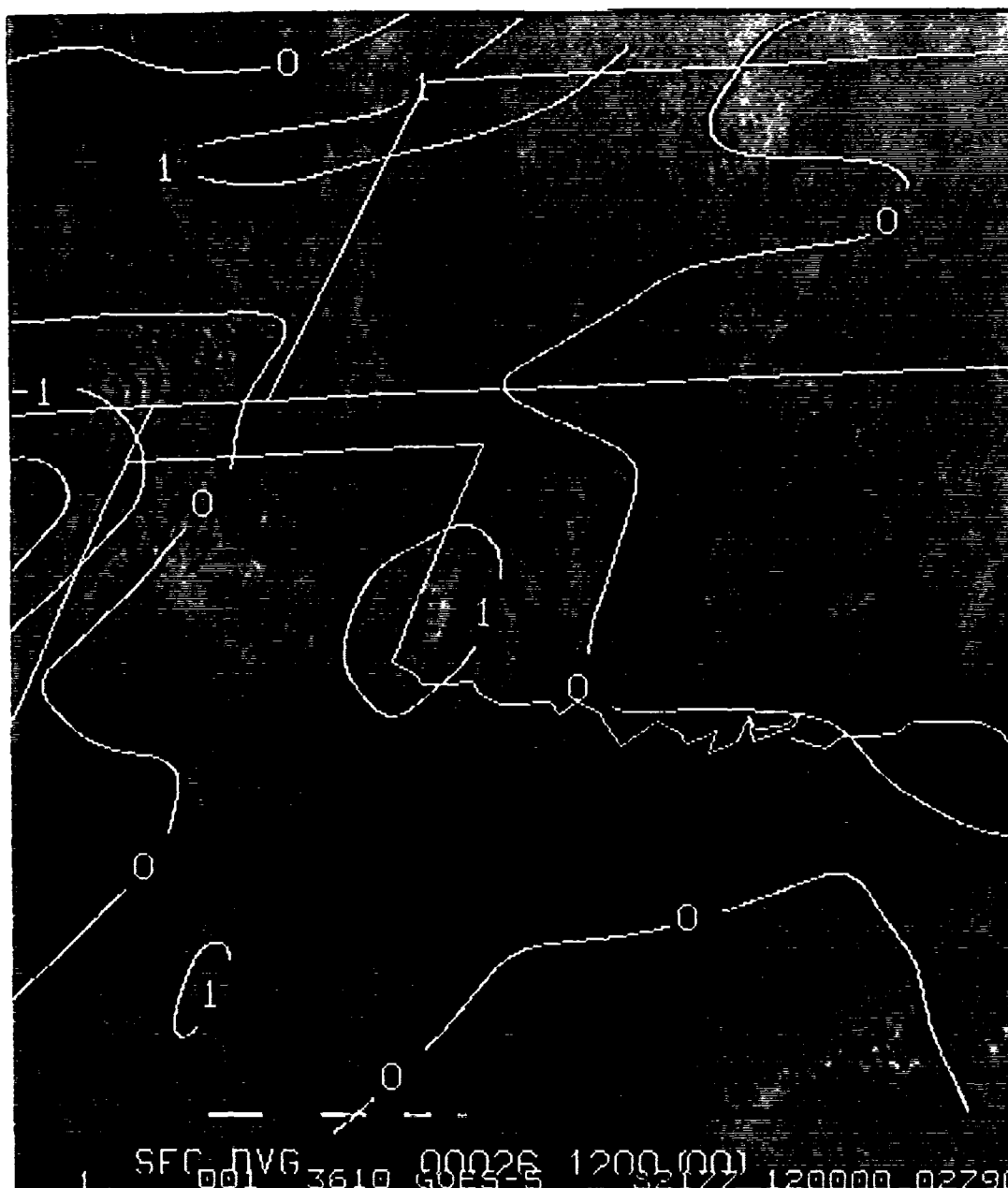


Fig. 34. Surface divergence overlaid upon GOES image for 1200 GMT 26 June 1982. Values are times 10^{-5} s $^{-1}$. A divergence maxima behind the first arc cloud is labeled "E".

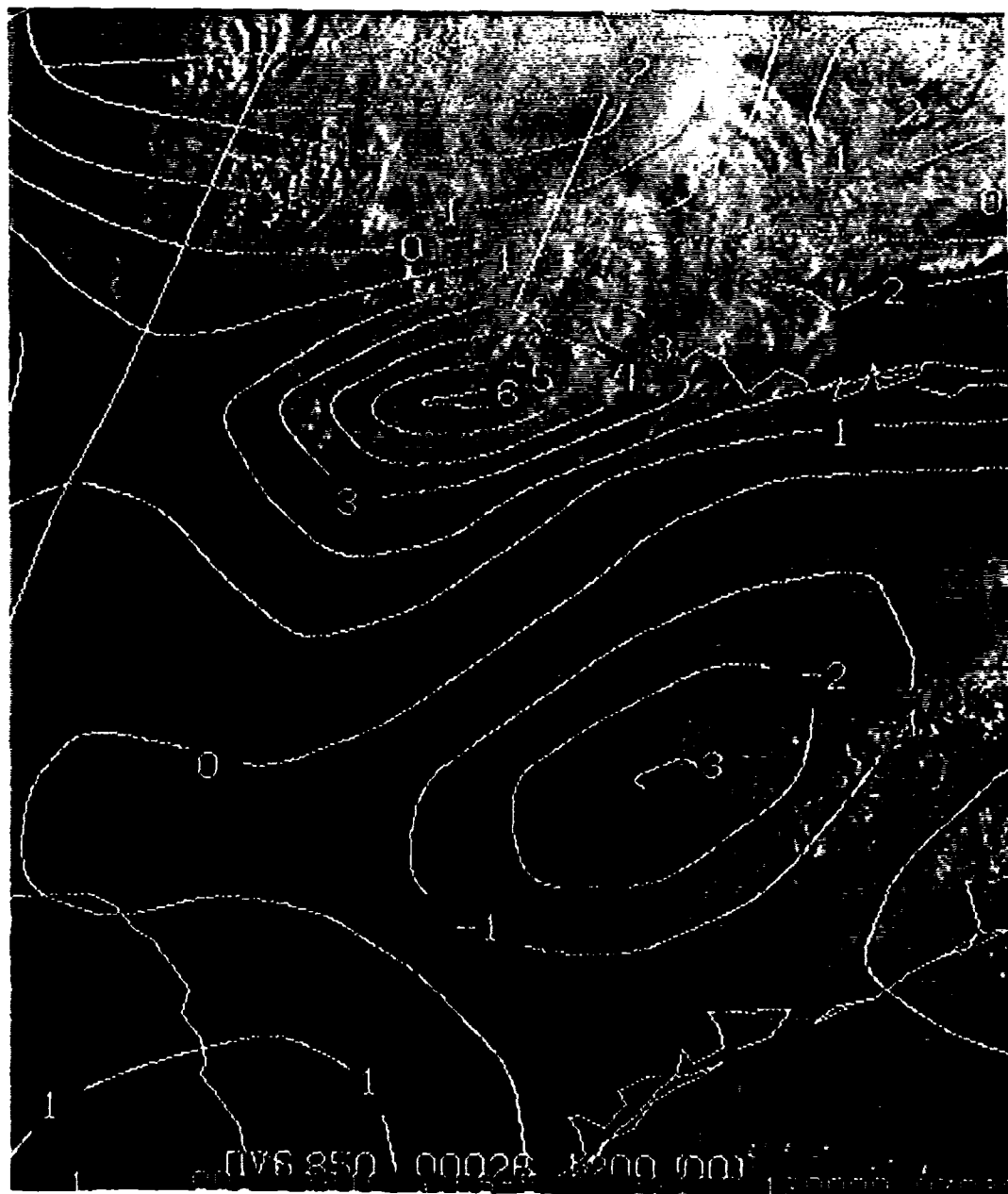


Fig. 35. 850 mb divergence overlaid upon GOES image for 1200 GMT 26 June 1982. Values are times 10^{-5} s^{-1} .

After 1400 GMT the areal extent of the cloud tops with coldest temperatures decreased significantly. The 1435 GMT radar chart (Fig. 36) indicated rain continuing to fall over the entire Texas and Oklahoma Panhandles. The strongest radar returns at this time (D/VIP=3) were located just behind the southeast portion of the second gust front. A surface divergence center within the MCS was located over the northeast Texas Panhandle behind the second gust front (Fig. 37). At the surface, lower θ_e values were located over the Texas Panhandle (Fig. 38). A surface convergence maximum is associated with the tongue of higher θ_e values along the Texas-New Mexico border, as it was earlier. By 1502 GMT, the second arc cloud (from "A" to "B" to "C" in Fig. 39) along with some partial clearing (labeled "D") behind it, was evident in the visual/IR composite GOES image. The change in the cloudiness was probably due to subsidence associated with the horizontal divergence near the surface. In Fig. 39, clouds with $T > -43^\circ \text{C}$ are not "enhanced" and appear as they would in any visual imagery. Cloud tops colder than -43°C are enhanced just as they would be when MB enhancement is used. This enhancement scheme is ideal for ACC investigation. The lower, warmer clouds which make up the arc cloud show up better in the visual than the IR imagery, while the enhancement of overshooting tops remains.

At 1600 GMT the divergence field (Fig. 40) centered in the Texas Panhandle, the packing of the surface isotherms (Fig. 41) behind the arc cloud, the pattern of θ_e (Fig. 42) within the ACC and at its edge, and the arc cloud location in the GOES image (Fig. 43), all correspond well with the pattern expected within outflow air. The largest θ_e

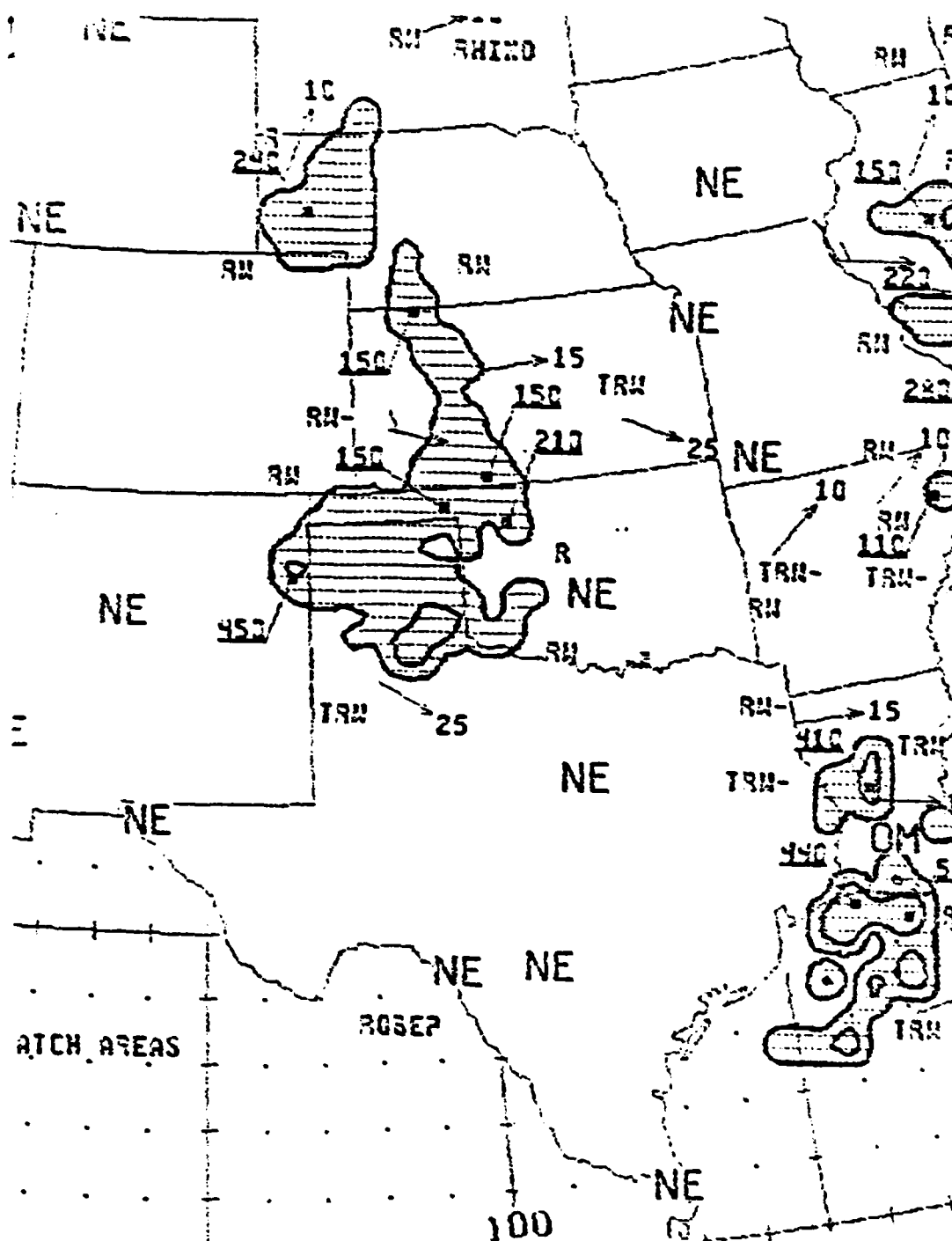


Fig. 36. Radar summary chart for 1435 GMT 26 June 1982. Shading indicates echo areas. Contours at echo intensities 1, 3, and 5; echo heights are in thousands of feet; cell movement given at end of arrows in knots; area and line movement given by pennant with full barb = 10 kt (U. S. Department of Commerce, 1981).

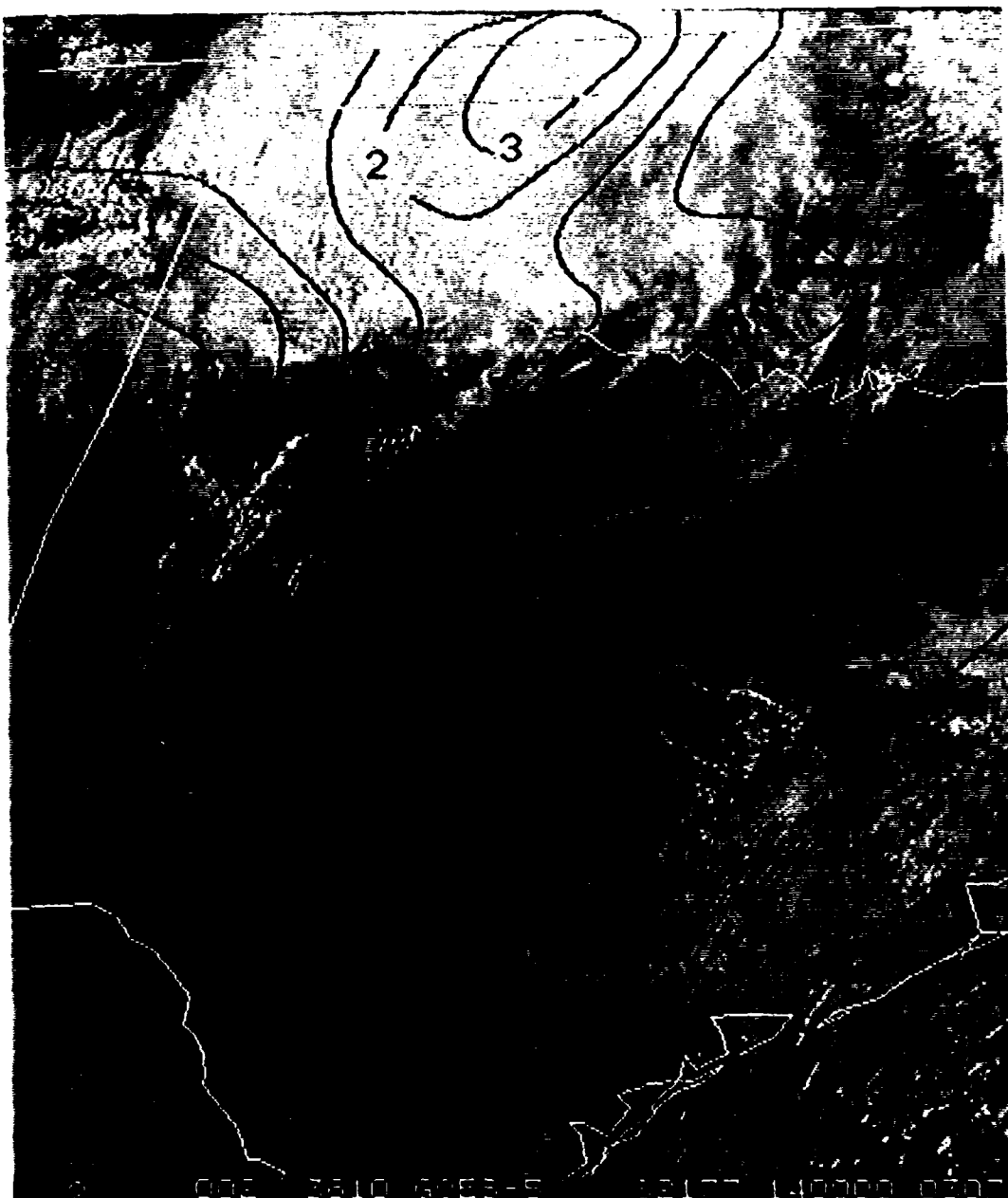


Fig. 37. Surface divergence overlaid upon GOES image for 1400 GMT 26 June 1982. Values are times 10^{-5} s^{-1} .

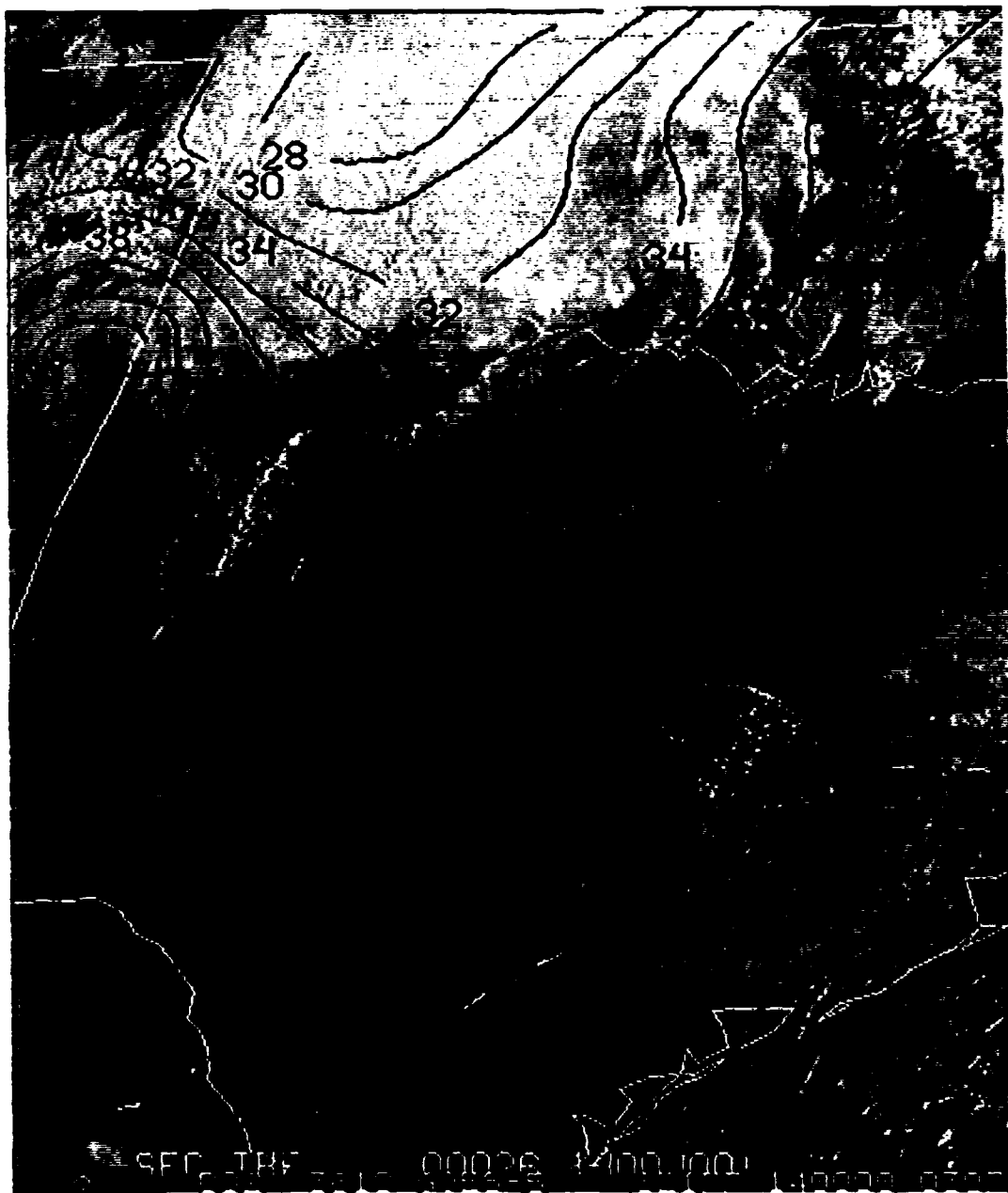


Fig. 38. Surface Θ_e (K) overlaid upon GOES image for 1400 GMT 26 June 1982. The leading digit, 3, is missing from the values.

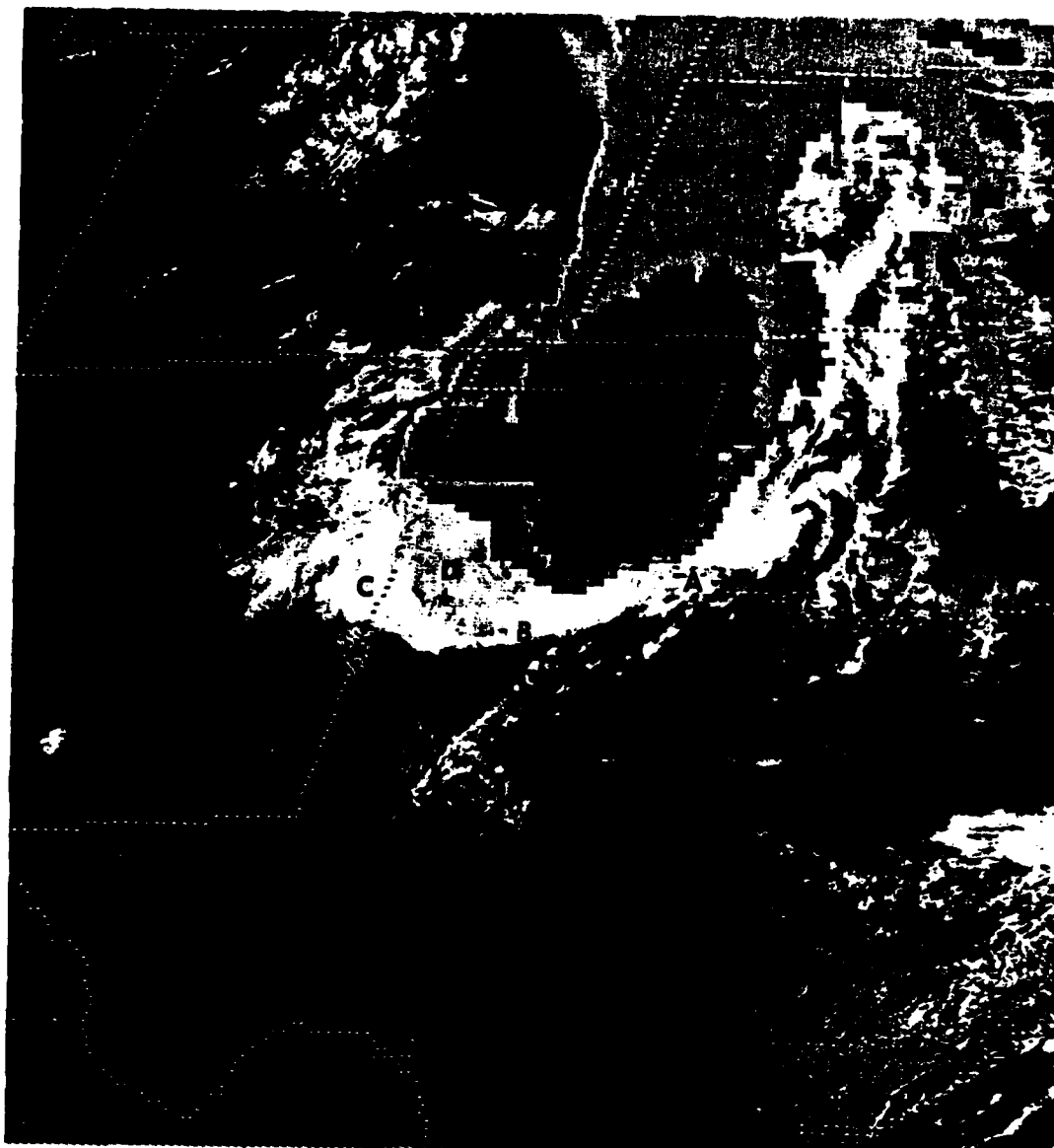


Fig. 39. GOES IR/Visual composite (C9 enhancement) for 1502 GMT 26 June 1982. The second arc cloud extended from "A" to "B" to "C". Partial clearing behind the arc cloud is evident at "D".

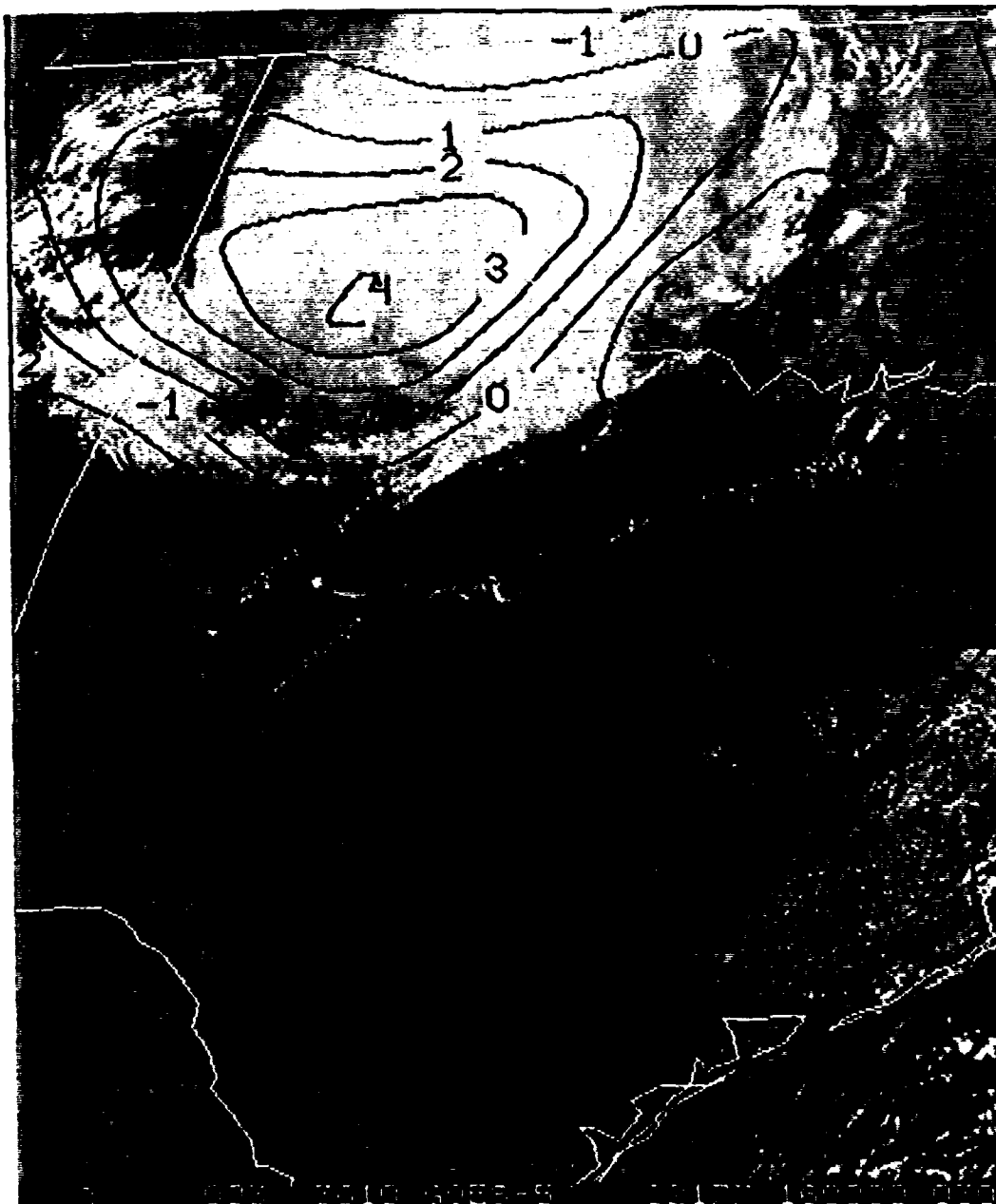


Fig. 40. Surface divergence overlaid upon GOES image for 1600 GMT 26 June 1982. Values are times 10^{-5} s^{-1} .

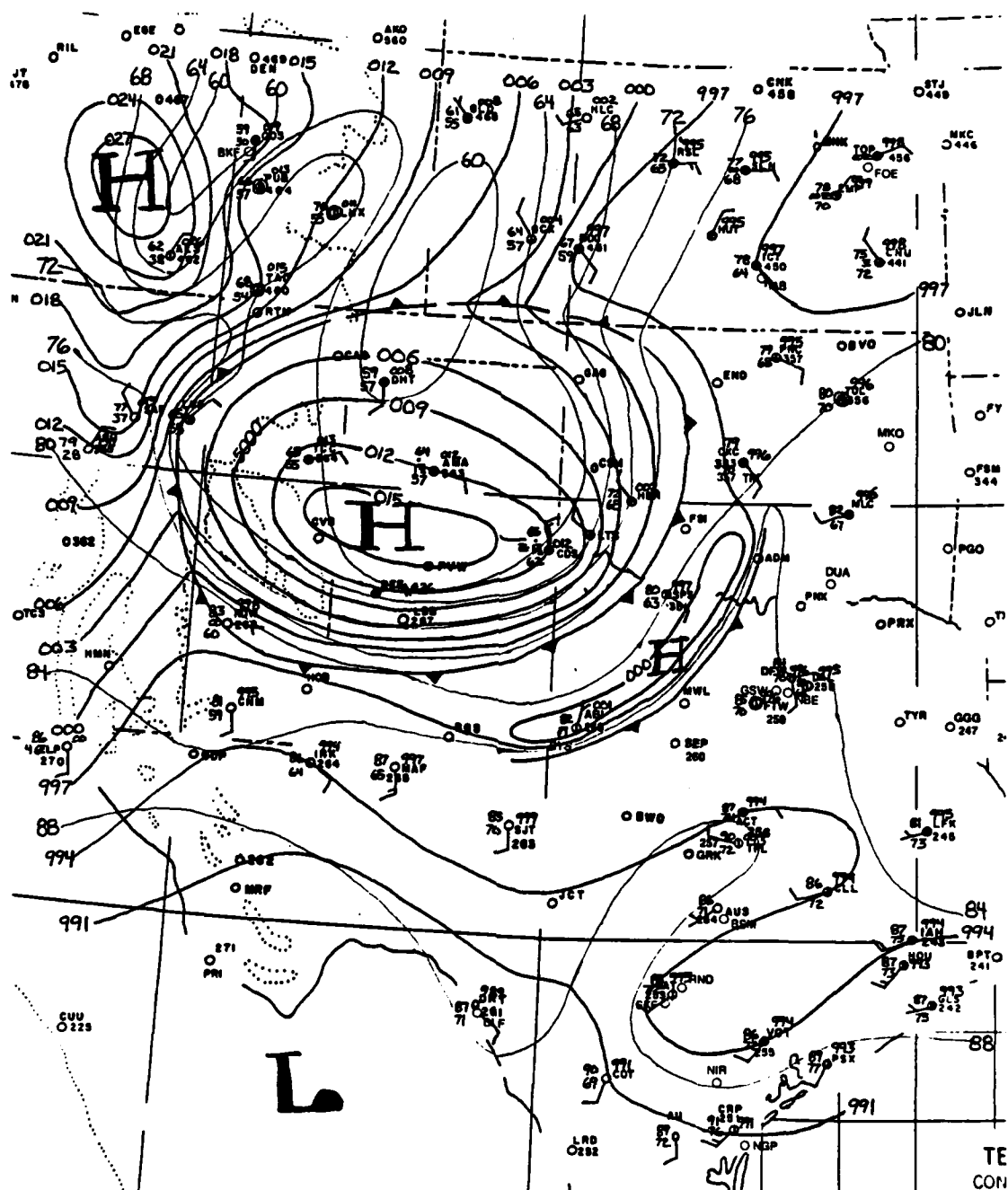


Fig. 41. Surface temperature and pressure fields for 1600 GMT 26 June 1982. Altimeter setting contours (thick lines) are every 0.03 in Hg; isotherms (thin lines) are every 4°F. The gust fronts are denoted by cold front symbols.

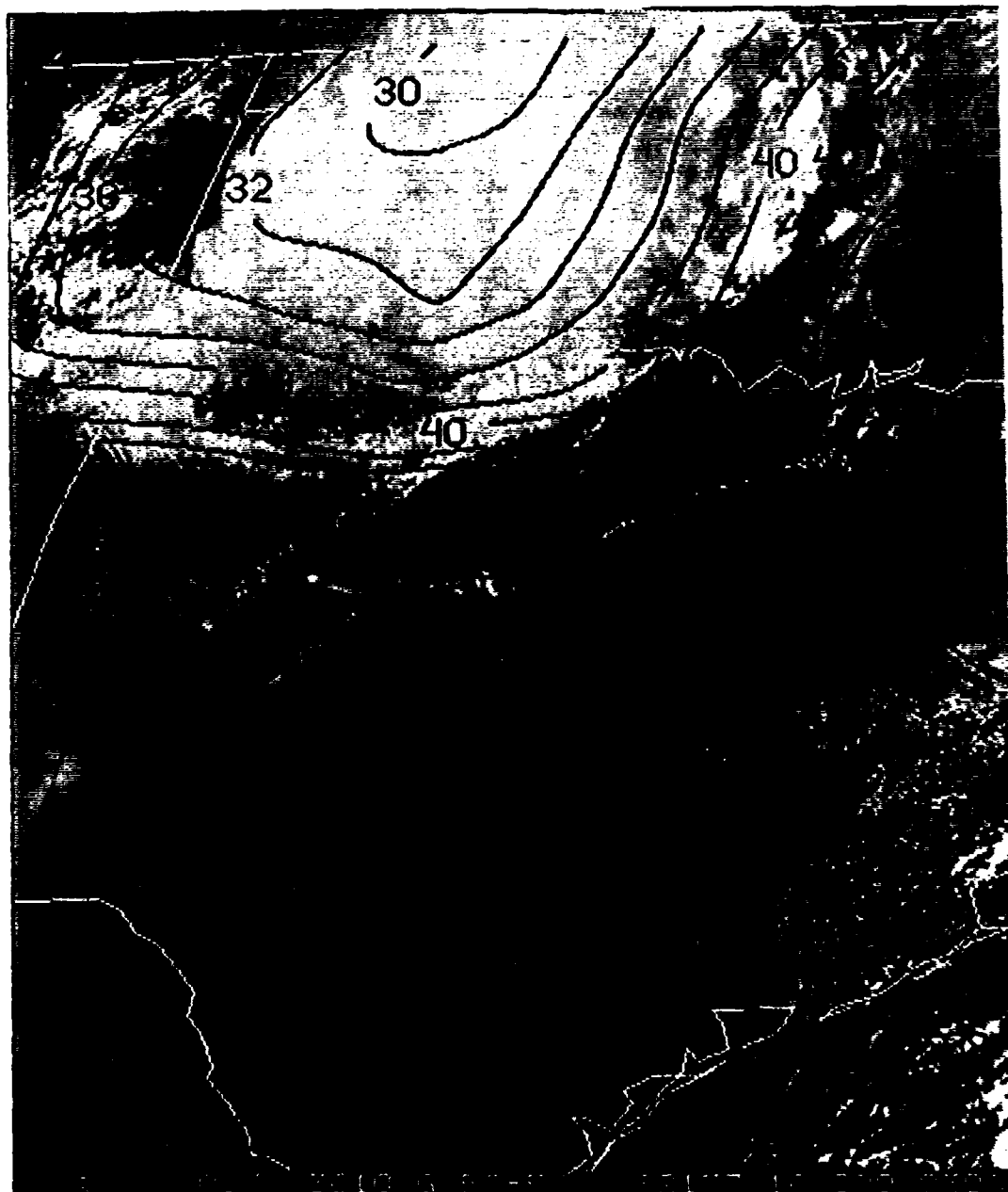


Fig. 42. Surface Θ_e (K) overlaid upon GOES image for 1600 GMT 26 June 1982. The leading digit, 3, is missing from the values.



Fig. 43. GOES IR/Visual composite (C9 enhancement) for 1602 GMT 26 June 1982.

gradients at this time were along the arc cloud. In addition, a band of θ_e isolines with smaller packing extended from the High Plains to the Texas-Louisiana border. Convection developed along this line later in the afternoon. It was at about this time that the ACC began to dissipate.

Over the period from 1700-1800 GMT the only area within the ACC with cloud tops at temperatures less than -59°C was over Hereford, southwest of Amarillo. This area corresponded to the largest rainfall rate in the area, the mesohigh center in the surface pressure analysis, low θ_e values, the surface divergence center, and strongest radar returns (cell "F" in Fig. 44). It is also evident in Fig. 44 (also see Fig. 41) that the arc cloud was acting as a thunderstorm trigger mechanism. Three cells ("A", "B", and "C") were evident along the eastern portion of the arc cloud, another cell ("D") along the western portion, and a fifth cell ("E") along the northern portion. Just to the west of the active cells along the eastern portion of the arc cloud, the θ_e values decreased by 2°K over the 2-h period from 1600-1800 GMT (Fig. 45). Convergence continued ahead of the entire gust front at the surface, and a center of divergence appeared over the south-central Texas Panhandle. The outflow of colder, dryer air from the original MCS was probably strong in this area. The main storm area of the ACC continued to dissipate.

An interesting feature appeared in the 1902 GMT image (surrounding "G" in Fig. 46) due to the stabilizing influence of the outflow air within the ACC. The cool, stably-stratified layer is ideal for the formation of banded clouds due to Helmholtz-type gravity

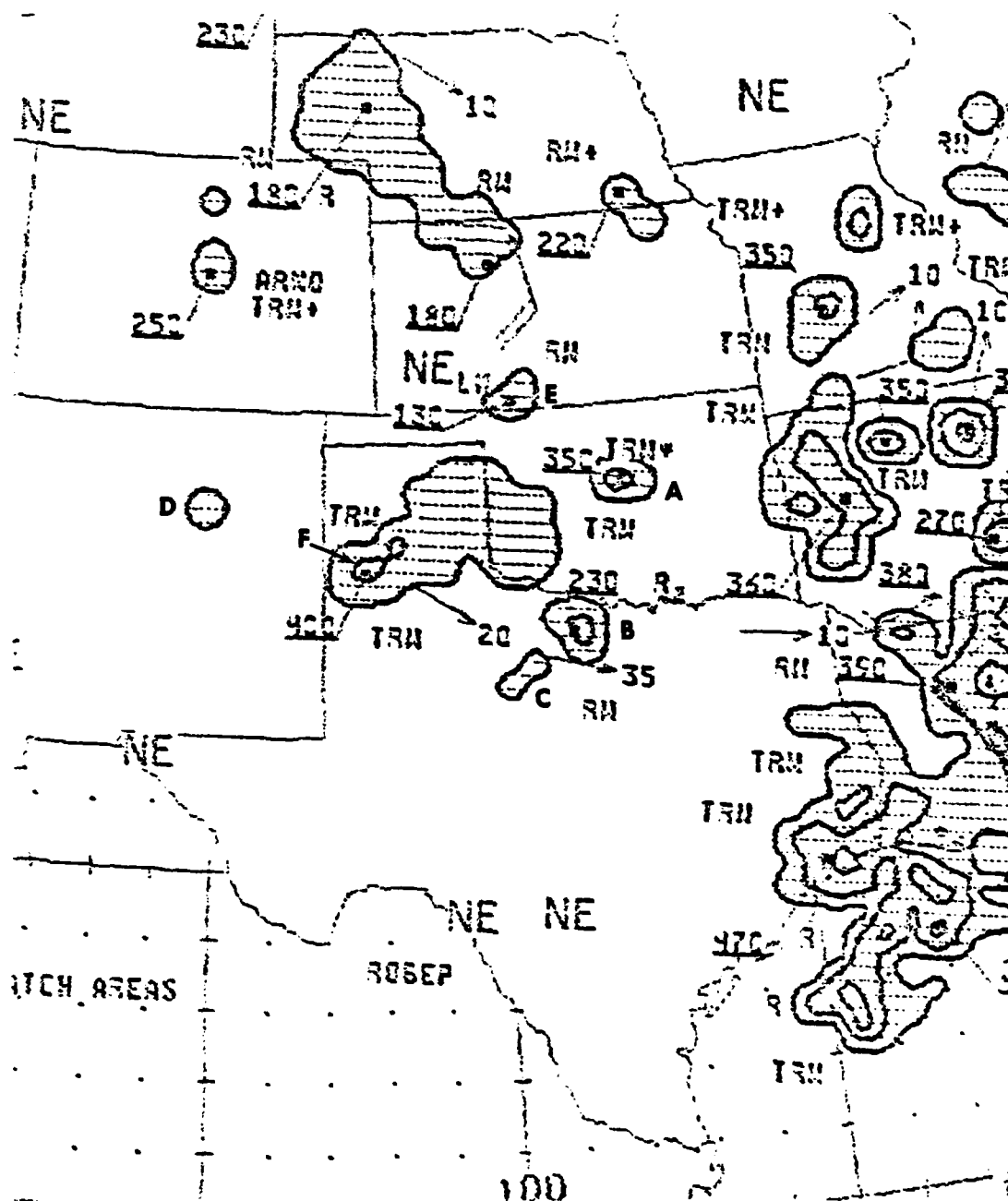


Fig. 44. Radar summary chart for 1735 GMT 26 June 1982. Shading indicates echo areas. Contours at echo intensities 1, 3, and 5; echo heights are in thousands of feet; cell movement given at end of arrows in knots; area and line movement given by pennant with full barb = 10 kt (U. S. Department of Commerce, 1981). Cells "A", "B", "C", "D", and "E" were along the second arc cloud. The strongest radar returns within the ACC are marked "F".



Fig. 45. Surface θ_e (K) 2-h change pattern (1800-1600 GMT) overlaid upon GOES image for 1800 GMT 26 June 1982.



Fig. 46. GOES IR/Visual composite (C9 enhancement) for 1902 GMT 26 June 1982. Banded clouds due to Helmholtz-type gravity waves were located at "G". New and rapid development of thunderstorms occurred at "J", "K", and "M".

waves in the southern part of the ACC. Banded clouds were revealed at a similar location and state relative to an ACCs' life cycle in an investigation by Brundidge (1983). At this time one can see that the arc cloud was acting as a thunderstorm triggering mechanism. New and rapid development of thunderstorms had occurred near Abilene ("J") and Wichita Falls ("K") as seen by the cold cloud tops in Fig. 46. The thunderstorm near Abilene is at the intersection of the arc cloud and a line of low level convection which runs towards Houston. Yet another significant but small cell can be seen along the arc cloud in the vicinity of Big Spring and Midland ("M"). In agreement with findings of Purdom (1979), these developments were a result of the movement of the strong but narrow field of upward motion along the leading edge of the arc cloud into a region with relatively moist and unstable air, as evidenced by the cumulus activity already present there. The convective cells along the lee of the New Mexico Rockies were designated the "first storms" of the MCC of 27 June 1982 by Rodgers et al. (1983).

Over the next 2 h, there was a southeastward drift of the ACC and the other features mentioned in Fig. 46. By 2102 GMT the main storm area of the ACC ("A" in Fig. 47) had undergone some rejuvenation while rapid growth had occurred in the Big Spring-Midland storm ("M" in Fig. 47). The Big Spring-Midland storm is seen to be the dominant convective area. The cirrus blowoff from this storm had merged with that of the rejuvenated center portion of the ACC. The area of precipitation and coldest tops within the ACC moved eastward, leaving the mesohigh behind. The Abilene thunderstorm ("J") had grown, but at



Fig. 47. GOES IR/Visual composite (C9 enhancement) for 2102 GMT 26 June 1982. The main storm area of the ACC is identified by "A". The storm near Hobbs is labeled "H"; "M" identifies the Midland storm, and "J" the Abilene storm.

a rate slower than the Midland thunderstorm. Another cell had developed along the arc cloud near Hobbs, New Mexico ("H"). At 2150 GMT radar indicated a possible tornado 80 km south-southeast of Abilene which moved to the south-southeast at 8 km h⁻¹. A tornado warning was issued by the NWS. At this same time, several large trees were uprooted by a tornado 80 km northwest of Abilene.

At this point it is useful to summarize the sequence of events involved in the formation of the second arc cloud. A convective cell developed to the lee of the Rockies and moved eastward. It collided with the first gust front, underwent further development, and contributed to the increase of cold cloud top coverage over the western Texas Panhandle. In this area, the troposphere was undergoing destabilization due to differential advection. It is hypothesized that the combination of low-level convergence, the low-level jet, and the tongue of higher θ_e at low levels fueled the convection, and was the source of the updraft air. An overshooting top, surface mesohigh, and gust front appeared. The source of the low-level cold air within the ACC was found to be near 700 mb just upstream of the storm. The areal extent of the cloud tops with coldest temperatures decreased significantly as the gust front came close to moving out from under the MCS cloud shield. An arc cloud appeared and the ACC dissipated. Intense convection formed where the arc cloud encountered areas favorable for convective development.

By 2202 GMT the cells at Hobbs, Midland, and the parent ACC thunderstorm had merged to form a new MCS. The center portion of this new MCS is seen to have cooled (Fig. 48). At 2148 GMT Midland's wind



Fig. 48. GOES IR/Visual composite (C9 enhancement) for 2202 GMT 26 June 1982.

had shifted to northerly. Over the next hour the temperature dropped from 97° F (2150 GMT) to 77° F (2249 GMT). The 0000 GMT sounding for 27 June at Midland (Fig. 49) shows the vertical extent of the outflow air. This outflow is from the thunderstorm which developed along the arc cloud, not from the ACC parent storm. Note the nearly isothermal layer from the surface to 825 mb in Fig. 49. The wind in this layer is from the east due to the fact that the thunderstorm producing the outflow is to the east. Except for the anomaly at 895 mb, all the air in this layer had the same θ_e value.

The highest tops of the new MCS at 2302 GMT (Fig. 50) were between Big Spring and Abilene. Little precipitation was occurring within the now dissipated ACC; most of it was associated with rapidly building thunderstorms along the arc cloud. Between 2305 and 2336 GMT golfball size hail occurred in Regan, Sterling, and Taylor Counties.

The availability of upper-air data at 0000 GMT 27 June made it possible to compare the synoptic features of the new storm complex with the ACC conditions 12 h earlier. The 500 mb short-wave trough had deepened, thus making it a more prominent feature (Fig. 51). The thermal structure of the short-wave trough also had changed. A cold pocket (delineated by the -10° C isotherm) was located in the western half of the trough. This placed the cold pocket along the northern edge of the MCS. At 300 mb, a warm-core high had developed over Missouri. The 300 mb thermal trough had broadened. The 200 mb flow remained diffluent downstream of the trough over Amarillo.

At 700 mb the short wave broadened with the trough extending from Childress to central Nebraska. A wind maximum of 25 kt ran from

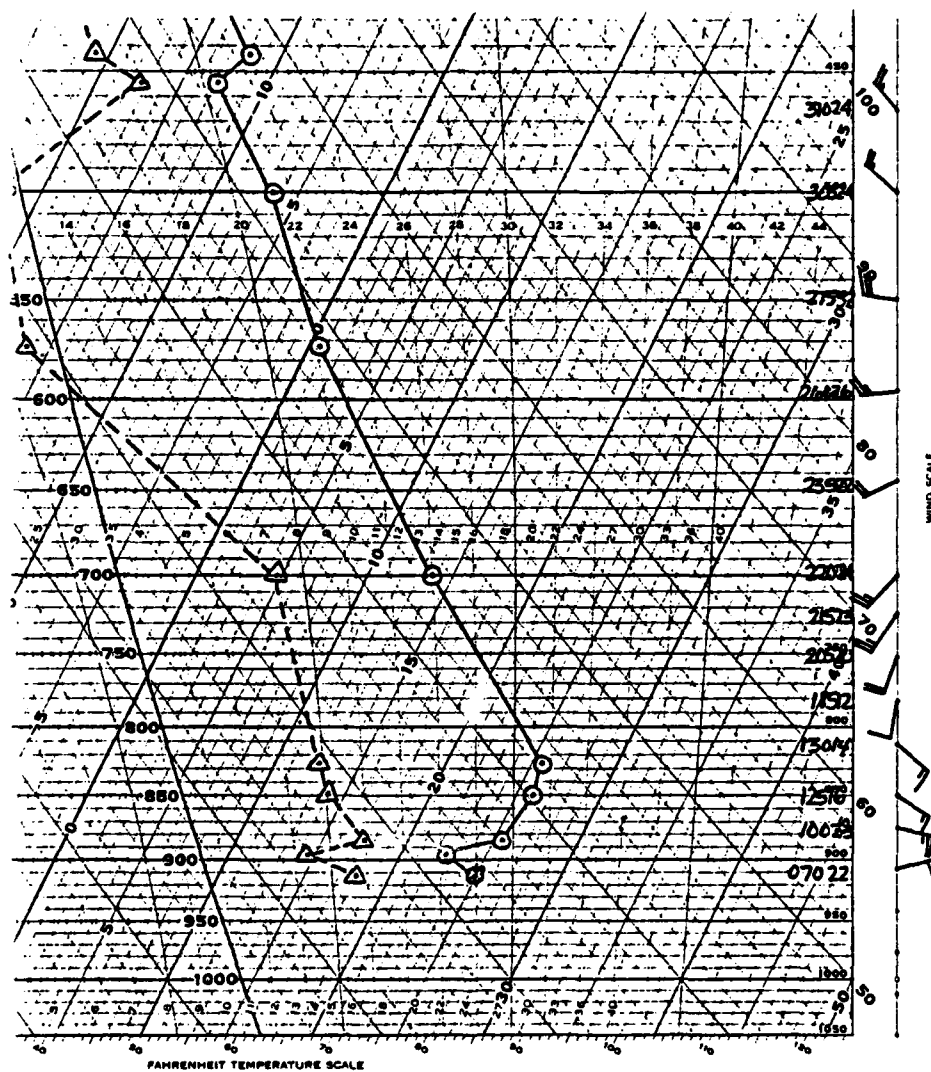


Fig. 49. Midland sounding at 0000 GMT 27 June 1982. Plot is on a skew-T log-P diagram.

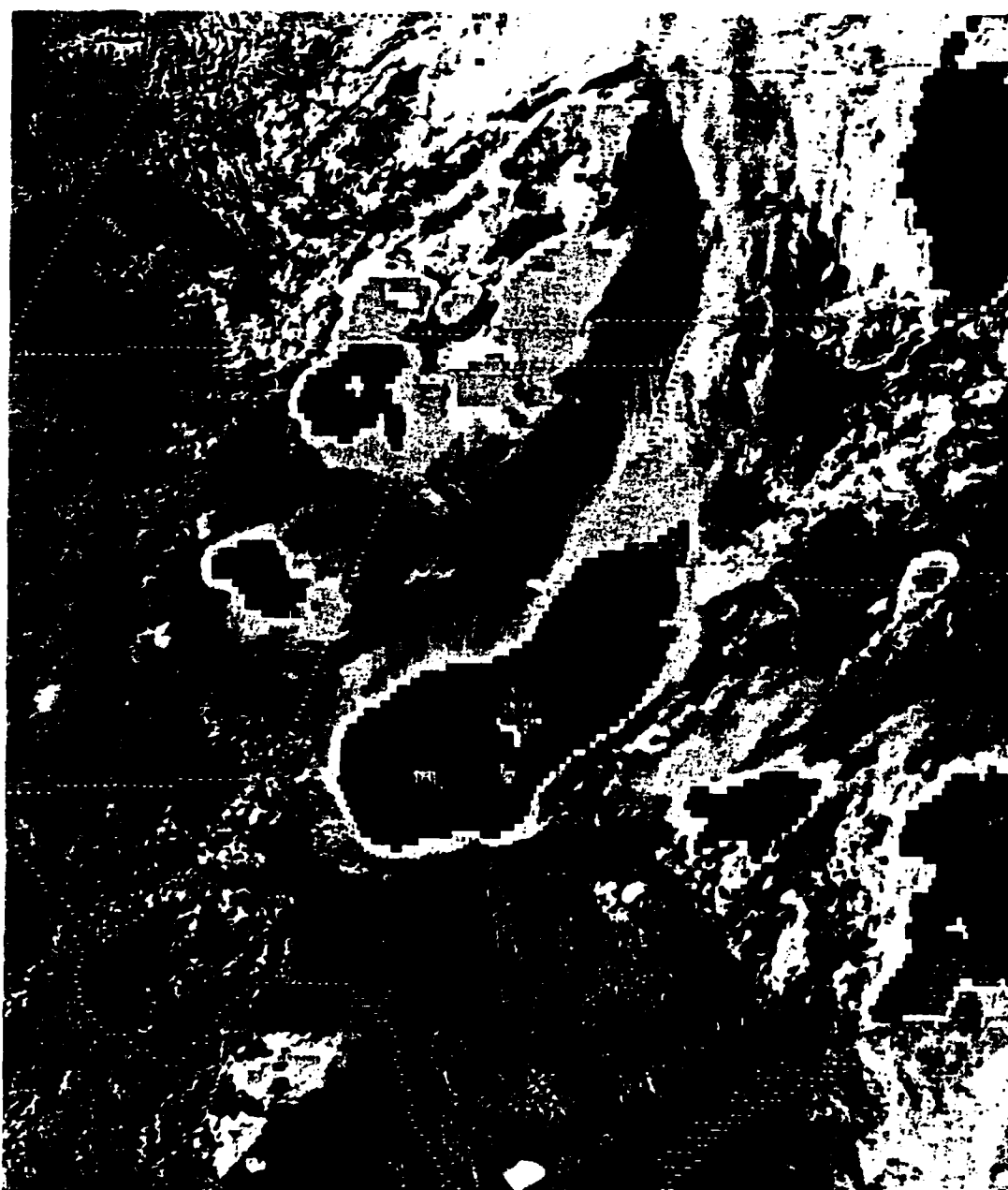


Fig. 50. GOES IR/Visual composite (C9 enhancement) for 2302 GMT 26 June 1982.

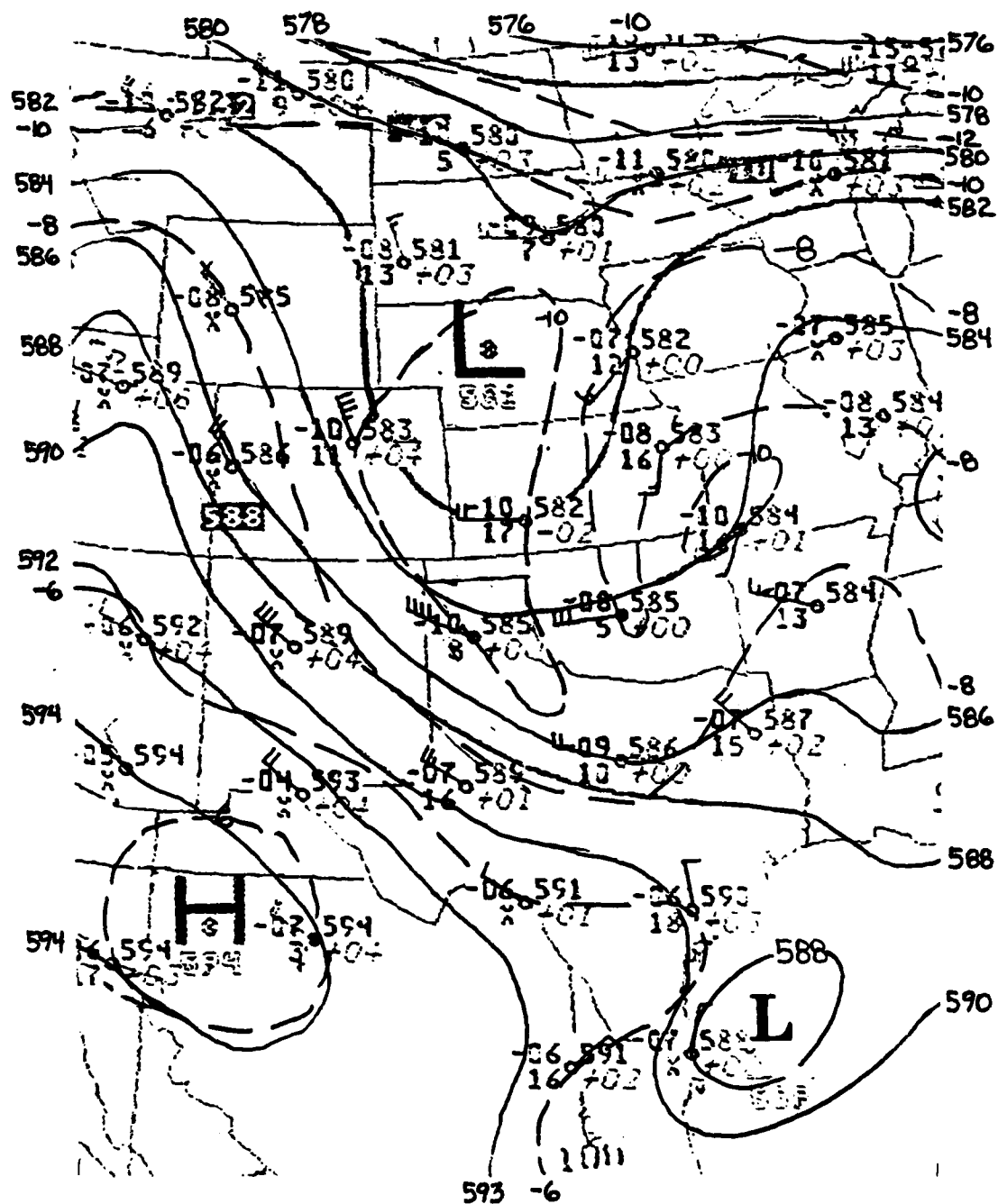


Fig. 51. 500 mb height (dm) and temperature ($^{\circ}\text{C}$) for 0000 GMT 27 June 1982. Height contours (solid lines) are every 20 m; isotherms (dashed lines) are every 2°C .

Midland towards Stephenville. At 850 mb, the height and isotherm pattern was similar to the pattern 12 h prior. The low-level jet no longer was evident. The flow over Oklahoma and North Texas now had a northerly instead of southerly component.

The divergence fields reveal interesting features within the now nearly-dissipated ACC and along its edge. Divergent flow at the surface (Fig. 52) within the arc cloud is still present with the maximum located east of Lubbock. The location of the gust front, where the surface divergence changes to convergence, corresponds well with the location of deep convection. Thus, the arc cloud continued to trigger and/or intensify convection after its parent thunderstorm had dissipated. Features which show the dissipation include convergent flow over Lubbock at 850 mb (Fig. 53), and the convergence located over Lubbock at 300 mb where divergence was noted 12 h prior. Divergence maxima at 300 mb are located along the east and west sides of the second arc cloud as seen in Fig. 54 over north central Texas and New Mexico, respectively. This indicates that the convection at certain locations along this gust front was substantial. A divergence maximum at 300 mb was also associated with the first arc cloud (marked "D") which was located over the Dallas-Fort Worth area. Lightning associated with a storm along this arc cloud critically injured a Garland woman at this time.

The series of satellite images (Figs. 55-60) covers up to the time of MCC initiation [0800 GMT 27 June 1982, (Rodgers et al., 1983)]. They show that the convection which was initiated to the lee of the New Mexico Rockies and then became intersected with the second

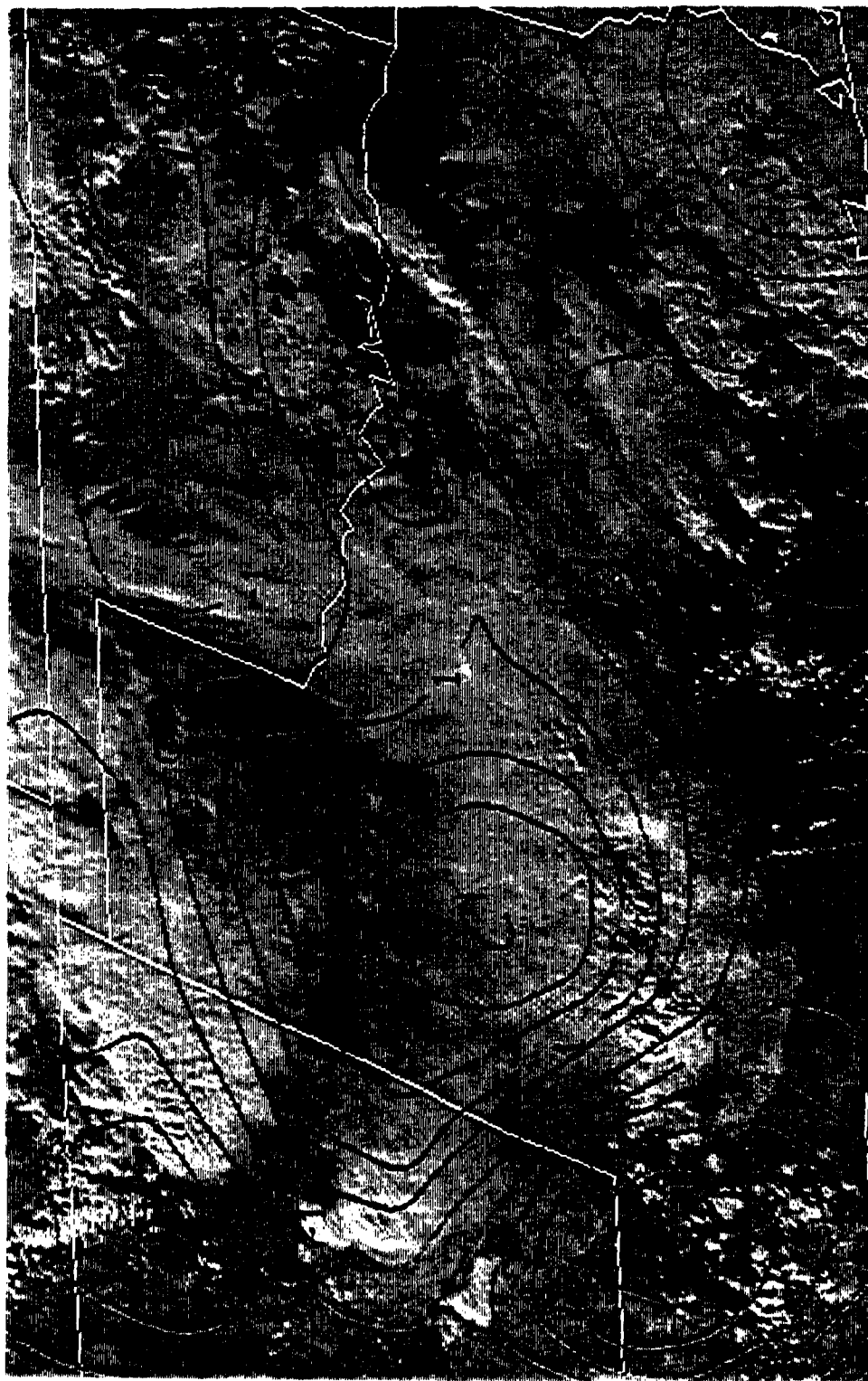


Fig. 52. Surface divergence overlaid upon GOES image for 0000 GMT 27 June 1982. Values are times 10-5 s-1.

AD-A145 384

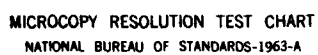
THE ARC CLOUD COMPLEX A CASE STUDY(U) AIR FORCE INST OF 272
TECH WRIGHT-PATTERSON AFB OH R L MILLER AUG 84
AFIT/C1/NR-84-52T

UNCLASSIFIED

F/G 4/2

NL





MICROCOPY RESOLUTION TEST CHART
NATIONAL BUREAU OF STANDARDS-1963-A



Fig. 53. 850 mb divergence overlaid upon GOES image for 0000 GMT 27 June 1982. Values are times 10-5 s-1.



Fig. 54. 300 mb divergence overlaid upon GOES image for 0000 GMT 27 June 1982. Values are times 10-5 s-1. A divergence maximum associated with the first arc cloud is labeled "D".



Fig. 55. GOES IR/Visual composite (C9 enhancement) for 0002 GMT 27 June 1982.



Fig. 56. GOES infrared image with MB enhancement at 0330 GMT 27 June 1982.



Fig. 57. GOES infrared image with MB enhancement at 0430 GMT 27 June 1982.

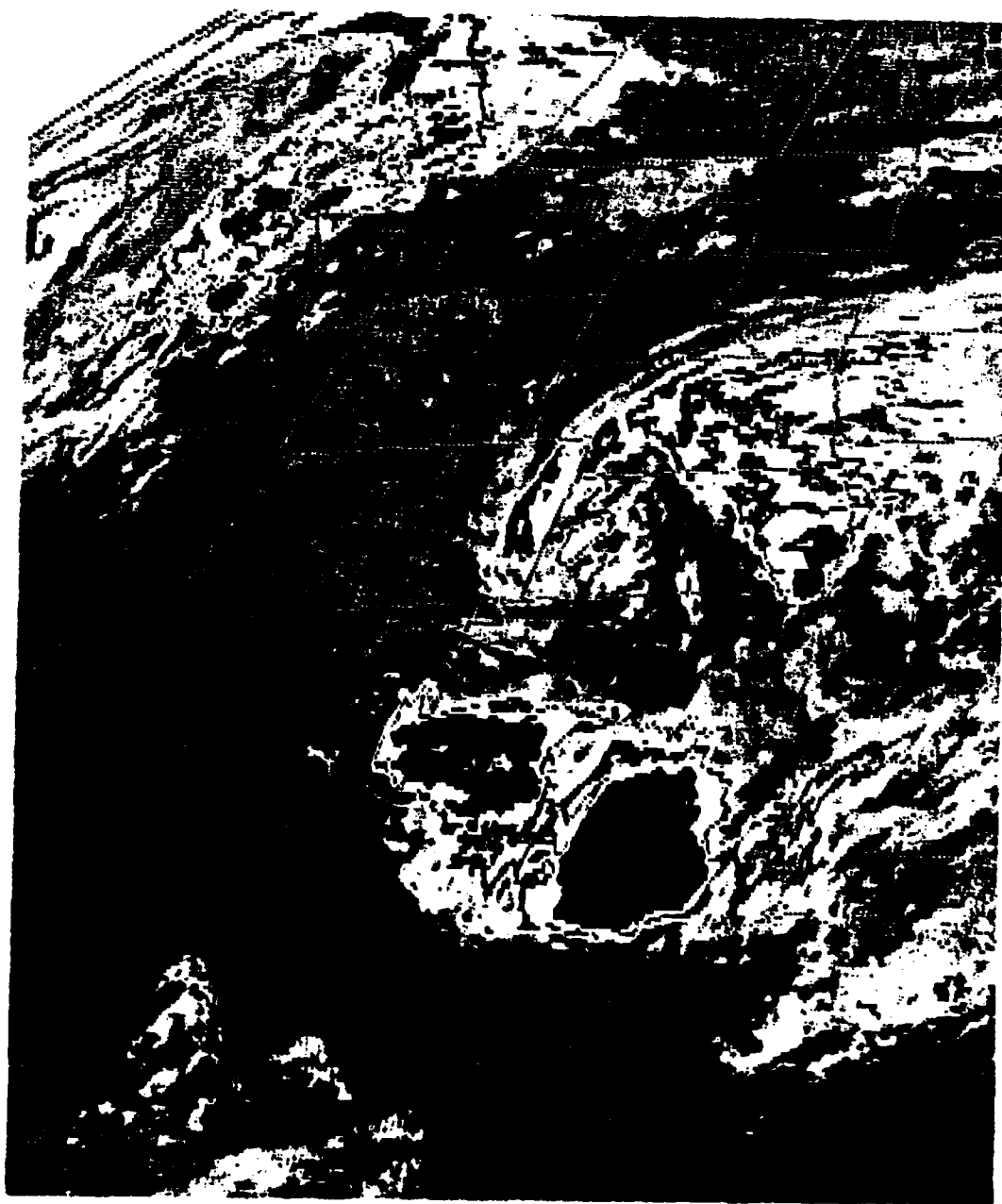


Fig. 58. GOES infrared image with MB enhancement at 0530 GMT 27 June 1982.



Fig. 59. GOES infrared image with MB enhancement at 0630 GMT 27 June 1982.

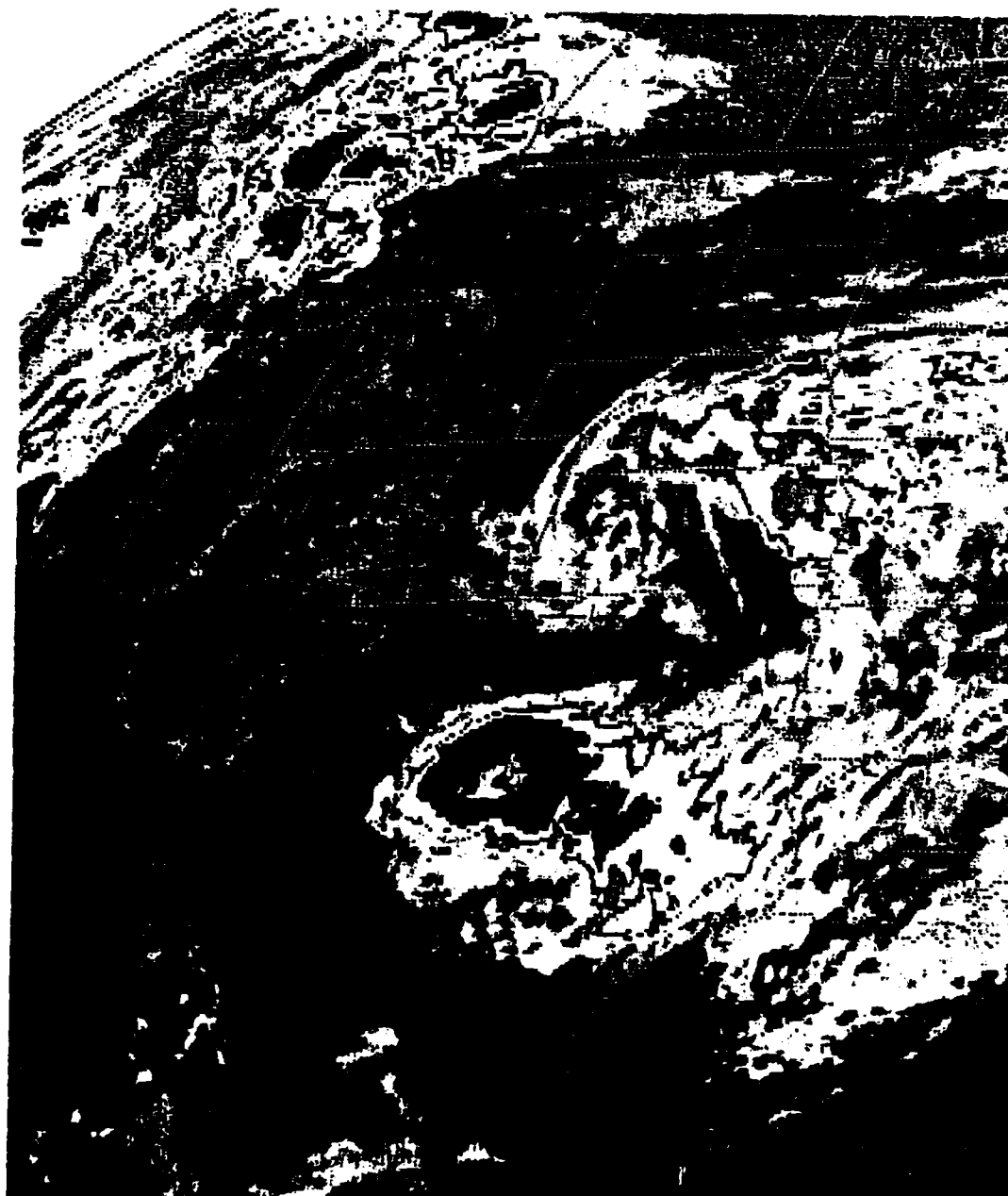


Fig. 60. GOES infrared image with MB enhancement at 0800 GMT 27 June 1982.

arc cloud, underwent considerable growth and became the main constituent of an MCC. Significant weather associated with this MCC included tornadoes, large hail, high winds, lightning damage, and flooding (Rodgers, et al., 1983).

SUMMARY AND RECOMMENDATIONS

Summary

The life cycle of an important type of convective weather system, the arc cloud complex, was qualitatively examined in this study. The chronological discussion showed that this arc cloud complex was responsible for widespread precipitation and severe weather. Convection formed along the arc cloud at different times during its life, thus a chain of storm events occurred, eventually resulting in the formation of an MCS much larger than the ACC.

A sequence of events was similar for both arc clouds. The sequence was as follows:

1. Thunderstorms developed along the foothills of the Rockies and moved eastward with an upper-level short-wave trough to form an MCS. The short-wave trough underwent modification, most likely due to interaction with the MCS.
2. The troposphere underwent destabilization due to differential advection.
3. The areal extent of the MCS cloud shield increased.
4. Overshooting tops appeared near the time that a surface mesohigh and spreading outflow were present. A gust front was located under the greatest IR temperature gradient in the satellite imagery. The origin of the downdraft air was near 700 mb; the updraft air was fed into the system by a southerly low-level jet.

5. Heavy precipitation in the form of a solid squall line was found along the southern and eastern sides of the gust front while the gust front was under the MCS cloud shield. Stratiform precipitation trailed the squall line.

6. The squall line decayed into isolated cells just prior to moving out from under the MCS cloud shield.

7. The areal extent of the MCS cloud shield decreased. The arc cloud appeared and acted as a "dry" gust front which continued to move away from the parent storm area. Meanwhile, the parent storm complex decayed.

8. Low-level divergent flow, mid-level convergence, and upper-level divergence were noted within the ACC. Convergent flow was noted along the arc cloud.

9. Severe thunderstorms formed where the arc cloud encountered areas favorable for convective development. A chain of storm events occurred, leading to the development of an MCS larger than the system which produced the arc cloud.

There are other phenomena not investigated in this paper which may relate to the ACC, namely gravity waves and conditional symmetric instability. It is evident that as the arc cloud moves outward from the main storm area, it leaves behind the downdraft source which initiated it. The fact that it can propagate over large distances while maintaining its identity implies some type of internal dynamics that may be somewhat akin to that of squall lines. Gravity waves may

be recognized as traveling disturbances which possess features similar in some respects to the arc cloud. Propagating gravity waves and the associated interrelationships between surface pressure, surface wind, and cloudiness variations have been established by Eom (1975). The role of gravity waves with wavelengths of 300-500 km acting as a thunderstorm trigger mechanism was investigated by Uccellini (1975) who stated, "Reintensification of preexisting storm cells or the development of new cells generally followed the passage of the (gravity) wave trough, with maximum rainfall intensity coinciding with the passage of the ridge." This statement points out what appears to be a rather significant difference between squall lines and the arc cloud. The latter is closely associated with low pressure with the high pressure lying under the main storm area. However, this picture of the pressure field of the ACC could be changed if one were dealing with pressure data which had been subjected to band-pass filtering to isolate the perturbation field, as was done by Uccellini.

Erickson and Whitney (1973) discussed a wave-cloud formation evident in a morning satellite image which was located to the southeast of dissipating nocturnal thunderstorm activity. They hypothesized that the cloud formation was due to "southeastward - moving gravity waves initiated by the earlier violent convection to the north and northwest". Ley and Peltier (1981) tested the hypothesis based upon a theoretical development and concluded it was unsatisfactory in part because the "source radius" of a severe storm required to produce such waves exceeded the physical dimensions of a "reasonable" severe storm and the propagation speed was several times the observed value. Their model source radius was nearly equal to 20

km, small compared to the MCS investigated in this paper. They go on to show that "the observed spatial scale and propagation speed (of the waves) may be found in the modal structure of the observed environmental conditions". Another phenomena which may relate to the arc cloud is the banded cloud and precipitation structure often observed to parallel frontal regions. Bennetts and Hoskins (1979) hypothesized that the bands, which are located approximately along the thermal wind, are a manifestation of "conditional symmetric instability."

Much more can be learned about the ACC. There are many other cases which may or may not follow the pattern described in this paper. The scale of the ACC and the density of our synoptic network make it difficult to obtain large numbers of pertinent surface and upper air observations. Questions which need to be answered include:

1. What factors determine how far the arc cloud will spread and how long it will be sustained?
2. How strong is the preference for arc clouds to form in the early (predawn) morning hours?
3. If there is a nocturnal preference, is it related to boundary layer stability changes?
4. How is arc cloud initiation related (if at all) to the appearance of an overshooting top in the GOES imagery?
5. Is a solid band of heavy precipitation always associated with the gust front while it is under the MCS

cloud shield?

6. What mid-tropospheric perturbations (if any) form during the life cycle of an ACC?

7. What percentage of the ACC's are responsible for new convective systems with weather more severe than that associated with the ACC parent storm?

8. What percentage of the MCC's undergoing dissipation become ACC's?

It is hoped that further research, preferably using a mesonetwork, will be devoted to study the ACC.

Recommendations

The arc cloud complex, by virtue of its occurrence and effect on human activities, deserves more detailed study. Further case studies using existing data would be valuable to further describe, both qualitatively and quantitatively, the nature of ACC's. To truly reveal the small scale aspects of the ACC, a mesonetwork of surface and upper air stations is required. Instrumented towers within and radar (both Doppler and conventional) coverage over such a mesonetwork would be very valuable. The use of satellite data processed upon an interactive system (such as McIDAS) would prove very useful.

Such research should be included in the National Stormscale Operational and Research Meteorology (STORM) Program (University Corporation for Atmospheric Research, 1982). It is consistent with the program's first goal:

"To enable meteorologists, public and private, to

observe and predict the occurrence of small-scale weather phenomena with substantially improved timeliness and accuracy."

Using mesonetwork data sets, development of ACC numerical models would provide an excellent tool for examining the cumulus, mesoscale, and synoptic features within the ACC environment.

REFERENCES

- Barnes, S. L., 1973: Mesoscale objective map analysis using weighted time-series observations. NOAA Tech. Memo. ERL NSSL-62, 60 pp.
- Bennetts, D. A., and B. J. Hoskins, 1979: Conditional symmetric instability - a possible explanation for frontal rainbands. Quart. J. Roy. Meteor. Soc., 105, 945-962.
- Brundidge, K. C., 1983: Investigation of the arc cloud complex. NASA Contract NGT 01-008-021, 23 pp.
- Byers, H. R., and R. R. Brahm, Jr., 1949: The Thunderstorm. U. S. Dept of Commerce, Weather Bureau, Washington, D.C., 287 pp.
- Charba, J., 1974: Application of gravity current model to analysis of squall-line gust front. Mon. Wea. Rev., 102, 140-156.
- Eom, J. K., 1975: Analysis of the internal gravity wave occurrence of 19 April 1970 in the Midwest. Mon. Wea. Rev., 103, 217-226.
- Erickson, C. O., and L. F. Whitney, Jr., 1973: Picture of the Month: Gravity waves following severe thunderstorms. Mon. Wea. Rev., 101, 708-711.
- Fritch, J. M., R. A. Maddox, L. R. Hoxit and C. F. Chappell, 1979: Convectively driven mesoscale pressure systems aloft. Preprints Fourth Conf. Numerical Weather Prediction, Silver Spring, Amer. Meteor. Soc., 398-406.
- _____, _____, and A. G. Barnston, 1981: The character of mesoscale convective complex precipitation and its contribution to warm season rainfall in the United States. Preprints Fourth Conf. Hydrometeorology, Reno, Amer. Meteor. Soc., 94-99.
- Fujita, T., 1963: Analytical mesometeorology: A review. Meteor. Monogr., No. 27, 77-125.
- Gamache, J. F., and R. A. Houze, Jr., 1982: Mesoscale air motions associated with a tropical squall line. Mon. Wea. Rev., 110, 118-135.
- Goff, R. C. 1976: Vertical structure of thunderstorm outflows. Mon. Wea. Rev., 104, 1429-1440.

Continued

- Greene, G. E. 1977: Wind shear characterization. U. S. Fed. Aviation Admin, Wash., D.C., Report No. FAA-RD-77-33, 120 pp.
- Gurka, J. J., 1976: Satellite and surface observations of strong wind zones accompanying thunderstorms. Mon. Wea. Rev., 104, 1484-1493.
- Houze, R. A., 1977: Structure and dynamics of a tropical squall-line system. Mon. Wea. Rev., 105, 1540-1567.
- Ley, B. E., and W. R. Peltier, 1981: Propagating mesoscale cloud bands. J. Atmos. Sci., 38, 1206-1219.
- Maddox, R. A., L. R. Hoxit and C. F. Chappell, 1979: Interactions between convective storms and their environment. Final Project Report NASA Contract S-40336B, 96 pp.
- _____, 1980a: Mesoscale convective complexes. Bull. Amer. Meteor. Soc., 61, 1374-1387.
- _____, 1980b: An objective technique for separating macroscale and mesoscale features in meteorological data. Mon. Wea. Rev., 108, 1108-1121.
- _____, 1983: Large-Scale meteorological conditions associated with midlatitude, mesoscale convective complexes. Mon. Wea. Rev., 111, 1475-1493.
- Mader, M. W., 1979: Gust front recognition using a single-doppler radar. U.S. Air Force Inst. of Tech., Wright-Patterson AFB, OH., Report No. AFIT-CI-79-283T-S.
- Mitchell, K. E., and J. B. Hovermale, 1977: A numerical investigation of the severe thunderstorm gust front. Mon. Wea. Rev., 105, 657-675.
- Orlanski, I., 1975: A rational subdivision of scales of atmospheric processes. Bull. Amer. Meteor. Soc., 56, 527-530.
- Purdom, J. F. W., 1973: Meso-highs and satellite imagery. Mon. Wea. Rev., 101, 180-181.
- _____, 1974: Satellite imagery applied to the mesoscale surface analysis and forecast. Preprints Fifth Conf. Weather Forecasting and Analysis, St. Louis, Mo., Amer. Meteor. Soc., 63-68.
- _____, 1979: The development and evolution of deep convection. Preprints Eleventh Conf. Severe Local Storms, Kansas City, Amer. Meteor. Soc., 143-150.

Continued

- Rodgers, D. M., K. W. Howard, and E. C. Johnson, 1983: Mesoscale convective complexes over the United States during 1982 - Annual summary. Mon. Wea. Rev., 111, 2363-2369.
- Sinclair, P. C., and J. F. W. Purdom, 1982: Integration of research aircraft data and 3 minute interval GOES data to study the genesis and development of deep convective storms. Preprints 12th Conf. Severe Local Storms, San Antonio, Amer. Meteor. Soc., 269-271.
- Uccellini, L. W., 1975: A case study of apparent gravity wave initiation of severe convective storms. Mon. Wea. Rev., 103, 497-513.
- University Corporation for Atmospheric Research, 1982: The National STORM Program, Framework for a Plan. NOAA Contract No. NA81RAC00123, 21 pp.
- U. S. Department of Commerce, 1981: Weather Radar Observations - Part B. FMH No. 7.
- _____, 1982a: Storm Data, 24, No. 6.
- _____, 1982b: National Weather Service Radar Code User's Guide.
- _____, 1982c: Hourly Precipitation Data, 32, No. 6.
- _____, 1983: The GOES User's Guide.
- Wakimoto, R. M., 1982: The life cycle of thunderstorm gust fronts as viewed with doppler radar and rawinsonde data. Mon. Wea. Rev., 110, 1060-1082.
- Wetzel, P. J., W. R. Cotton, and R. L. McNelly, 1982: The dynamic structure of the mesoscale convective complex - Some case studies. Preprints 12th Conf. Severe Local Storms, San Antonio, Amer. Meteor. Soc., 265-268.
- Zipser, E. J., 1977: Mesoscale and convective-scale downdrafts as distinct components of squall-line structure. Mon. Wea. Rev., 105, 1568-1589.

VITA

Robert L. Miller was born in New York City, New York on 30 October 1954. His parents are Robert W. Miller and Marjorie J. (Moore) Miller. He was raised in Central Square, New York (20 miles north of Syracuse), where he graduated from P.V. Moore High School in 1972.

From 1972 through 1976 he attended Texas A&M University and was enrolled in Air Force ROTC. In May of 1976 he received his Bachelor of Science Degree in Meteorology, and his Air Force Commission. From August, 1976 through November, 1979, he served as Wing Weather Officer at Plattsburgh AFB, New York. After serving one year as Defense Meteorological Satellite Coordinator at Osan Air Base, South Korea, he served as Assistant Operations Officer with 26th Weather Squadron, Barksdale AFB, Louisiana.

Rob returned to Texas A&M University in August, 1982 to pursue the degree of Master of Science in Meteorology, under the auspices of the Air Force Institute of Technology, United States Air Force. His next assignment will be with 7th Weather Squadron, Heidelberg, Germany, APO New York 09403.

He married the former Karen E. Williams, and they have a daughter, Kate. His permanent mailing address is: 312 Tanglewood, New Braunfels, Texas 78130.

The typist for this thesis was the author.

END

FILMED

10-84

DTIC